



U.S. Department  
of Transportation

**National Highway  
Traffic Safety  
Administration**



---

DOT HS 812 845

June 2020

# **Parameter Study of the OMDB Test Procedure**

## **DISCLAIMER**

This publication is distributed by the U.S. Department of Transportation, National Highway Traffic Safety Administration, in the interest of information exchange. The opinions, findings, and conclusions expressed in this publication are those of the authors and not necessarily those of the Department of Transportation or the National Highway Traffic Safety Administration. The United States Government assumes no liability for its contents or use thereof. If trade or manufacturers' names or products are mentioned, it is because they are considered essential to the object of the publication and should not be construed as an endorsement. The United States Government does not endorse products or manufacturers.

Suggested APA Format Citation:

Reichert, R., & Kan, C.-D. (2020, June). *Parameter study of the OMDB test procedure* (Report No. DOT HS 812 845). National Highway Traffic Safety Administration.

## Technical Report Documentation Page

<b>1. Report No.</b> DOT HS 812 845	<b>2. Government Accession No.</b>	<b>3. Recipient's Catalog No.</b>	
<b>4. Title and Subtitle</b> Parameter Study of the OMDB Test Procedure		<b>5. Report Date:</b> June 2020	
		<b>6. Performing Org. Code:</b>	
<b>7. Authors:</b> Reichert, R., Kan, C.-D.		<b>8. Performing Organization Report No.</b>	
<b>9. Performing Organization Name and Address</b> Center for Collision Safety and Analysis George Mason University 4087 University Drive, Suite 2100 Fairfax, VA 22030		<b>10. Work Unit No. (TRAIS)</b>	
		<b>11. Contract or Grant No.</b> DTNH2217R00098	
<b>12. Sponsoring Agency Name and Address</b> National Highway Traffic Safety Administration 1200 New Jersey Aveue SE Washington, DC 20590		<b>13. Type of Report and Period Covered</b> Final Report Oct. 2017–March 2019	
		<b>14. Sponsoring Agency Code</b>	
<b>15. Supplementary Notes</b>			
<b>16. Abstract</b> Oblique impact configurations account for a significant amount of real-world accidents. Compared to co-linear frontal crash configurations, these impacts have different occupant kinematics and vehicle intrusion patterns. Consequently, a new oblique impact test is being developed and investigated by the National Highway Traffic Safety Administration. Variations in impact conditions and occupant seating positions are immanent in full-scale crash testing. For example, offset moving deformable barrier (OMDB) impact velocity and occupant seating position can only be controlled within certain limits. Therefore, it is important to understand the effect of relevant parameters related to NHTSA's advanced test and occupant positioning procedure. Finite element simulations, consisting of detailed computer models of a vehicle, the OMDB, the Test Device for Human Occupant Restraints (THOR), and relevant restraints and interiors, were used by the Center for Collision Safety and Analysis at the George Mason University to conduct this research funded by NHTSA. Advanced design-of-experiment (DoE) methods were applied to determine the importance of parameters and their effect on the vehicle and occupant criteria.			
<b>17. Key Word</b> oblique frontal impact, FE simulation, DoE, test procedure, and seating position study		<b>18. Distribution Statement</b> Document is available through the National Technical Information Service, <a href="http://www.ntis.gov">www.ntis.gov</a> .	
<b>19. Security Classif. (of this report)</b> Unclassified	<b>20. Security Classif. (of this page)</b> Unclassified	<b>21. No. of Pages</b> 137	<b>22. Price</b>

Form DOT F 1700.7 (8-72)

Reproduction of completed page authorized

## Executive Summary

Oblique impact configurations account for a significant amount of real-world crashes. Compared to co-linear frontal crash configurations, these impacts have different occupant kinematics and vehicle intrusion patterns. Consequently, a new oblique impact test is being developed and investigated by NHTSA. Variations in impact conditions and occupant seating positions are immanent in full-scale crash testing. For example, offset moving deformable barrier (OMDB) impact velocity and occupant seating position can only be controlled within certain limits. Therefore, it is important to understand the effect of relevant parameters related to NHTSA's test and occupant positioning procedure. Finite element simulations, consisting of detailed computer models of a vehicle, the OMDB, the Test Device for Human Occupant Restraints (THOR), and relevant restraints and interiors, were used by GMU to conduct this research. Design-of-experiment (DoE) methods were applied to determine the importance of parameters and their effect on the vehicle and occupant criteria.

In the Test Procedure Study," the effect of variations in OMDB impact angle, vertical misalignment, overlap, mass, and impact speed, was evaluated:

- (1) Repeatability Study: Good test repeatability was found when changing parameters within defined test tolerances. Impact speed was the most important factor for vehicle pulse in x-direction and impact angle was most dominant for vehicle y-pulse.
- (2) Sensitivity Study: More significant effects were seen when changing parameters beyond defined test tolerances. Impact speed was the most important factor for driver and passenger injury risk.
- (3) Impact Angle Study: Significant differences in vehicle yaw motion were observed when changing the impact angle from 0° co-linear to 20° oblique. Overall injury risk was similar for the driver, while higher overall injury risk was seen for more oblique impact conditions for the far-side passenger. BrIC values tended to be higher for more oblique impact conditions

A THOR position study determined the effect and importance of parameters relevant for positioning the THOR. Parameters included the H-point x-, y-, and z-coordinate, the head/torso angle, and the position of the lower extremities:

- (1) Repeatability Study: Relevant parameters for positioning the THOR on the driver seat were changed within defined positioning tolerances. For example, the head/torso angle was varied by +/-1°. CORA values above 0.8 indicated good correlation of time-history data, when compared to the designated seating position.
- (2) Sensitivity Study: Relevant parameters for positioning the THOR on the passenger seat were changed within ranges that are beyond defined tolerances. For example, head/torso angle was varied by +/-5°. Differences in occupant kinematics and injury risk were larger than for the driver side due to the larger range for respective parameters and less controlled

kinematics of the far-side occupant. Despite these observations, it was found that 37 out of 41 conducted simulations showed similar overall injury risk. CORA values above 0.7 indicated good to acceptable correlation of time history data.

In summary, NHTSA's oblique frontal offset impact test showed overall good repeatability with respect to vehicle kinematics and injury risk when relevant parameters were changed within defined tolerances.

## Table of Contents

<b>Executive Summary .....</b>	<b>ii</b>
<b>1. Introduction.....</b>	<b>1</b>
1.1 Objective .....	3
1.2 Baseline Simulation .....	4
<b>2. Methods.....</b>	<b>10</b>
2.1 Design of Experiments (DoE) .....	11
2.2 Response Surface Construction .....	12
2.3 Data Analysis and Comparison .....	13
2.4 CORA – Objective Correlation Method .....	16
<b>3. Test Procedure Repeatability Study .....</b>	<b>17</b>
3.1 Parameters and Ranges .....	17
3.2 Results – Vehicle .....	18
3.3 Results – Driver .....	20
3.4 Results – Passenger .....	23
<b>4. Test Procedure Sensitivity Study .....</b>	<b>27</b>
4.1 Evaluated Parameters and Ranges .....	27
4.2 Results – Vehicle .....	29
4.3 Results – Driver .....	31
4.4 Results – Passenger .....	35
<b>5. Test Procedure Impact Angle Study .....</b>	<b>39</b>
5.1 Evaluated Parameters and Ranges .....	39
5.2 Results – Vehicle .....	40
5.3 Results – Driver .....	42
5.4 Results – Passenger .....	45
<b>6. Test Procedure Study Summary .....</b>	<b>48</b>
<b>7. THOR Position Study.....</b>	<b>50</b>
7.1 Parameters and Ranges .....	50
<b>8. THOR Position Repeatability Study (Driver) .....</b>	<b>54</b>
8.1 Driver Simulation Results Overview .....	54
8.2 Driver Star Rating .....	54
8.3 Driver Head .....	56
8.4 Driver Neck .....	58
8.5 Driver Chest and Abdomen .....	59
8.6 Driver Acetabulum and Femur .....	60
8.7 Driver Tibia .....	61

8.8 THOR Position Repeatability Study Summary (Driver) .....	62
<b>9. THOR Position Sensitivity Study (Passenger).....</b>	<b>64</b>
9.1 Passenger Simulation Results Overview.....	64
9.2 Passenger Overall Score.....	65
9.3 Passenger Head.....	66
9.4 Passenger Neck.....	68
9.5 Passenger Chest and Abdomen .....	69
9.6 Passenger Acetabulum and Femur.....	71
9.7 Passenger Tibia.....	72
9.8 THOR Position Sensitivity Study Summary (Passenger) .....	73
<b>10. Limitations.....</b>	<b>75</b>
<b>11. Conclusion.....</b>	<b>76</b>
<b>APPENDIX A: Test Procedure Study Additional Graphs .....</b>	<b>A-1</b>
A1. Test Versus Simulation for Driver and Passenger .....	A-2
A2. Test Versus Simulation for Vehicle Intrusion and Pulse .....	A-3
A3. Test Procedure Repeatability Study – Simulation Matrix.....	A-4
A4. Repeatability Study – Vehicle Results Near-Side .....	A-5
A5. Repeatability Study – Vehicle Results Far-side .....	A-7
A6. Repeatability Study – Driver Results.....	A-8
A7. Repeatability Study – Passenger Results .....	A-9
A8. Sensitivity Study – Simulation Matrix.....	A-10
A9. Sensitivity Study – Vehicle Results Near-Side .....	A-11
A10. Sensitivity Study – Vehicle Results Far-Side.....	A-12
A11. Sensitivity Study – Driver Results .....	A-13
A12. Sensitivity Study – Passenger Results .....	A-14
A13. Impact Angle Study – Vehicle Results .....	A-15
A14. Impact Angle Study – Driver Results .....	A-16
A15. Impact Angle Study – Passenger Results.....	A-17
A16. Test Procedure Parametric Study – Overview Vehicle.....	A-18
A17. Test Procedure Parametric Study – Overview Driver.....	A-19
A18. Test Procedure Parametric Study – Overview Passenger .....	A-21
A19. Driver BRIC & Chest – 80km/h Versus. 90km/h.....	A-22
<b>APPENDIX B: THOR Position Study Additional Graphs .....</b>	<b>B-1</b>
B1. THOR Position Simulation Matrix – Driver & Passenger .....	B-2
B2. Knee-to-Knee Distance in 64 Full-Scale Tests.....	B-3
B3. Repeatability Study – Driver Results Runs 1–16 .....	B-4
B4. Repeatability Study – Driver Results Runs 17–28 .....	B-5

B5. Repeatability Study – Driver Results Runs 29–41 .....	B-6
B6. Driver Star-Rating – Effect of Individual Parameters.....	B-7
B7. Driver HIC – Effect of Individual Parameters.....	B-8
B8. Driver BrIC – Effect of Individual Parameters.....	B-9
B9. Driver Neck – Effect of Individual Parameters .....	B-10
B10. Driver Chest – Effect of Individual Parameters.....	B-11
B11. Driver Abdomen – Effect of Individual Parameters .....	B-12
B12. Driver Acetabulum – Effect of Individual Parameters.....	B-13
B13. Driver Femur – Effect of Individual Parameters .....	B-14
B14. Driver Tibia – Effect of Individual Parameters .....	B-15
B15. Sensitivity Study – Passenger Results Runs 1–16 .....	B-16
B16. Sensitivity Study – Passenger Results Runs 17–28 .....	B-17
B17. Sensitivity Study – Passenger Results Runs 29–41 .....	B-18
B18. Passenger Point Score – Response Surface .....	B-19
B19. Passenger BrIC – Response Surface .....	B-20
B20. Passenger Neck – Response Surface.....	B-21
B21. Passenger Chest – Response Surface .....	B-22
B22. Passenger Abdomen – Response Surface.....	B-23
B23. Passenger Femur – Response Surface.....	B-24
B24. Passenger Tibia – Response Surface.....	B-25
B25. THOR Position Study Results Overview .....	B-26
B26. THOR Position Study Summary.....	B-27

## Figures

Figure 1. NHTSA’s Oblique Impact Configuration.....	2
Figure 2. THOR: (a) Driver Seat; (b) Passenger Seat.....	4
Figure 3. THOR Kinematics in Test and Simulation: (a) Near-Side; (b) Far-Side.....	5
Figure 4. Lower Leg Kinematics in Test and Simulation.....	5
Figure 5. Overall Star Rating: (a) Driver; (b) Passenger.....	8
Figure 6. Test Versus Simulation – Driver.....	8
Figure 7. Test Versus Simulation – Passenger.....	9
Figure 8. Test Procedure Simulation Plan Flow Chart.....	10
Figure 9. Box-Behnken DoE Design Example.....	11
Figure 10. An Example of Variation of Single Parameter.....	13
Figure 11. 3-Dimensional RS Example obtained from the Variation of 2 Parameters.....	14
Figure 12. An Example of Parameter Importance Index Obtained From ANOVA.....	15
Figure 13. CORA – Objective Correlation Rating Methodology.....	16
Figure 14. Repeatability Study Parameters and Ranges.....	17
Figure 15. (a) Toe-pan; (b) IP and Steering Intrusion Measurement Points.....	18

Figure 16. Vehicle x-Pulse: (a) Parameter Importance Index; (b) Effect of Parameters...	18
Figure 17. Vehicle y-Pulse: (a) Parameter Importance Index; (b) Effect of Parameters...	19
Figure 18. Maximum Toe-Pan Intrusion: (a) Importance Index; (b) Effect of Parameters.....	19
Figure 19. Passenger Kinematics: (a) Test and Simulation; (b) Head trajectory.....	20
Figure 20. Driver Points: (a) Importance Index; (b) Effect of Parameters; (c) RS Example. ....	21
Figure 21. Driver BrIC: (a) Importance Index; (b) Effect of Parameters; (c) RS Example. ....	21
Figure 22. Driver Femur: (a) Importance Index; (b) Effect of Parameters; (c) RS Example. ....	22
Figure 23. Passenger Kinematics: (a) Test and Simulation; (b) Head Trajectory.....	23
Figure 24. Passenger Points: (a) Importance Index; (b) Effect of Param; (c) RS Example. ....	24
Figure 25. Passenger BrIC: (a) Importance Index; (b) Effect of Parameters.....	24
Figure 26. Passenger Chest: (a) Importance Index; (b) Effect of Parameters.....	25
Figure 27. Passenger Femur: (a) Importance Index; (b) Effect of Parameters. ....	25
Figure 28. Passenger Tibia: (a) Importance Index; (b) Effect of Parameters. ....	26
Figure 29. Sensitivity Study – Parameters and Ranges. ....	27
Figure 30. Sensitivity Study – Extreme Cases.....	28
Figure 31. Vehicle x-Pulse: (a) Importance Index; (b) Effect of Parameters; (c) RS Example.....	29
Figure 32. Vehicle y-Pulse: (a) Importance Index; (b) Effect of Parameters; (c) RS Example.....	29
Figure 33. Toe-Pan Intrusion: (a) Importance Index; (b) Effect of Parameters; (c) RS Example. ....	30
Figure 34. Driver Head y-Displacement: (a) Lowest; (b) Highest.....	31
Figure 35. Driver Points: (a) Importance Index; (b) Effect of Parameters; (c) RS Example. ....	32
Figure 36. Driver BrIC: (a) Importance Index; (b) Effect of Parameters; (c) RS Example. ....	32
Figure 37. Driver Chest: (a) Importance Index; (b) Effect of Parameters; (c) RS Example. ....	33
Figure 38. Driver Tibia: (a) Importance Index; (b) Effect of Parameters; (c) RS Example. ....	33
Figure 39. Driver Head Trajectory: (a) Best Case; (b) Worst Case. ....	35
Figure 40. Passenger Points: (a) Importance Index; (b) Effect of Parameters; (c) RS Example. ....	36
Figure 41. Passenger BrIC: (a) Importance Index; (b) Effect of Parameters; (c) RS Example. ....	36
Figure 42. Driver Chest: (a) Importance Index; (b) Effect of Parameters; (c) RS Example. ....	37
Figure 43. Passenger Femur: (a) Importance Index; (b) Effect of Parameters; (c) RS Example. ....	37

Figure 44. Passenger Tibia: (a) Importance Index; (b) Effect of Parameters; (c) RS Example. ....	38
Figure 45. Impact Angle Study – Initial Positions for 0° to 20°.....	39
Figure 46. Impact Angle Study – Deformed Shape: (a) 0° Impact; (b) 20° Impact.....	40
Figure 47. Impact Angle Study: (a) Delta-V; (b) Vehicle Yaw.....	41
Figure 48. Driver Head Trajectory y-Excursion: (a) Lowest Value; (b) Highest Value. ...	42
Figure 49. Driver Head Motion: (a) y-Direction; (b) x-Direction.....	42
Figure 50. Impact Angle Study: (a) Points Driver; (b) BrIC Driver. ....	44
Figure 51. Impact Angle Study Head Excursion: (a) Best Case; (b) Worst Case.....	45
Figure 52. Passenger Head Motion: (a) y-Direction; (b) x-Direction. ....	46
Figure 53. Impact Angle Study: (a) Passenger Points; (b) Passenger BrIC.....	47
Figure 54. Impact Angle Study – Maximum Tibia Moment Passenger.....	47
Figure 55. THOR Position Repeatability Study Parameters and Ranges.....	51
Figure 56. (a) HP-x -20/0/+20mm; (b)HP-z 0/+10/+20mm. ....	52
Figure 56. (c) Head Angle – 5/0/+5°; (d) Knee-to-Knee Distance 0/+30/+60 mm .....	52
Figure 57. Driver Star Rating: (a) Importance Index; (b) Response Surface. ....	55
Figure 58. Driver Head y-Trajectory: (a) Importance Index; (b) Kinematics. ....	56
Figure 59. Driver HIC: (a) Importance Index; (b) Response Surface. ....	56
Figure 60. Driver BrIC: (a) Importance Index; (b) Response Surface. ....	57
Figure 61. Driver Neck: (a) Importance Index; (b) Response Surface.....	58
Figure 62. Driver Chest: (a) Importance Index; (b) Response Surface. ....	59
Figure 63. Driver Abdomen: (a) Importance Index; (b) Response Surface.....	59
Figure 64. Driver Acetabulum: (a) Importance Index; (b) Response Surface. ....	60
Figure 65. Driver Femur: (a) Importance Index; (b) Response Surface.....	60
Figure 66. Driver Tibia: (a) Importance Index; (b) Response Surface.....	61
Figure 67. Passenger Overall Score: (a) Importance Index; (b) Effect of Parameters. ....	65
Figure 68. Passenger Head x-Trajectory: (a) Importance Index; (b) Kinematics. ....	66
Figure 69. Passenger HIC: (a) Importance Index; (b) Effect of Parameters.....	67
Figure 70. Passenger BrIC: (a) Importance Index; (b) Effect of parameters.....	67
Figure 71. Passenger Neck: (a) Importance Index; (b) Effect of Parameters. ....	68
Figure 72. Passenger Chest: (a) Importance Index; (b) Effect of Parameters.....	69
Figure 73. Passenger Abdomen: (a) Importance Index; (b) Effect of Parameters. ....	70
Figure 74. Passenger Acetabulum: (a) Importance Index; (b) Effect of Parameters.....	71
Figure 75. Passenger Femur: (a) Importance Index; (b) Effect of Parameters. ....	71
Figure 76. Passenger Tibia: (a) Importance Index; (b) Effect of Parameters. ....	72

## Tables

Table 1. Injury Criteria With Upper and Lower Boundaries .....	6
Table 2. 5 Star Rating Scale (100 Point Scale) .....	7
Table 3. Repeatability Study – Parameter Ranges and Levels .....	11

# 1. Introduction

Consumer information rating crash tests, such as the National Highway Traffic Safety Administration's New Car Assessment Program (NCAP) full frontal impact and the Insurance Institute for Highway Safety (IIHS) small and moderate frontal overlap impacts, have advanced vehicle safety and reduced injury risks. Recent studies, such as *Fatalities in Frontal Crashes Despite Seat Belts and Air Bags*,<sup>1</sup> indicate that oblique offset crashes are a common real-world crash pattern related to belted occupant fatalities. Another study compared the number of annual driver Maximum Abbreviated Injury Scale (MAIS) 3+ injuries by body region for oblique and co-linear frontal impacts.<sup>2</sup> The study showed that drivers in left oblique impacts experienced more MAIS 3+ injuries in almost all body regions than drivers in co-linear crashes. Oblique impacts capture real world crashes, and the development of countermeasures for restraints and vehicle structures will potentially further improve vehicle safety and reduce injury risk.

NHTSA has developed a laboratory test procedure for oblique offset moving deformable barrier impacts.<sup>3</sup> Figure 1 depicts a schematic of the new oblique test configuration. An offset moving deformable barrier (OMDB) was optimized to produce target vehicle crush patterns like real world cases. It has a weight of 2,486 kilograms (kg) and impacts a stationary vehicle at a speed of 90 km/h. The vehicle is placed at a 15-degree angle from the OMDB longitudinal axis. The impact is set up such that a 35-percent overlap occurs between the OMDB and the front end of the struck vehicle at initial contact.

---

<sup>1</sup> Bean, J. D., Kahane, C. J., Mynatt, M., Rudd, R. W., Rush, C. J., & Wiacek, C. (2009, September). *Fatalities in frontal crashes despite seat belts and air bags – Review of all CDS cases – Model and calendar years 2000-2007 – 122 fatalities* (Report No. DOT HS 811 202)., Washington, DC: National Highway Traffic Safety Administration. Retrieved from <https://crashstats.nhtsa.dot.gov/Api/Public/ViewPublication/811102>.

<sup>2</sup> NASS-CDS (2000-2013), Number of Annual Driver MAIS 3+ Injuries by Body Region in Co-liner and Left Oblique Crashes.

<sup>3</sup> National Highway Traffic Safety Administration. (2015, December 5). Laboratory Test Procedure for Oblique Offset Moving Deformable Barrier Impact Test - Memorandum/Report [Oblique Test Procedure - Draft 7-22-2015, NHTSA-2015-0119-0017]. Washington, DC: Author. Retrieved from [www.regulations.gov/contentStreamer?documentId=NHTSA-2015-0119-0017&attachmentNumber=1&contentType=pdf](http://www.regulations.gov/contentStreamer?documentId=NHTSA-2015-0119-0017&attachmentNumber=1&contentType=pdf).

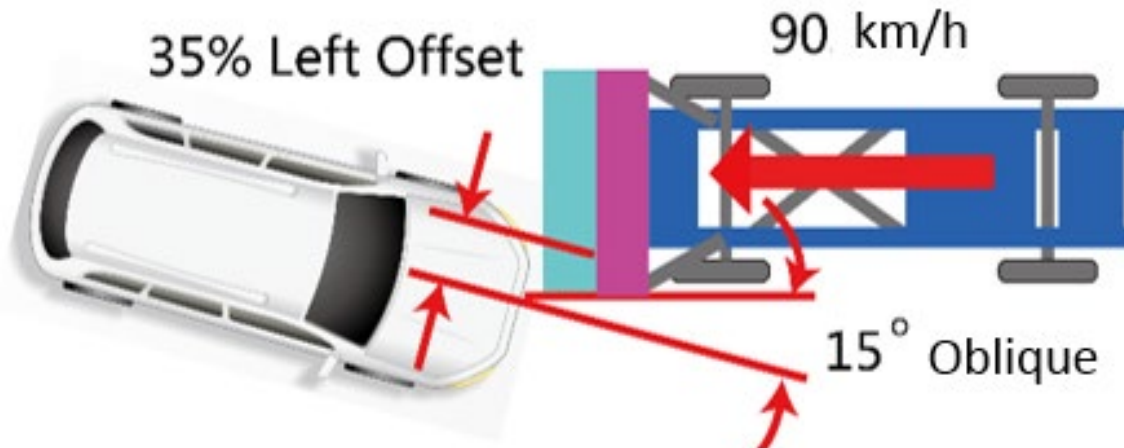


**Figure 1. NHTSA's Oblique Impact Configuration.**

When developing the oblique test procedure, NHTSA defined tolerances for test parameters, since they cannot be completely controlled. A finite element (FE) study using available models for vehicle, barrier, interior, restraints, and Test Device for Human Occupant Restraint (THOR) occupants is being used to evaluate the effect of test configuration tolerances, such as small differences in impact angle, impact location, impact mass, and velocity (repeatability study). To understand how vehicle and occupant outcomes are affected when parameters are changed beyond current test tolerances, a sensitivity study is conducted. Similar studies are conducted to understand the effect of parameters relevant for positioning the THOR occupants in the vehicle.

## 1.1 Objective

The study has two main objectives. The first objective consists of determining the effects of different test configuration parameters on the vehicle and occupant results using FE computer models. The parameters to be varied and evaluated:

- Impact angle
- OMDB vertical misalignment
- OMDB horizontal misalignment (overlap)
- OMDB mass
- Impact speed

The effect of each parameter, as well as combinations of these parameters, was investigated. Variations in vehicle and occupant (driver and passenger) responses were studied.

The second objective is to determine the effect of varying occupant seating positions within and beyond defined tolerances using FE simulations. The seating parameters to be varied and evaluated:

- Dummy x position
- Dummy y position
- Dummy z position
- Head/torso angle
- Heel and knee position

Here again the effect of each seating parameter, as well as combinations of these parameters, was analyzed. Variations of the occupant (driver and passenger ATDs) responses was assessed.

## 1.2 Baseline Simulation

A baseline simulation for NHTSA left oblique impact condition was conducted with an FE model of a mid-size sedan vehicle (NHTSA Test #8789: 2014 Honda Accord 4-door sedan) with a THOR occupant in the driver and front passenger seat. THOR ATD's were positioned in the baseline simulation model using coordinate measuring machine (CMM) measurement data provided by NHTSA's Vehicle Research Technical Center. Occupants were seated according to the latest seating procedures. Figure 2 shows the final seating position for the driver (a) and for the passenger (b).



**Figure 2. THOR: (a) Driver Seat; (b) Passenger Seat.**

Vehicle kinematics, vehicle pulse, occupant kinematics, and occupant injury criteria were compared with results from a full-scale test of the same vehicle. Kinematics and injury criteria compared reasonably well with the specific test results for all body regions. Kinematics and injury values were in a range that has been seen in many full-scale tests of similar sedan vehicles.

Figure 3 (a) shows the typical occupant kinematics of the near-side occupant in test and simulation. The driver's motion is controlled by the seat belt and the driver and side curtain air bag. Figure 3 (b) represents the far-side occupant in test and simulation, which shows that the passenger upper body slides out of the shoulder-belt and the head moves towards the middle of the vehicle with significant head rotation due to the interaction with the passenger air bag.

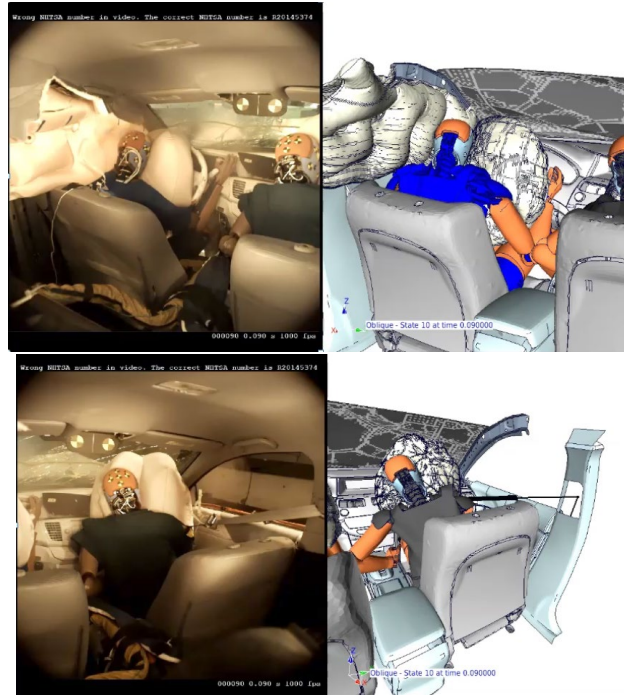


**Figure 3. THOR Kinematics in Test and Simulation: (a) Near-Side; (b) Far-Side.**

Realistic occupant kinematics and injury risk were observed for driver and passenger. Vehicle kinematics, pulse, and intrusion characteristics were also well captured. Figure 4 shows a comparison of the lower extremity kinematics in test and simulation for the near-side occupant.



**Figure 4. Lower Leg Kinematics in Test and Simulation.**

Injury risk was analyzed by calculating injury criteria for the head (HIC, BrIC), neck (Nij), chest (peak resultant deflection), abdomen (peak compression), upper leg (peak resultant acetabulum force, peak femur axial force), and lower leg (peak tibia axial force, peak tibia resultant moment). For each injury metric, an upper and lower boundary was defined, as shown in Table 1.

**Table 1. Injury Criteria With Upper and Lower Boundaries**

Head	HIC15	500	700
	BrIC	0.71	1.05
Neck	Ntf	0.39	0.85
	Ncf	0.39	0.85
	Nte	0.39	0.85
	Nce	0.39	0.85
Chest	Deflection - UPR LH [mm]	37.9	52.3
	Deflection - UPR RH [mm]	37.9	52.3
	Deflection - LWR LH [mm]	37.9	52.3
	Deflection - LWR RH [mm]	37.9	52.3
Abdomen	Deflection - LH [mm]	NA	88.6
	Deflection - RH [mm]	NA	88.6
Femur	Resultant Acetabulum Force - LH [N]	2583	3486
	Resultant Acetabulum Force - RH [N]	2583	3486
	Femur Force - LH [N]	5331	8558
	Femur Force - RH [N]	5331	8558
Lower Leg	Upper Tibia Fz - LH [N]	4235	5577
	Upper Tibia Fz - RH [N]	4235	5577
	Lower Tibia Fz - LH [N]	3573	5861
	Lower Tibia Fz - RH [N]	3573	5861
	Upper Tibia resultant Moment - LH [Nm]	178	240
	Upper Tibia resultant Moment - RH [Nm]	178	240
	Lower Tibia resultant Moment - LH [Nm]	178	240
	Lower Tibia resultant Moment - RH [Nm]	178	240

Upper and lower injury criteria boundaries and a potential 5-star rating scale that relates the crashworthiness total point score are based on a “request for comments” document that discussed potential updates to the New Car Assessment Program (NCAP).<sup>4</sup>

A point system was used, with a total of 100 points, resulting from a maximum of 25 points for each of the four body regions (head, neck, chest, and legs). Injury assessment values (IAVs) below the lower boundary receive 25 points; IAVs above the upper boundary receive 0 points; and IAVs between the lower and upper boundaries are calculated using linear interpolation, according to Equation 1.

$$Score = \left[ 1 - \frac{IAV - lower\ boundary}{upper\ boundary - lower\ boundary} \right] \times 25\ points \quad (Eq. 1)$$

<sup>4</sup> NHTSA, Docket No. NHTSA-2015-0119, New Car Assessment Program, Request for comments.

For example, head injury criteria (HIC) values below 500 would be considered low risk of injury and receive 25 points; HIC values above 700 would be considered high risk of injury and receive 0 points; and a HIC value of 620 would fall between the upper and lower boundaries and would receive 10 points based on linear interpolation. Where more than one criterion is available for an individual body region (for instance, HIC and BrIC for the head), the minimum score from the available criteria was used for the given body region. A star rating ranging from 0 stars to 5 stars in ½-star increments was calculated based on the overall points using Equation 2, where FLOOR is an Excel function that rounds a given number to the nearest specified multiple.

$$\text{Star Rating} = f(\text{Overall Score}) = \text{FLOOR}\left(\frac{\text{Overall Score} + 5}{20}, 0.5\right) \quad (\text{Eq. 2})$$

The resulting star rating based on the overall point score is shown in Table 2.

**Table 2. 5 Star Rating Scale (100 Point Scale)**

<b>Lower Total Point Score (Greater than or equal to)</b>	<b>Crashworthiness Stars</b>	<b>Upper Total Point Score (Less than)</b>
0	No stars	5
5	½	10
10	1	20
20	1-½	30
30	2	40
40	2-½	50
50	3	60
60	3-½	70
70	4	80
80	4-½	90
90	5	100

The original baseline model (BM) was set up by another organization and provided by NHTSA.<sup>5</sup> It was updated to better represent occupant kinematics and injury risks, as seen in full-scale oblique impact tests. The improved model is called updated BM or baseline simulation in the remainder of this document.

The new baseline simulation showed the same overall star rating for the passenger side as a full-scale crash test conducted with the respective mid-size sedan. A higher BrIC value than in the test was observed for the driver side. Aside from BrIC, injury risk for all other body regions were

---

<sup>5</sup> Singh, H., Ganesan, V., Davies, J., Paramasuwoom, M., & Gradischnig. (2018, May). *Vehicle interior and restraints modeling development of full vehicle finite element model including vehicle interior and occupant restraints systems for occupant safety analysis using THOR dummies* (Report No. DOT HS 812 545). Washington, DC: National Highway Traffic Safety Administration. Retrieved from [https://www.nhtsa.gov/sites/nhtsa.dot.gov/files/documents/report\\_13548-edag\\_vehicle\\_interior\\_restraint\\_modeling\\_050318\\_v2.pdf](https://www.nhtsa.gov/sites/nhtsa.dot.gov/files/documents/report_13548-edag_vehicle_interior_restraint_modeling_050318_v2.pdf).

well captured. Instead of further validating the baseline model to better capture driver BrIC, it was decided to proceed as is, since BrIC in the model is between the upper and lower limits, which makes it more sensitive to changes given the rating system described above. As a result, a more conservative estimate was used. Without considering BrIC, the same star rating as in the test was captured by the baseline model for the driver as well, as shown in Figure 5. The more conservative values for BrIC were considered in the conducted repeatability and sensitivity studies.

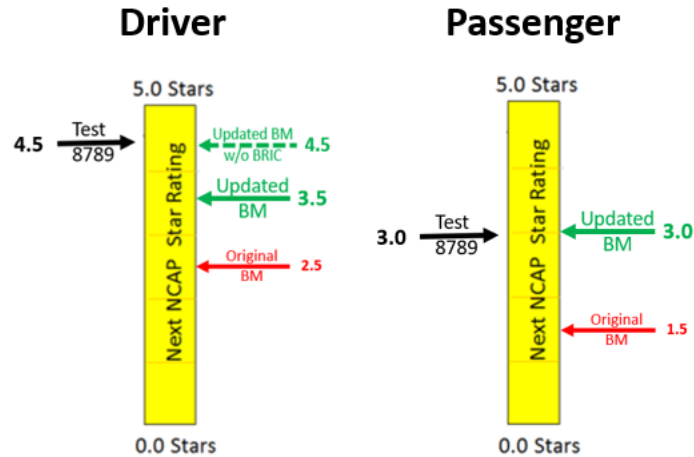


Figure 5. Overall Star Rating: (a) Driver; (b) Passenger.

Examples of time-history comparisons between simulation and available test results are shown in Figure 6 for the driver side. The baseline simulation, represented by green lines, showed realistic injury characteristics and maximum loads for all body regions for the THOR on the driver seat.

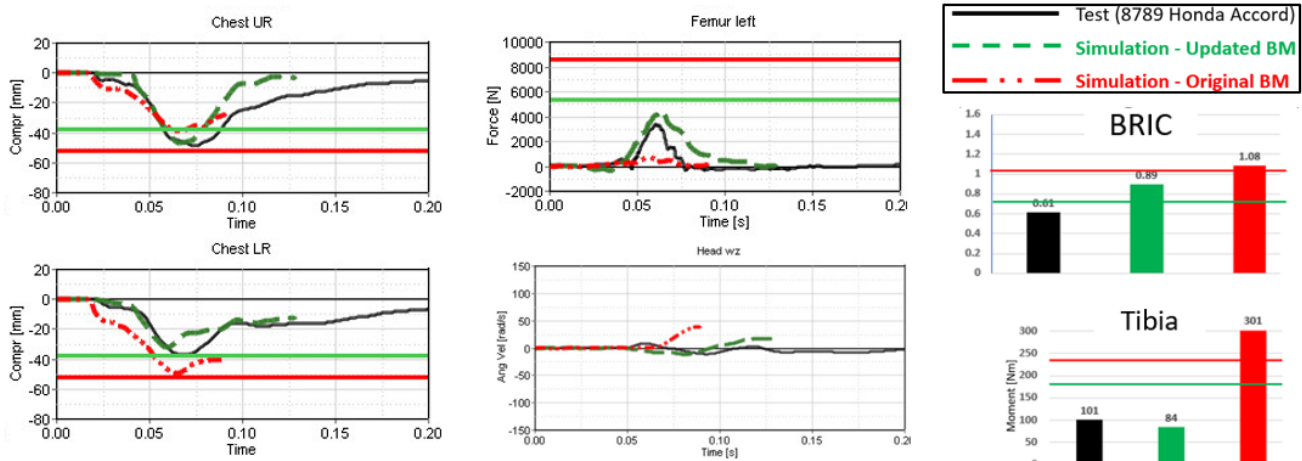


Figure 6. Test Versus Simulation – Driver.

Examples of time-history comparisons between simulation and available test results are shown in Figure 7 for the passenger side. The baseline simulation, represented by green lines, showed realistic injury characteristics and maximum loads for all body regions.

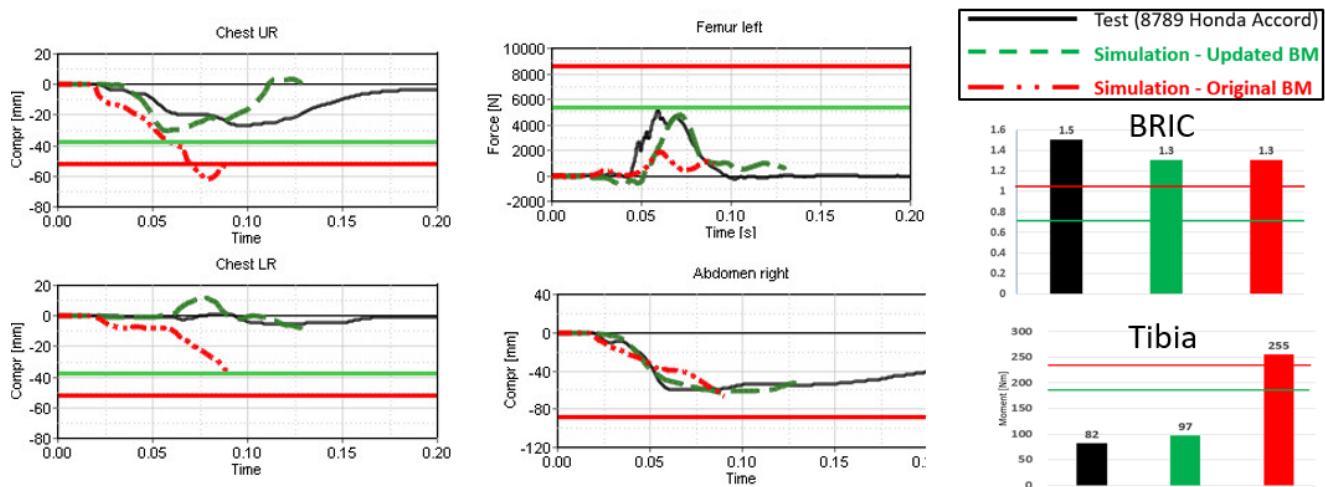
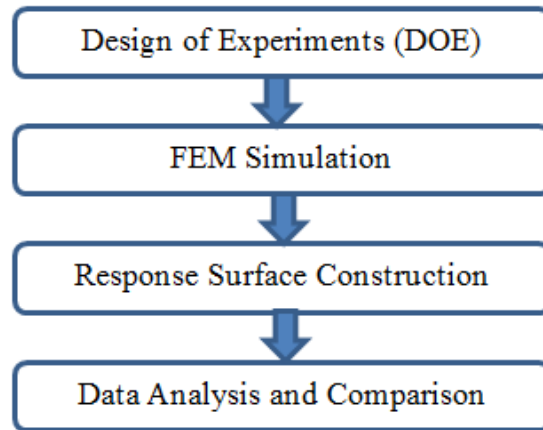


Figure 7. Test Versus Simulation – Passenger.

The baseline simulation for NHTSA’s left oblique impact condition, conducted with an FE model of a mid-size sedan vehicle with a THOR occupant in the driver and front passenger seat, was found to show realistic vehicle kinematics, vehicle pulse, occupant kinematics, and occupant injury criteria. All evaluated criteria were in a range that can be seen in many full-scale tests of sedan vehicles. It can therefore be considered a good baseline model to conduct parametric studies to understand the effect of different test configuration and THOR seating position parameters. A comparison of all vehicle and occupant criteria for test and baseline simulation can be found in **Appendix A1** and **A2**.

## 2. Methods

The flow chart of the test procedure and THOR position simulation study is shown in Figure 8. The procedure includes four main components: DoE, FE simulations, response surface (RS) construction, and data analysis and comparison. Constructed response surfaces were used in the data analysis to do the sensitivity study for each parameter and calculate the importance index for each parameter.



**Figure 8. Test Procedure Simulation Plan Flow Chart.**

## 2.1 Design of Experiments (DoE)

To evaluate the effects each parameter and the combinations of these parameters have on the outcome of the vehicle and THORs, the DoE-based method was adopted. Specifically, the Box-Behnken method was used to define the samples of the design. The Box-Behnken approach is an independent quadratic design in which the treatment combinations are at the midpoints of edges of the process space and at the center. These designs are rotatable (or near rotatable) and require three levels for each factor. An example of a Box-Behnken design for three parameters is shown in Figure 9.

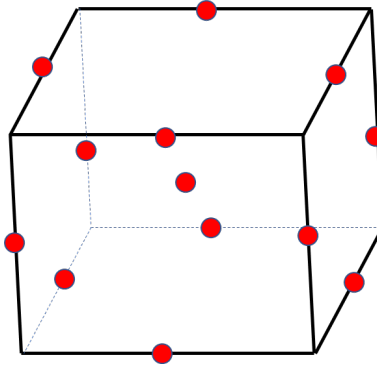


Figure 9. Box-Behnken DoE Design Example.

In the test procedure repeatability study, we have five parameters and their respective variation range was divided into three levels, as listed in Table 3.

Table 3. Repeatability Study – Parameter Ranges and Levels

Parameters	Levels		
	0	1	2
Impact angle (degree)	14	15	16
Horizontal misalignment Y direction (mm)	-50	0	50
Vertical misalignment Z direction (mm)	-50	0	50
OMDB mass [kg]	-50	0	50
Impact speed (km/h)	89	90	91

## 2.2 Response Surface Construction

Response surfaces, also called surrogate models, approximate models, or machine learning models, are used to estimate the representation of the real objective function, which is unknown. Thus, the obtained response surface can be used for the prediction of the objective function. There are many different types of response surface models, such as linear surface, polynomial surface, radial basis function model, Kriging model, support vector machine model, and neural network model. In the present study, the open source python machine learning library “scikit-learn” was used to build the response surface.

To consider the influences of parameters on the responses of the vehicle and THORs, toe-pan intrusion, change in velocity, occupant head kinematics, injury criteria, and occupant kinematics relative to seat belt and air bag were analyzed. A set of response surfaces were constructed based on the data obtained from the FE simulations.

During the procedure of the response surface construction, two main types of models were used: second order polynomials and support vector machine regression models. K-fold cross-validation strategy was adopted to optimize the response surface for each parameter and combination of parameters. Cross-validation is a resampling procedure used to evaluate response surface models on a limited data sample. The procedure has a single parameter, called  $k$ , that refers to the number of groups that a given data sample is to be split into. As such, the procedure is often called  $k$ -fold cross-validation. When a specific value for  $k$  is chosen, it may be used in place of  $k$  in the reference to the model, such as  $k=5$  becoming 5-fold cross-validation.

The general procedure for the  $k$ -fold cross-validation is conducted in four steps. (1) The dataset is randomly shuffled. (2) The dataset is split into  $k$  groups. (3) For each group (a) use the group as a hold out or test data set, (b) take the remaining groups as a training data set, (c) fit a response surface model on the training set and evaluate it using the test set, (d) obtain the evaluation score or predict value and discard the model. (4) Summarize the skill of the model using the sample of the model evaluation scores or predict values.

If the obtained model is accurate enough according to the cross-validation scores, the model is kept and used in the data analysis stage. Otherwise, the model is discarded, and different models are tried.

## 2.3 Data Analysis and Comparison

In the stage of data analysis, comparisons are conducted of responses for each parameter, with varied ranges between baseline results and simulation cases. Figure 10 shows an example of response curves obtained from variation of single design factors. Parameters are evaluated one at a time, keeping the other values at the baseline value. For instance, the yellow line represents the effect of the impact speed on the BrIC value, when keeping all other parameters at the mid-level.

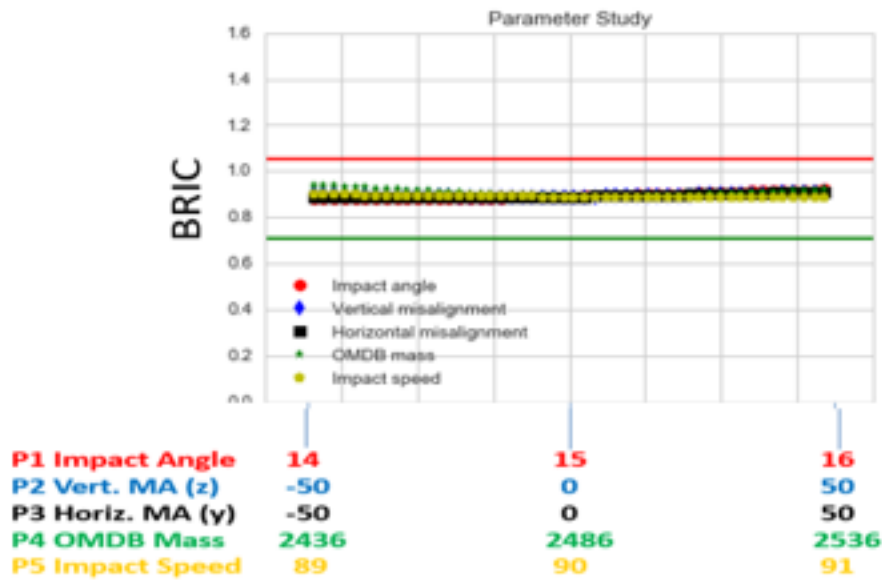
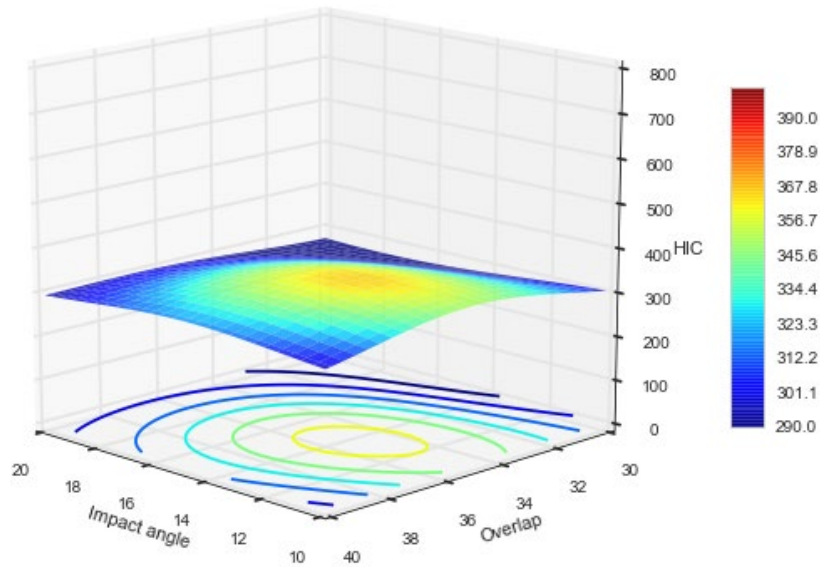


Figure 10. An Example of Variation of Single Parameter.

Figure 11 shows an example of the response surface obtained from variation of two design factors. The 3-dimensional response surface shows the combined effect of OMDB to vehicle overlap percentage and impact angle on the head injury criteria (HIC).



**Figure 11. 3-Dimensional RS Example obtained from the Variation of 2 Parameters.**

In addition, the ANOVA method<sup>6</sup> and other sensitivity analysis methods<sup>7</sup> are used to quantify the importance of each parameter based on the response surfaces. In the present study, an open source sensitivity analysis library, SALib, was used for implementation of the sensitivity analysis. An example of the parameter importance index is shown in Figure 12.

<sup>6</sup> Kim, H. Y., Jeong, S. K., Yang, C., & Noblesse, F. (2011). *Hull form design exploration based on response surface method*. In 21st International Society of Offshore and Polar Engineering Conference, Maui, HA.

<sup>7</sup> Saltelli, A., Tarantola, S., & Chan, K. P.-S. (1999). A quantitative model-independent method for global sensitivity analysis of model output. *Technometrics*, 41(1).

## Parameter Importance Index

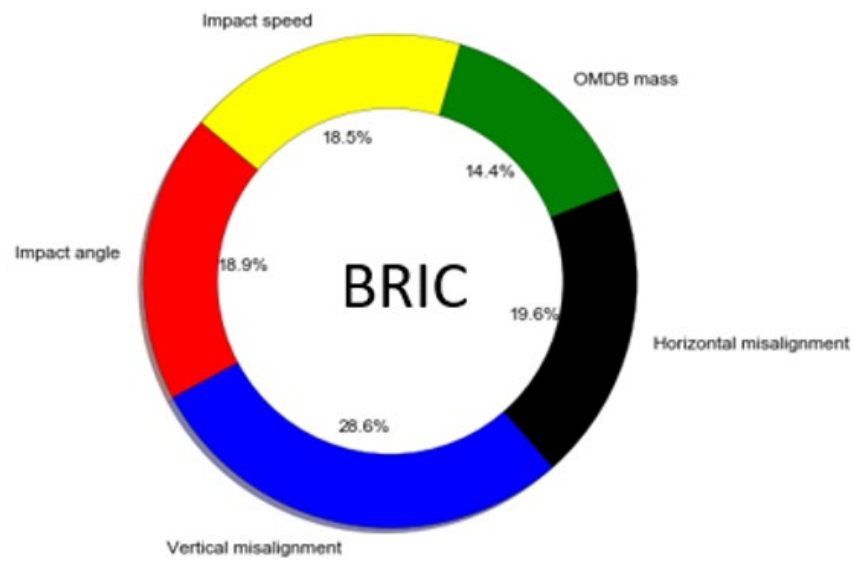
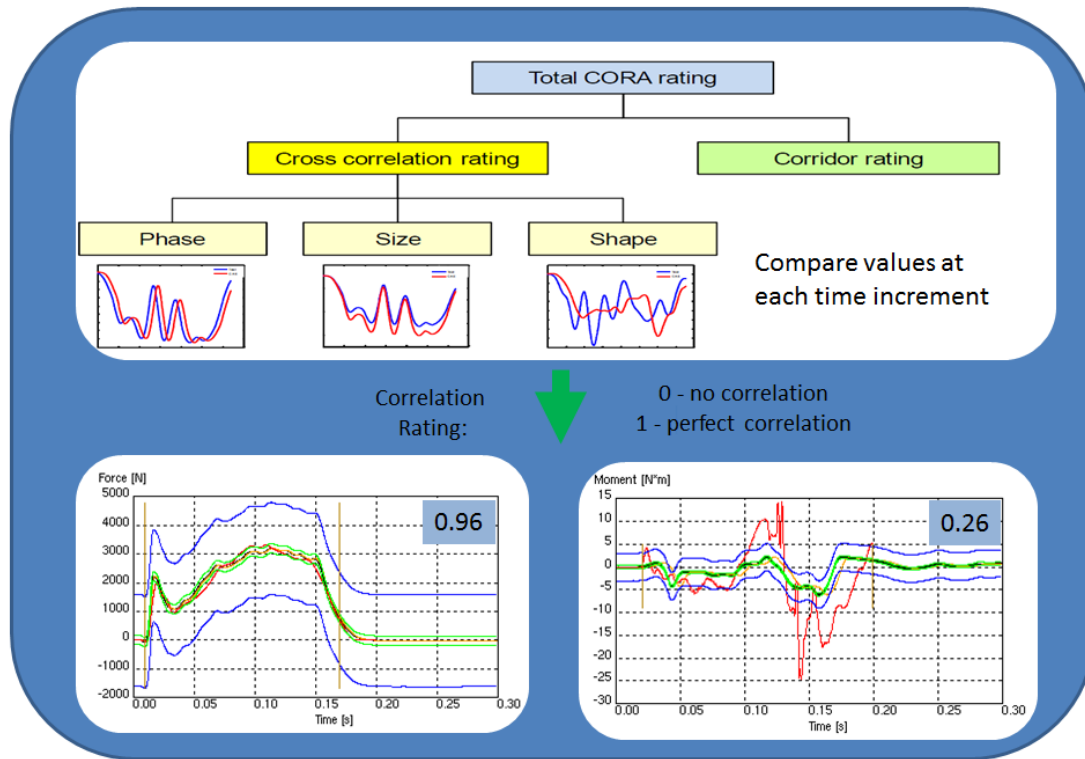


Figure 12. An Example of Parameter Importance Index Obtained From ANOVA.

## 2.4 CORA – Objective Correlation Method

The objective curve correlation rating tool CORA (CORrelation and Analysis)<sup>8</sup> was used to quantify differences in time history results between select parametric cases and the baseline simulation. The CORA tool was developed by the Partnership for Dummy Technology and Biomechanics (PDB) and takes phase shift, size, shape, as well as the comparison of values at each time increment, into account. Using these criteria, an "objective rating" is given that indicates how well a curve (e.g., parametric simulation) compares to a reference curve (e.g., baseline simulation). Rating results range between 0 and 1, where 0 means no correlation and 1 means (close to) perfect correlation.

Figure 13 shows the CORA comparison and rating process. Two general examples of curve comparisons are shown at the bottom. Inner and outer corridors are depicted in green and blue, respectively. The example on the right shows a reference result in black and a simulation curve in red. A correlation rating of 0.26 was given by CORA, and therefore the correlation can be judged as poor. The example on the left shows an example where test in black and simulation in red correlate very well and a close-to-perfect rating of 0.96 was given. For the current study, a CORA value above 0.8 was considered “GOOD” and values between 0.6 and 0.8 was considered “FAIR” or ACCEPTABLE.” The used rating scheme is adopted from ISO.<sup>9</sup>



**Figure 13. CORA – Objective Correlation Rating Methodology.**

<sup>8</sup> Thunert, C. (2017). CORAplus User's Manual, Version 4.0.4. Gaimersheim, Germany: Partnership for Dummy Technology and Biomechanics.

<sup>9</sup> International Organization for Standardization. (2013). Road vehicles — Objective rating metric for non-ambiguous signals, ISO 18571. Geneva: Author.

### 3. Test Procedure Repeatability Study

#### 3.1 Parameters and Ranges

For the test procedure repeatability study, parameters were varied within defined test tolerances, as shown in Figure 14. The OMDB impact angle was varied by +/- 1 degree, i.e., between 14 and 16 degrees relative to the vehicle longitudinal centerline. The vertical position (z) of the OMDB was evaluated at level to the vehicle and 50 mm higher and lower relative to the target vehicle. A range of +/- 50 mm was also used for the horizontal misalignment of the OMDB. This represents an overlap of 33 percent and 38 percent compared to the 35 percent overlap of the OMDB with the target vehicle in the baseline simulation. The OMDB mass was varied by +/- 50 kg. An additional study was conducted to evaluate the influence of having an OMDB with small differences of moments of inertia. Finally, the impact speed was evaluated for a range of +/- 1 km/h.

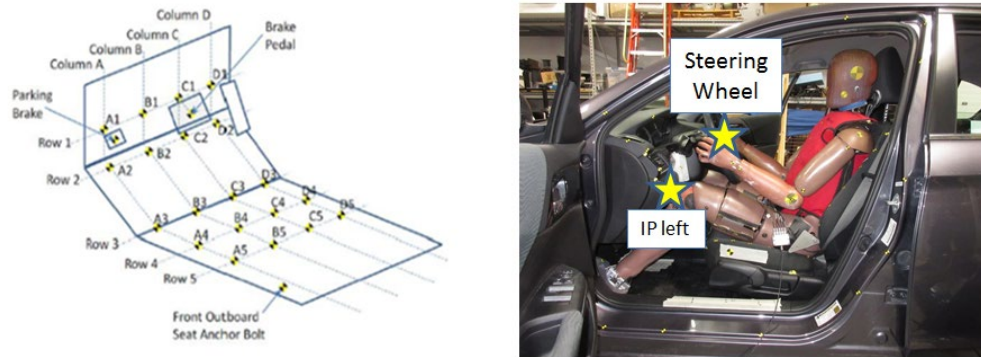
Parameter	Range			
Impact angle [degree]	14	15	16	Baseline
Vertical Misalign. [mm] (Overlap)	-50 (33%)	0 (35%)	50 (38%)	
Horizontal misalignment [mm]	-50	0	50	Within current test tolerance
OMDB Mass [kg]	-50	2486	+50	
Impact speed [km/h]	89	90	91	

Figure 14. Repeatability Study Parameters and Ranges.

Using a Box-Behnken DoE method with five parameters and three levels, 41 simulations were run to determine the effect and importance of the different parameters. The simulation matrix can be found in **Appendix A3**.

### 3.2 Results – Vehicle

An accelerometer was placed at the far-side rear sill to record the vehicle pulse during the impact. Intrusion into the occupant compartment was recorded at the brake pedal and at 5 rows with 4 points each on the toe-pan, as shown in Figure 15 (a). Intrusions were also evaluated for the Steering Column and the left and right Instrument Panel (IP), as shown in Figure 15 (b). Deformation in the longitudinal vehicle x-direction was the dominant component and was used to compare occupant compartment intrusions.



**Figure 15. (a) Toe-pan; (b) IP and Steering Intrusion Measurement Points.**

Impact speed was found to be the most important parameter for the vehicle x-pulse, represented by a 46 percent parameter importance index, as shown in Figure 16 (a). Higher impact speed tended to show marginally higher delta-v in longitudinal vehicle direction, as shown in Figure 16 (b). Values ranged from 14.5 m/s to 15.1 m/s. Varying parameters within the test tolerance showed good test repeatability with little effect on the vehicle x-pulse.

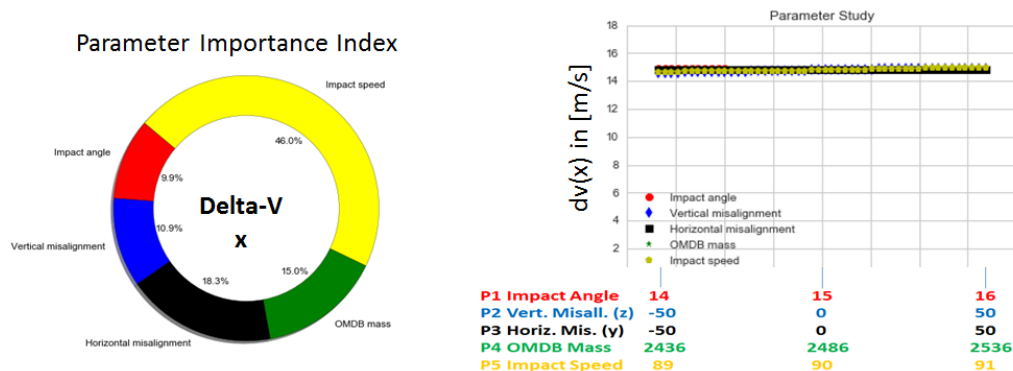


**Figure 16. Vehicle x-Pulse: (a) Parameter Importance Index; (b) Effect of Parameters.**

Impact angle was found to be the most significant parameter for the vehicle y-pulse, represented by a 49 percent importance index, as shown in Figure 17 (a). Larger impact angle, i.e., more oblique configuration, tended to show marginally higher delta-v in vehicle y-direction, as shown in Figure 17 (b). Values ranged from 5.6 m/s to 6.2 m/s, as shown in **Appendix A4**. Varying

parameters within the test tolerance showed good test repeatability with little effect on the vehicle y-pulse.

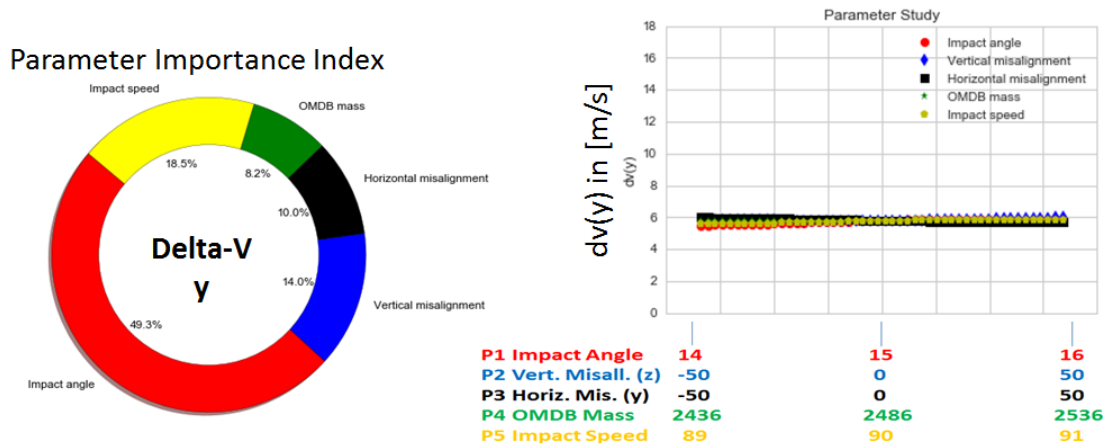


Figure 17. Vehicle y-Pulse: (a) Parameter Importance Index; (b) Effect of Parameters.

Horizontal misalignment was found to be the most significant parameter for the maximum toe-pan intrusion, represented by a 26 percent importance index, as shown in Figure 18 (a). A value of +50 mm represents a larger overlap (38%) compared to the baseline model (35%). More overlap tended to show lower maximum toe-pan intrusion, as shown in Figure 18 (b). Maximum values ranged from 128 mm to 157 mm. Varying parameters within the test tolerance showed good test repeatability with little effect on the occupant compartment intrusions. It can also be noticed that a more oblique impact angle, higher OMDB mass, and higher impact speed caused marginally higher occupant compartment intrusions.

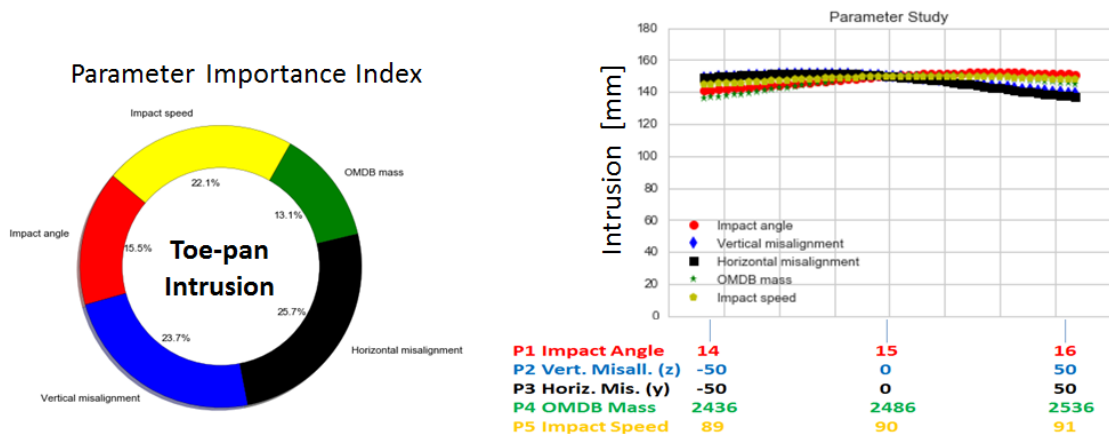
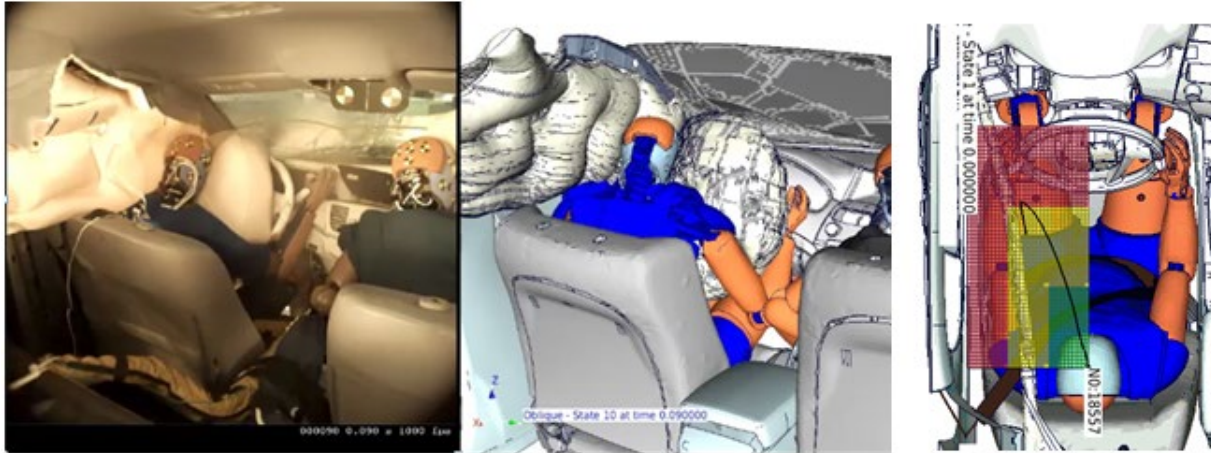


Figure 18. Maximum Toe-Pan Intrusion: (a) Importance Index; (b) Effect of Parameters.

Respective points at the toe-pan and instrument panel were also evaluated on the far-side occupant compartment, relevant for the front passenger seating position. Maximum intrusion was considerably smaller than for the near-side. Differences when varying parameters within test tolerances were not significant, ranging from 14 mm to 25 mm, as shown in **Appendix A5**.

### 3.3 Results – Driver

The effect of varying parameters within defined full-scale test tolerances (repeatability study) was evaluated by analyzing occupant kinematics and injury metrics for a 50 percent THOR in the driver seat. Figure 19 (a) shows the typical near-side occupant kinematics in test and simulation. The THOR moves towards the A-pillar and is being restrained by the seat belt, driver air bag and side curtain air bag. Figure 19 (b) shows an example of the trajectory of the head center of gravity. Head movement ranged from 396 mm to 408 mm in x-direction and from 167 mm to 188 mm in y-direction.



**Figure 19. Passenger Kinematics: (a) Test and Simulation; (b) Head Trajectory.**

Injury risk was analyzed using upper and lower boundaries, as defined in **Appendix A6**. For example, maximum chest deflection values below 37.9 mm would be considered low risk of injury and no points for the overall rating would be deducted. Chest deflection values above 52.3 mm would be considered high risk of injury and 0 points would be given for the chest. Linear interpolation is used to calculate the amount of points for chest values between the lower and upper boundary. A total of 100 points can be achieved, resulting from the maximum 25 points for each of the body regions, head, neck, chest, and lower extremities. A star rating was calculated based on the overall points.

Vertical misalignment (MA) was the most important parameter for the overall injury risk, represented by a 31 percent index, as shown in Figure 20 (a). Higher OMDB position tended to show more points, i.e., lower overall injury risk, as shown in Figure 20 (b). Overall points, when using all combinations of parameters, ranged from 54 (3 stars) to 70 (3.5 stars). Figure 20 (c) shows an example of a 3-dimensional response surface visualizing the effect of horizontal misalignment and impact speed, which illustrates that the combination of smaller overlap (i.e., 33 percent overlap compared to 35 percent for the baseline simulation) and higher impact speed was the most critical (i.e., least amount of points) with respect to overall injury risk.

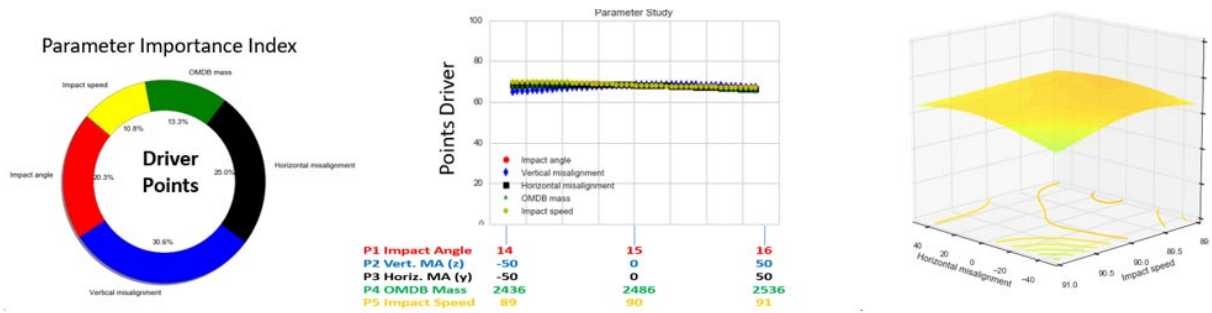


Figure 20. Driver Points: (a) Importance Index; (b) Effect of Parameters; (c) RS Example.

Vertical misalignment (MA), impact angle, and impact velocity were the most important parameters, represented by a 24 percent to 30 percent index for the driver BrIC, as shown in Figure 21 (a). BrIC ranged from 0.85 to 0.96, where higher values were associated with higher pitch component, i.e., higher angular head velocity around the local y-axis. The effect on BrIC was small, yet noticeable when taking all combinations of parameters into account. Figure 21 (c) depicts the 3-dimensional response surface for the impact angle and vertical misalignment, showing that a more oblique impact configuration and higher OMDB position tended to show higher driver BrIC values. The influence for each individual parameter was small, when keeping the other parameters at the baseline simulation value, as shown in Figure 21 (b).

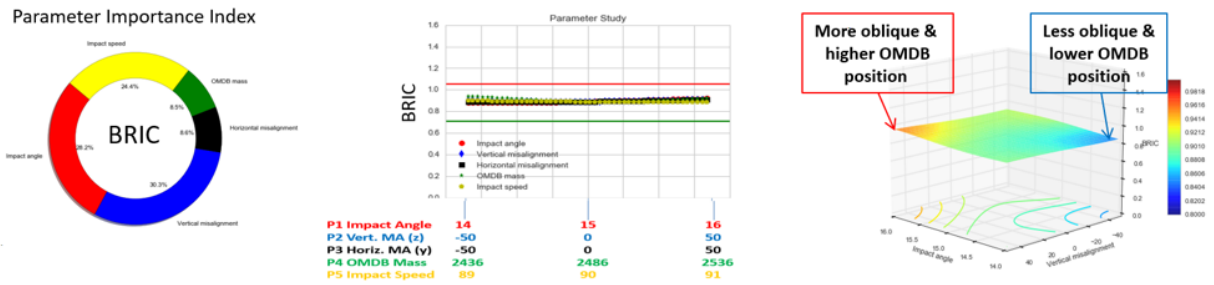
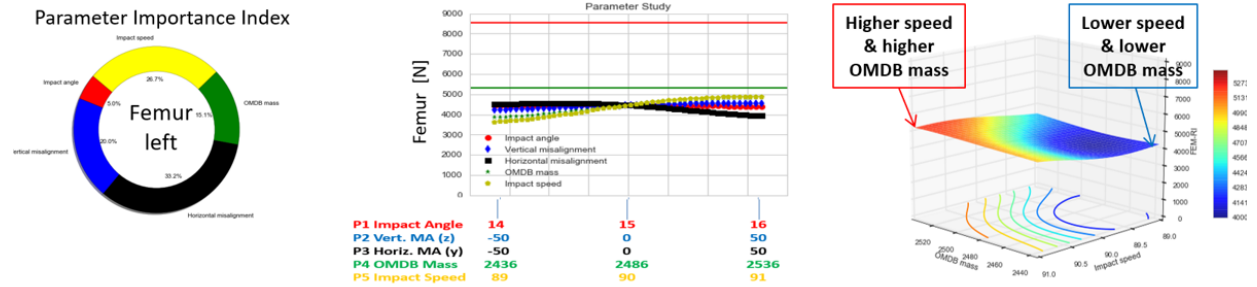


Figure 21. Driver BrIC: (a) Importance Index; (b) Effect of Parameters; (c) RS Example.

Impact speed was found to be the most important factor for the maximum chest deflection, which occurred at the upper right measurement point for the THOR in the driver seat due to interaction with the seat belt. Higher impact velocity correlated with higher chest deflection, where differences were small, ranging from 47 mm to 49 mm.

Horizontal misalignment was the most important factor for the left femur load of the driver, as shown in Figure 22 (a). Less overlap tended to show higher femur loads. Higher impact velocity and higher OMDB mass also correlated with higher femur loads, as shown in Figure 22 (b). When taking all combinations of parameters into account, values for the maximum femur load ranged from 3,421 N to 5,324 N. Figure 22 (c) shows an example of a 3-dimensional response surface for the parameters OMDB mass and impact speed. It can be noticed that higher speed and higher OMDB mass clearly correlate with higher femur loads.



**Figure 22. Driver Femur: (a) Importance Index; (b) Effect of Parameters; (c) RS Example.**

Time history data compared well between simulations with varying parameters and the baseline simulation, represented by overall CORA scores of 0.85 to 0.96 for all simulations.

### 3.4 Results – Passenger

The effect of varying parameters within defined test tolerances (repeatability study) was evaluated by analyzing occupant kinematics and injury metrics for a 50 percent THOR in the passenger seat. Figure 23 (a) shows the typical far-side occupant kinematics in test and simulation. The THOR moves towards the middle of the vehicle, sliding out of the seat belt, which slips over the shoulder and down on the upper right arm, resulting in little interaction between shoulder-belt and chest. Since there is no head curtain air bag in the middle of the vehicle and most current passenger air bags are not capable of controlling the head motion in a far-side oblique impact condition, higher angular velocities of the head can be observed. Significant head yaw motion, i.e., high angular velocity around the local z-axis of the head, lead to high BrIC values in many cases. Figure 23 (b) shows an example of the trajectory of the head center of gravity. It can be noticed that head motion is larger in both x- and y-directions, when compare to the near-side occupant on the driver side.

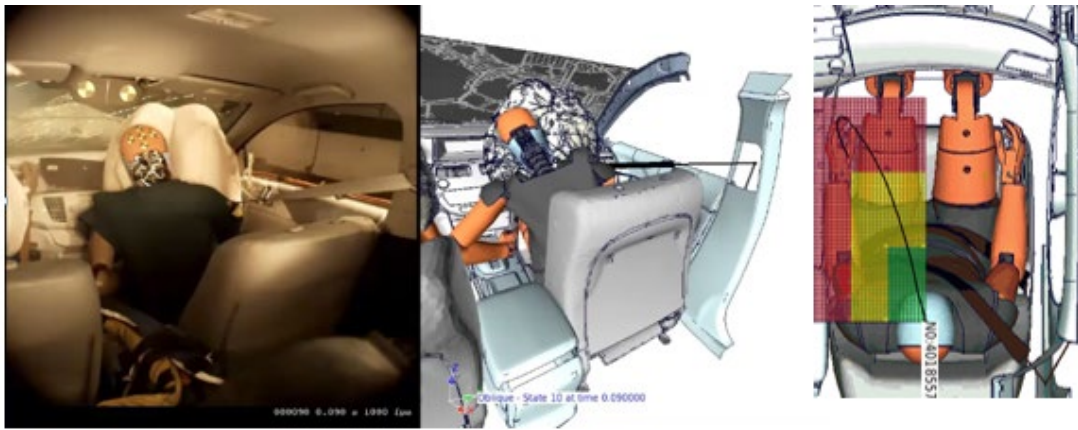


**Figure 23. Passenger Kinematics: (a) Test and Simulation; (b) Head Trajectory.**

Injury risk was analyzed using upper and lower boundaries, as defined in **Appendix A7**. HIC values below 500 would be considered low risk of injury and no points for the overall rating would be deducted. HIC values above 700 would be considered high risk of injury and 0 points would be given for the Head. Linear interpolation is used to calculate the amount of points for HIC values between the lower and upper boundary. A total of 100 points can be achieved, resulting from the maximum 25 points for each of the body regions, head, neck, chest, and lower extremities. A star rating was calculated based on the overall points, ranging from 0 stars for 4 or less points to 5 stars for 90 or more points.

Impact speed was the most important parameter, represented by a 27 percent index, as shown in Figure 24 (a). Lower impact speed tended to show more points, i.e., lower overall injury risk, as shown in Figure 24 (b). Overall points, when using all combination of parameters, ranged from 40 (2.5 stars) to 67 (3.5 stars). Figure 24 (c) shows an example of a 3-dimensional response surface visualizing the effect of vertical misalignment and impact speed. It can be noticed that the combination of lower OMDB position and higher impact speed was the most critical (i.e., least amount of points) with respect to overall injury risk.

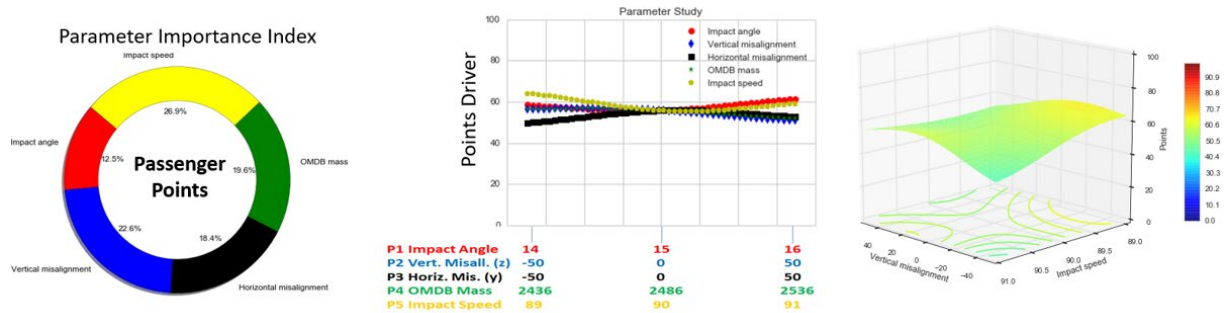


Figure 24. Passenger Points: (a) Importance Index; (b) Effect of Param; (c) RS Example.

BrIC values were above the upper limit, resulting in 0 points for the head. Maximum chest deflection values were lower than for the driver due to the limited interaction with the shoulder-belt. They ranged from 37 mm to 41 mm. Overall rating was therefore mostly influenced by varying neck and lower extremity criteria. Neck values varied noticeably due to different head motion, which is less controlled by restraints compared to the driver. Lower extremities also showed a significant difference, ranging from 6 to 23 points. It was found that differences in overall occupant kinematics for the far-side passenger, i.e., larger amount of head and upper body motion, contributed to these observations. Overall kinematics were larger than for the near-side occupant, since restraints are less capable of controlling the far-side THOR in the oblique impact configuration. On the other hand, occupant compartment intrusions were small with little variation and can be considered not significant with respect to the lower extremity injury criteria evaluated.

All five evaluated parameters were of similar importance for BrIC. Vertical misalignment was found to have the highest (27%) and OMDB mass the lowest (14%) index, as shown in Figure 25 (a). In contrast to the near-side driver seating position, small changes in parameters resulted in noticeable differences in BrIC, as shown in Figure 25 (b). All values were above the upper limit, ranging from 1.11 to 1.57. Higher impact speed and lower OMDB vertical position correlated with higher BrIC values. The results also indicate the lower OMDB mass tended to produce higher BrIC values, mainly due to higher angular head velocities around the local x-axis (pitch) and z-axis (yaw).

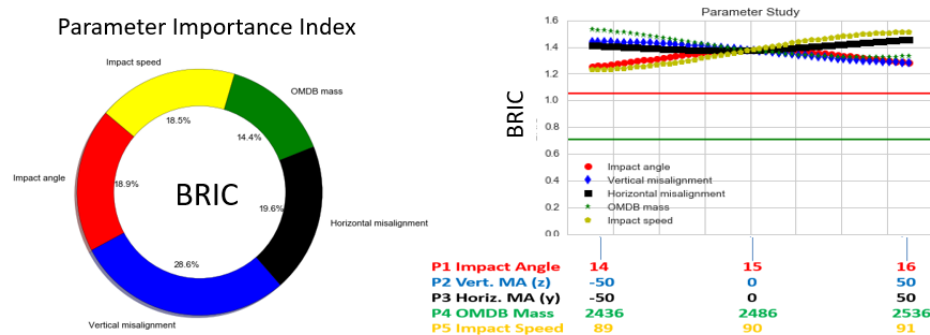


Figure 25. Passenger BrIC: (a) Importance Index; (b) Effect of Parameters.

Vertical misalignment was found to be the most important factor (44%) for the maximum chest deflection, as shown in Figure 26 (a). Highest values occurred at the lower left measurement point for the THOR in the passenger seat, since there was limited interaction between the upper torso and the shoulder-belt due to the observed kinematics of the far-side occupant. Differences were small, ranging from 37 mm to 41 mm, when taking all combinations of parameters into account. No significant trend was observed for any of the parameters when evaluating the effect of individual parameters while keeping the others at the baseline simulation value, as shown in Figure 26 (b).

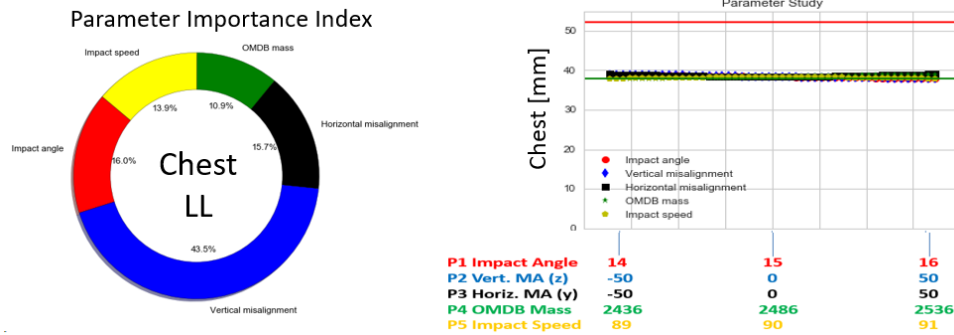


Figure 26. Passenger Chest: (a) Importance Index; (b) Effect of Parameters.

Impact speed was the most important factor for the passenger femur forces, represented by a 42 percent index, as shown in Figure 27 (a). Values ranged from 3,847 N to 5,623 N, when taking all combinations of parameters into account. Higher impact speed, higher OMDB mass, and larger overlap percentage correlated with higher femur loads, as shown in Figure 27 (b).

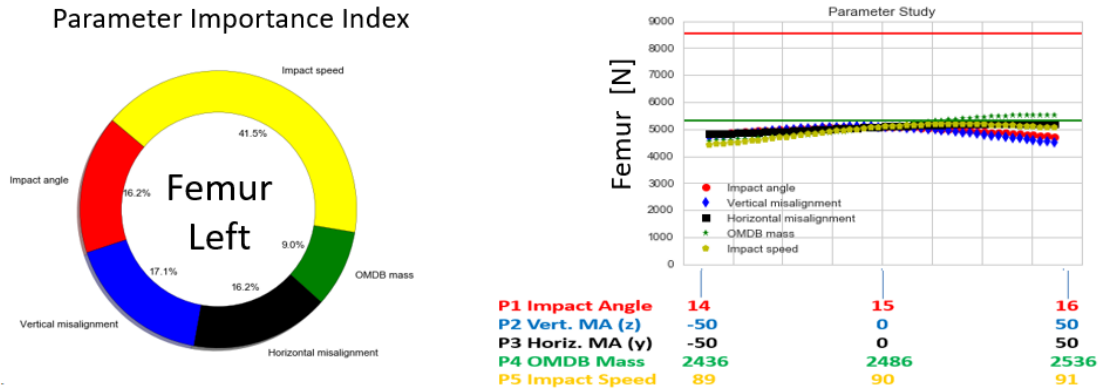
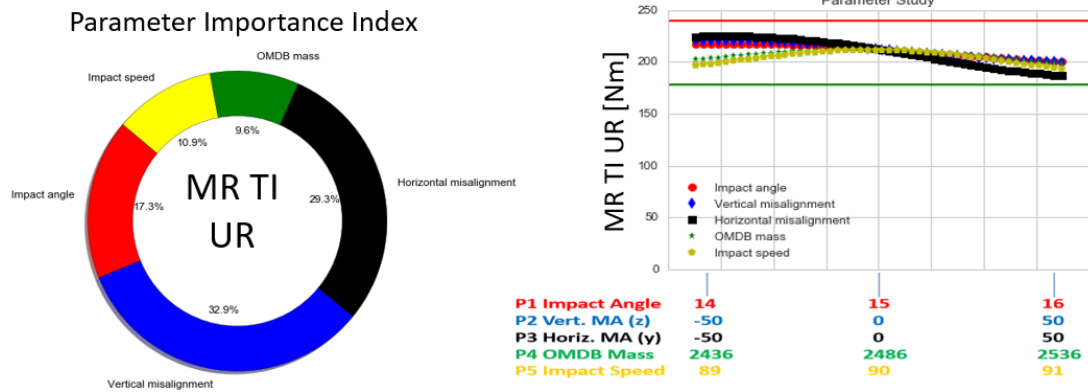


Figure 27. Passenger Femur: (a) Importance Index; (b) Effect of Parameters.

Vertical and horizontal misalignment were the most important parameters for the maximum resultant moment of the tibia, with 33 percent and 29 percent, respectively, as shown in Figure 28 (a). The values ranged from 174 Nm to 231 Nm, when taking all combinations of parameters into account.



**Figure 28. Passenger Tibia: (a) Importance Index; (b) Effect of Parameters.**

The observed variations in lower extremity injury risk was caused by differences in overall far-side occupant kinematics rather than toe-pan intrusion, which was small. Higher maximum moments of the upper right tibia correlated with lower OMDB vertical position, smaller overlap percentage, and less oblique impact angle. No clear trend could be observed for impact speed and OMDB mass, as shown in Figure 27 (b).

In addition to evaluating the effect of different OMDB masses with +/- 50 kg of the baseline weight, different moments of inertias, based on measurements provided by Calspan and Karco, were evaluated. Little effect on either vehicle or occupant responses was observed for values within typical tolerances.

## 4. Test Procedure Sensitivity Study

### 4.1 Evaluated Parameters and Ranges

A Sensitivity Study was conducted, where parameters were varied beyond full-scale test tolerances to understand how vehicle characteristics, occupant kinematics, and injury risks of the driver and front passenger are affected by a wider range of impact conditions. The impact angle was changed by  $\pm 5^\circ$  relative to the  $15^\circ$  baseline value, resulting in impact angles between  $10^\circ$  and  $20^\circ$ . The overlap percentage was varied by  $\pm 5$  percent compared to the 35 percent baseline value, resulting in a range of 30 percent to 40 percent overlap of the OMDB and the target vehicle. The OMDB mass was evaluated for a range between 2,000 kg and 2,500 kg. A value of 2,250 kg was chosen as the mid-level for the conducted DoE analysis. The impact speed was evaluated for a range between 80 km/h and 90 km/h, with 85 km/h being the mid-level for the DoE analysis. Parameters and ranges are summarized in Figure 29.

Parameter	Range				
Impact angle [degree]		10	15	20	Baseline
Overlap [%]		30	35	40	
OMDB Mass [kg]	2000	2250	2500		Beyond current test tolerance
Impact speed [km/h]	80	85	90		

**Figure 29. Sensitivity Study – Parameters and Ranges.**

Using a Box-Behnken DoE method with four parameters and three levels, a total of 25 simulations were run to determine their relative importance and the effect each parameter and combinations of parameters have on the vehicle and occupants seated in the driver and front passenger seat. The simulation matrix can be found in **Appendix A8**.

Figure 30 shows a top view of the configuration for two extreme cases. The OMDB shown in green represents a case where the barrier was positioned at a  $10^\circ$  angle, having a 40 percent overlap relative to the target vehicle. The OMDB shown in red represents a case where the barrier was positioned at a  $20^\circ$  angle, having a 30 percent overlap relative to the target vehicle.

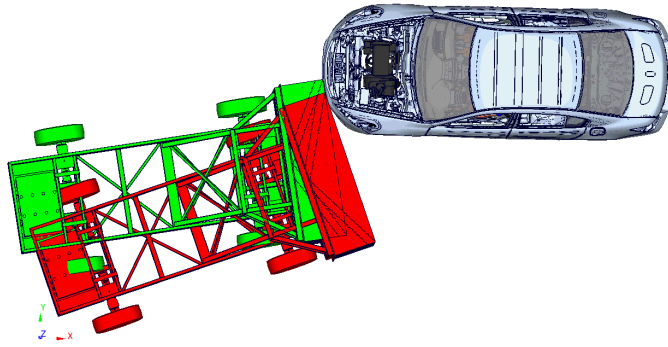


**Figure 30. Sensitivity Study – Extreme Cases.**

## 4.2 Results – Vehicle

Impact speed and OMDB mass were found to be the most important parameters for the vehicle x-pulse, represented by a 46 percent and 41 percent index, respectively, as shown in Figure 31 (a). Higher impact speed and higher OMDB mass tended to show higher delta-v in longitudinal vehicle direction, as shown in Figure 31 (b). Values ranged from 11.8 m/s to 14.8 m/s when taking all combinations of parameters into account. Figure 31 (c) shows an example of a 3-dimensional response surface for the parameters OMDB mass and overlap percentage. It can be noticed that a larger overlap and higher OMDB mass correlate with a more severe vehicle x-pulse. Results for all simulations can be found in **Appendix A9**.

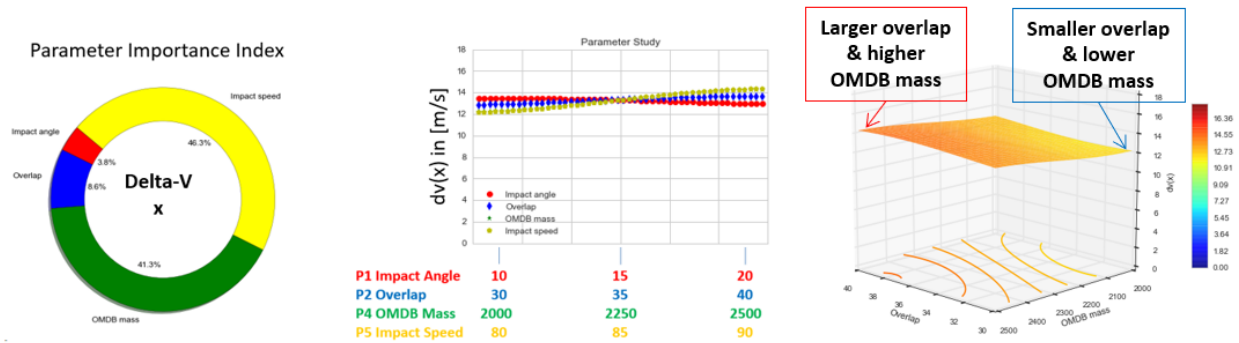


**Figure 31. Vehicle x-Pulse: (a) Importance Index; (b) Effect of Parameters; (c) RS Example.**

Impact angle was found to be the most significant parameter for the vehicle y-pulse, represented by a 64 percent index, as shown in Figure 32 (a). Larger impact angle, i.e., more oblique configuration, showed higher delta-v in vehicle y-direction, as shown in Figure 32 (b). Values ranged from 4.2 m/s to 6.4 m/s. Figure 32 (c) shows the effect of impact angle and impact speed. A more oblique impact at higher speed showed the highest delta-v in vehicle y-direction and vice versa.

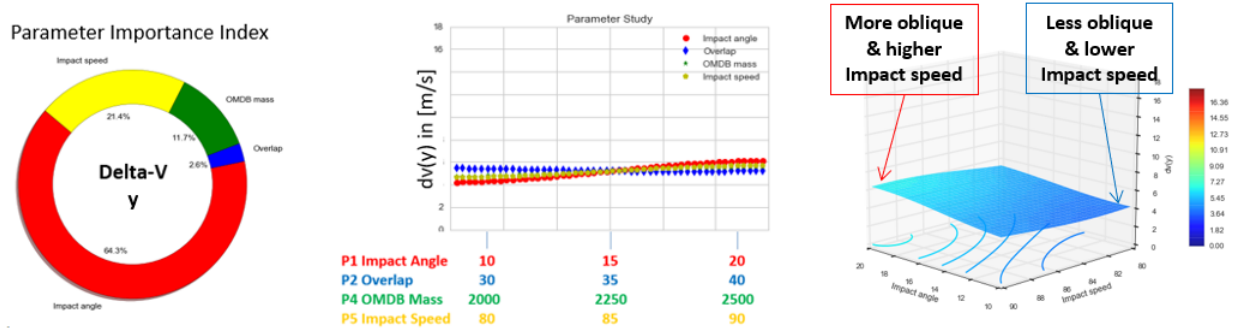


**Figure 32. Vehicle y-Pulse: (a) Importance Index; (b) Effect of Parameters; (c) RS Example.**

Impact speed was found to be the most significant parameter for the maximum toe-pan intrusion, represented by a 62 percent importance index, as shown in Figure 33 (a). Higher OMDB speed and higher mass correlated with higher maximum toe-pan intrusion, as shown in Figure 33 (b). More oblique configurations and more overlap tended to show marginally lower maximum

intrusions. Values ranged from 91 mm to 150 mm, when all combinations of parameters are considered, as listed in **Appendix A9**. Figure 33 (c) visualizes the significant difference in occupant compartment intrusion for the parameters impact speed and OMDB mass.

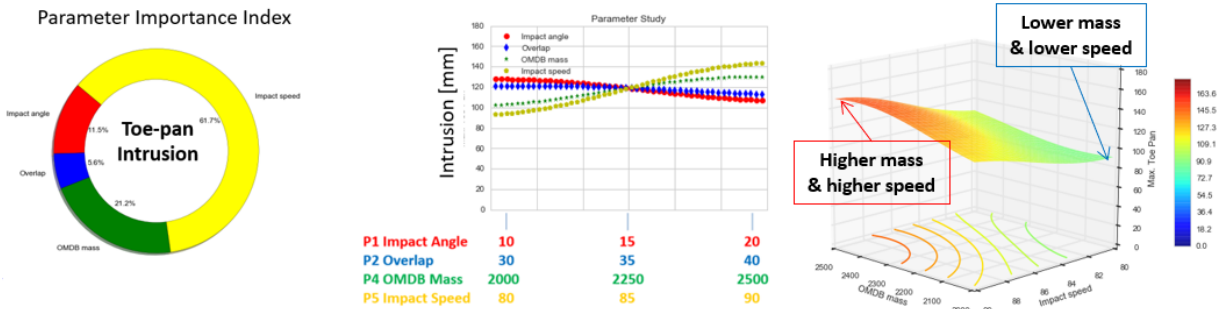


**Figure 33. Toe-Pan Intrusion: (a) Importance Index; (b) Effect of Parameters; (c) RS Example.**

Respective points at the toe-pan and instrument panel were evaluated on the far-side occupant compartment, relevant for the front passenger seating position. Maximum intrusion was considerably smaller than for the near-side. Differences were not significant, ranging from 4 mm to 20 mm, as shown in **Appendix A10**.

### 4.3 Results – Driver

In the Sensitivity Study,” the effect of varying parameters within a wider range compared to full-scale test tolerances was examined. Occupant kinematics and injury metrics for a 50 percent THOR in the driver seat were analyzed. Figure 34 (a) shows the head trajectory of the simulation with the lowest head excursion in y-direction. Figure 34 (b) shows the head trajectory of the simulation with the largest head excursion in y-direction. The differences of THOR movement towards the A-pillar was more significant than for the cases studied in the repeatability study. At the same time, the near-side occupant was well restrained by the seat belt, driver air bag, and side curtain air bag for all analyzed cases and no contact with the A-pillar or other interior parts of the vehicle was observed.

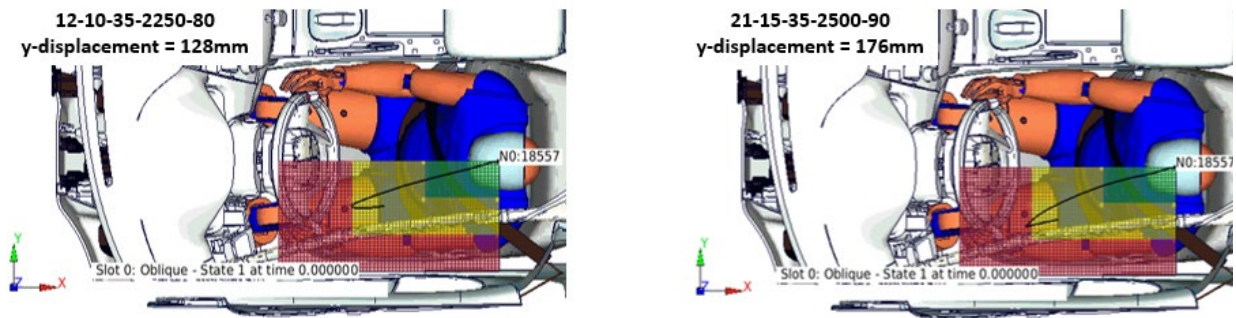
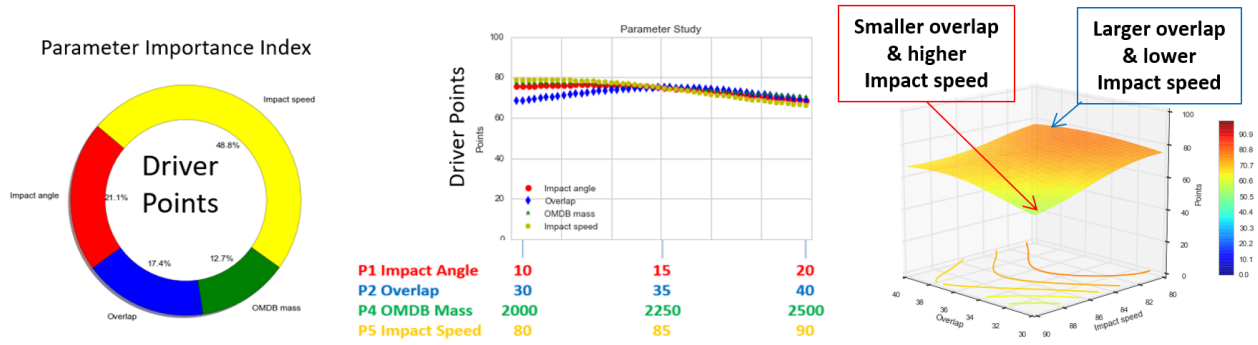


Figure 34. Driver Head y-Displacement: (a) Lowest; (b) Highest.

Injury risk was analyzed using upper and lower boundaries, as defined in **Appendix A11**. For example, maximum femur load values below 5331 N would be considered low risk of injury and no points for the overall rating would be deducted. Femur load values above 8558 N would be considered high risk of injury and 0 points would be given for the Femur. Linear interpolation is used to calculate the amount of points for femur values between the lower and upper boundary. A total of 100 points can be achieved, resulting from the maximum 25 points for each of the body regions, head, neck, chest, and legs. A star rating was calculated based on the overall points, ranging from 0 stars for 4 or less points to 5 stars for 90 or more points.

Impact speed was the most important parameter, represented by a 49 percent index, as shown in Figure 35 (a). Higher impact speed showed less points, i.e., higher overall injury risk, as shown in Figure 35 (b). Overall points, when using all combination of parameters, ranged from 57 (3 stars) to 79 (4 stars).



**Figure 35. Driver Points: (a) Importance Index; (b) Effect of Parameters; (c) RS Example.**

Figure 35 (c) shows an example of a 3-dimensional response surface visualizing the combined effect of overlap percentage and impact speed. It can be noticed that the combination of smaller overlap and high impact speed is the most critical (i.e., least amount of points).

Impact angle and impact velocity were the most important parameters, represented by a 41 percent to 40 percent index for the driver BrIC, as shown in Figure 36 (a). When taking all combinations of parameters into account, BrIC ranged from 0.85 to 1.08, where higher values were mainly associated with a higher yaw component, i.e., higher angular head velocity around the local z-axis. Especially the impact angle showed a significant effect, where more oblique conditions created higher BrIC values, as shown in Figure 36 (b), as well as when analyzing the combined effect of impact angle and overlap percentage, shown in Figure 36 (c). The 3-dimensional response surface indicates that BrIC values were highest for a more oblique condition with smaller overlap percentage, where the effect of impact angle was clearly more significant to the effect of overlap, as seen from the color coding in Figure 36 (c) and the close to horizontal blue trendline representing the effect of overlap in Figure 36 (b).

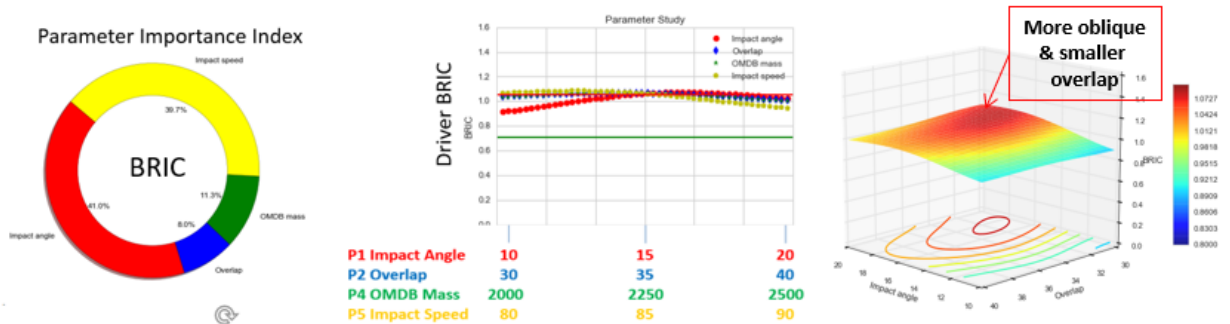


**Figure 36. Driver BrIC: (a) Importance Index; (b) Effect of Parameters; (c) RS Example.**

Impact speed (72% index) and OMDB mass (26% index) were the most important factors for the maximum chest deflection, which occurred at the upper right measurement point for the THOR in the driver seat due to interaction with the seat belt. Impact angle and overlap percentage with an index of 1-2 percent were not important for the maximum chest deflection of the near-side occupant, as shown in Figure 37 (a). Values ranged from 30 mm to 47 mm, when taking all combinations of parameters into account. The most significant trend when evaluating individual parameters was the impact speed, where higher values correlated with higher chest deflection, as

shown by the yellow line in Figure 37 (b). The same trend can be seen in Figure 37 (c), which represents the 3-dimensional response surface for the combined effect of impact speed and OMDB mass. The combination of higher mass and higher impact speed created the highest chest deflection values and vice versa.

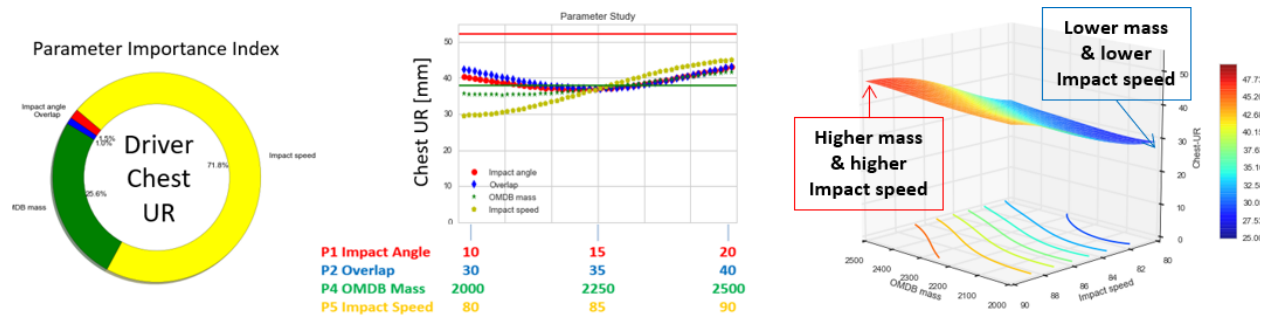


Figure 37. Driver Chest: (a) Importance Index; (b) Effect of Parameters; (c) RS Example.

Abdomen deflection was not critical for any of the conducted simulations with values around 50 mm, which is significantly less than the critical value of 89 mm. There was little sensitivity to any of the parameters, which also were of similar importance.

Impact speed was the most important factor for the left (50% index) and right (65% index) femur load of the driver. Higher speed correlated with higher femur loads.

Axial force of the lower right tibia was mostly influenced by the impact angle with an importance index of 54 percent, as shown in Figure 38 (a). Values ranged from 2598 N to 4042 N when taking all combinations of parameters into account. More oblique impact conditions caused higher maximum tibia loads, as shown in Figure 38 (b). The same observation can be made from the response surface for the combined effect of impact angle and impact speed, as shown in Figure 38 (c). OMDB mass was the least important parameter with an index of 4 percent, showing little effect on the lower leg axial forces.

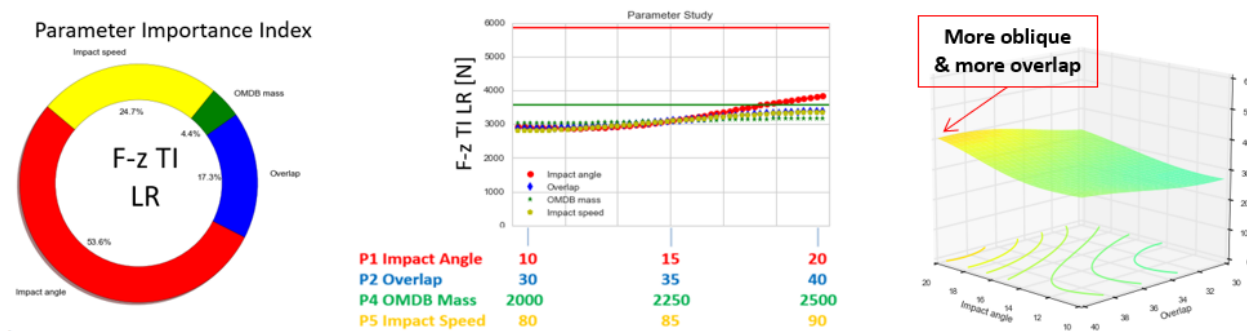


Figure 38. Driver Tibia: (a) Importance Index; (b) Effect of Parameters; (c) RS Example.

Time history data showed more differences between simulations with varying parameters and the baseline simulation than observed in the repeatability study. Overall CORA scores fell between 0.71 and 0.87.

#### 4.4 Results – Passenger

In the Sensitivity Study,” the effect of varying parameters within a wider range compared to full-scale test tolerances, as described in Chapter 4.1, was evaluated by analyzing occupant kinematics and injury metrics for a 50 percent THOR in the passenger seat. Figure 39 (a) shows the head trajectory of the simulation with the lowest head excursion in y-direction, i.e., 146 mm. Figure 39 (b) shows the head trajectory of the simulation with the largest head excursion in y-direction, i.e., 271 mm. Head trajectories with higher y-displacement were mainly correlated with more oblique impact conditions. The extent of THOR movement towards the middle of the vehicle was more significant than for the cases studied in the repeatability study and more significant than for the near-side seating position. The far-side occupant slides out of the shoulder seat belt and is being restrained mainly by the pelvis-belt and the passenger air bag. Consequently, larger movement of the upper body and head can be observed, making it more likely to have contact with the interior of the vehicle and experience less controlled head motion.

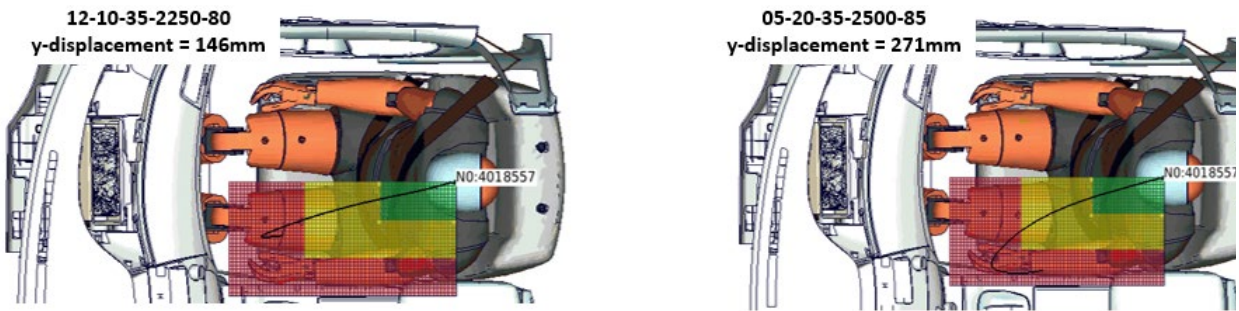


Figure 39. Driver Head Trajectory: (a) Best Case; (b) Worst Case.

Injury risk was analyzed using upper and lower boundaries, as defined in **Appendix A12**. For example, maximum tibia moment values below 178 Nm would be considered low risk of injury and no points for the overall rating would be deducted. Resultant tibia moment values above 240 Nm would be considered high risk of injury and 0 points would be given for the tibia. Linear interpolation is used to calculate the amount of points for tibia values between the lower and upper boundary. A total of 100 points can be achieved, resulting from the maximum 25 points for each of the body regions, head, neck, chest, and lower extremities. A star rating was calculated based on the overall points, ranging from 0 stars for 4 or less points to 5 stars for 90 or more points.

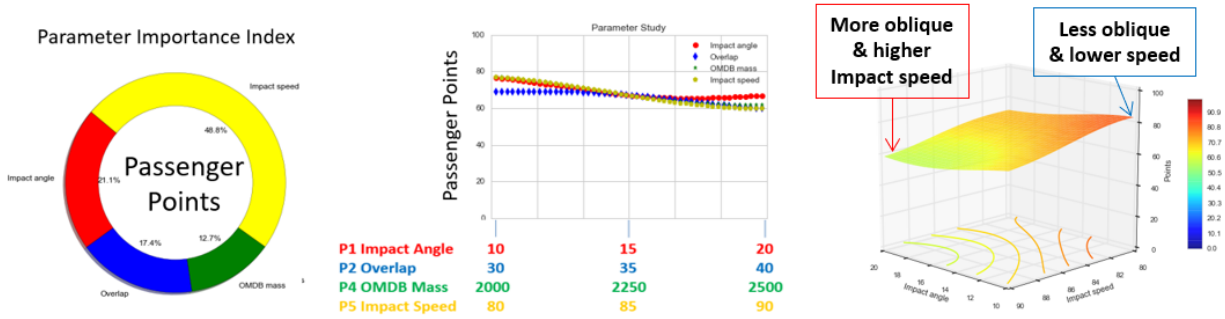


Figure 40. Passenger Points: (a) Importance Index; (b) Effect of Parameters; (c) RS Example.

Impact speed was the most important parameter, represented by a 49 percent index, as shown in Figure 40 (a). Higher impact speed showed less points, i.e., higher overall injury risk, as shown in Figure 40 (b). Overall points, when using all combination of parameters, ranged from 56 (3 stars) to 83 (4.5 stars).

A combination of more oblique impact angle and higher impact velocity showed the highest overall injury risk, as shown in Figure 40 (c).

Impact speed was also the most important parameter for passenger BrIC, represented by a 69 percent index, as shown in Figure 41 (a). When taking all combinations of parameters into account, BrIC ranged from 0.89 to 1.3, where higher values were mainly associated with a higher yaw component, i.e., higher angular head velocity around the local z-axis. Higher impact velocity resulted in higher contact forces of the head with the passenger air bag, which generated higher head angular velocities. This can also be noticed when analyzing the combined effect of impact angle and impact speed, shown in Figure 41 (c). The 3-dimensional response surface indicates that BrIC values were highest for a more oblique condition with higher impact speed.

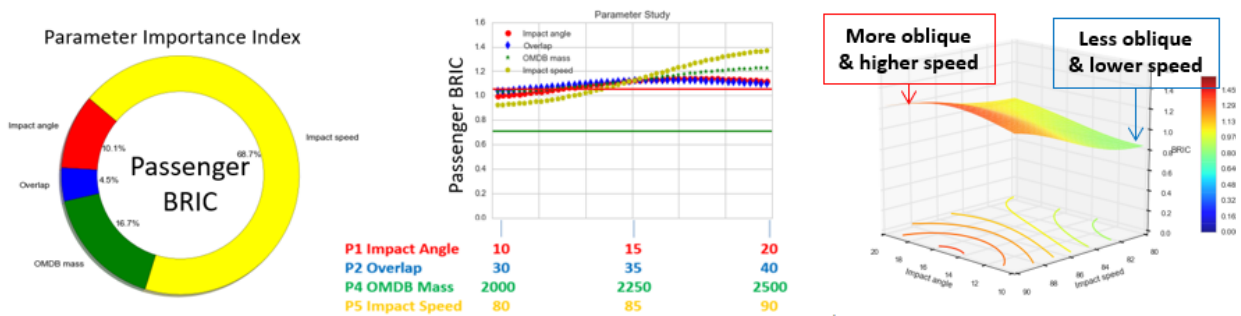
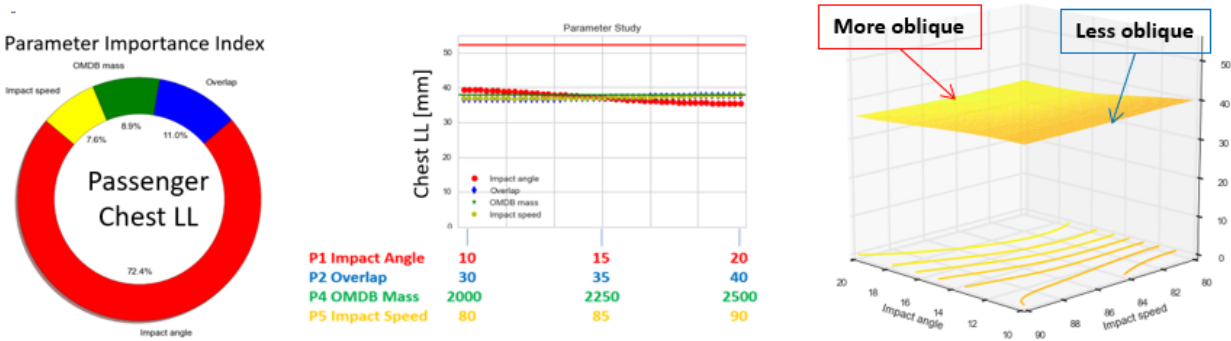


Figure 41. Passenger BrIC: (a) Importance Index; (b) Effect of Parameters; (c) RS Example.

Impact angle (72 percent index) was the most important factor for the maximum chest deflection, as shown in Figure 42 (a). Highest values occurred at the lower left measurement point for the THOR in the passenger seat due to limited interaction of the seat belt with the upper torso. More oblique impact angle correlated with lower chest deflection. Differences were small, ranging from 35 mm to 40 mm, when taking all combinations of parameters into account. The 3-dimensional response surface for the combined effect of impact speed and impact angle is shown

in Figure 42 (c). A limited effect of parameters on chest deflection for the far-side occupant was observed.



**Figure 42. Driver Chest: (a) Importance Index; (b) Effect of Parameters; (c) RS Example.**

Abdomen deflection was not critical for any of the conducted simulation, with values around 60 mm, which is significantly less than the critical value of 89 mm. The most important factor (55% index) for the abdomen was the impact velocity.

Impact speed was also the most important factor for the left femur load, with a 70 percent index of the far-side passenger, as shown in Figure 43 (a). The most significant correlation between any of the parameters and high femur loads can be seen for higher velocities, as shown in Figure 43 (b). Maximum femur loads ranged from 1241 N to 4142 N when taking all combinations of parameters into account. Figure 43 (c) visualizes the combined effect of impact speed and OMDB mass.

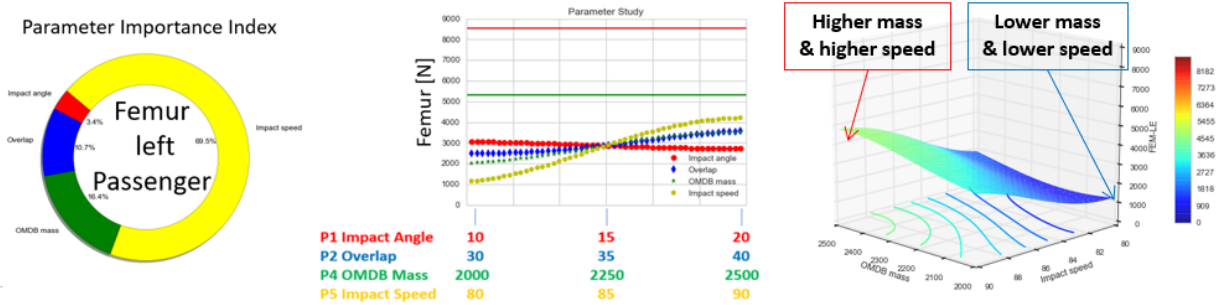


**Figure 43. Passenger Femur: (a) Importance Index; (b) Effect of Parameters; (c) RS Example.**

Resultant moment of the upper right tibia at the passenger side was mostly influenced by the impact angle, with an importance index of 58 percent, as shown in Figure 44 (a). Values ranged from 163 Nm to 220 Nm. More oblique impact conditions caused higher maximum tibia loads, as shown in Figure 44 (b). The same observation can be made from the response surface for the combined effect of impact angle and OMDB mass, shown in Figure 44 (c). Differences occurred in the absence of significant toe-pan intrusion.

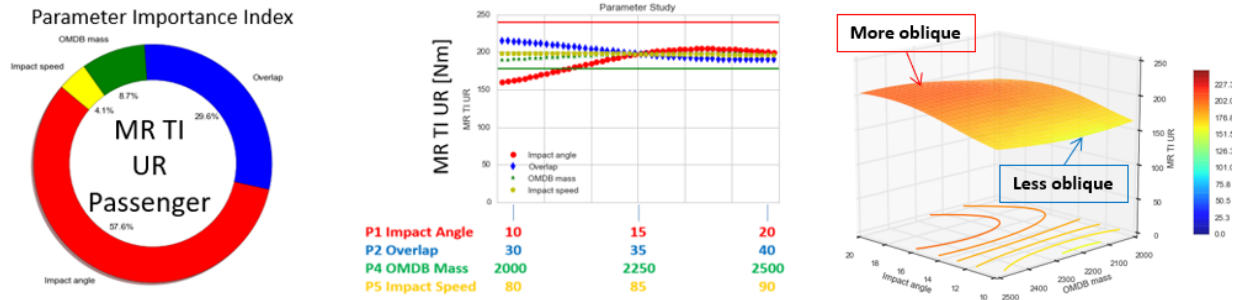


Figure 44. Passenger Tibia: (a) Importance Index; (b) Effect of Parameters; (c) RS Example.

Time history data showed more differences between simulations with varying parameters and the baseline simulation than for the repeatability study. Overall CORA scores ranged between 0.71 and 0.87.

## 5. Test Procedure Impact Angle Study

### 5.1 Evaluated Parameters and Ranges

An extended sensitivity study for the impact angle was conducted. OMDB mass and a 35 percent overlap were kept unchanged for all simulations. The impact angle was changed in 5° increments from 0° to 20°. The study was conducted for an impact velocity of 80 km/h and 90 km/h. Figure 45 shows the initial positions of the OMDB relative to the target vehicle.

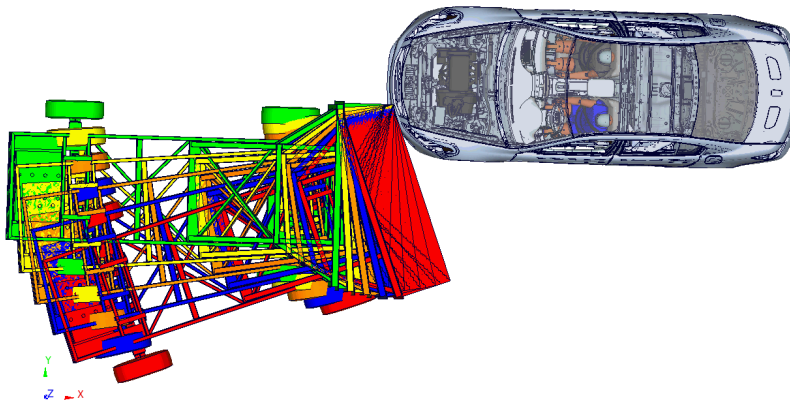
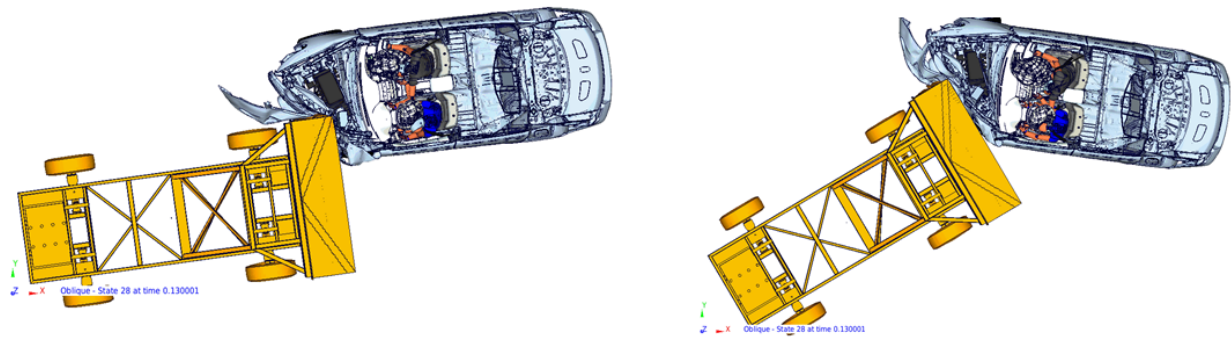


Figure 45. Impact Angle Study – Initial Positions for 0° to 20°.

## 5.2 Results – Vehicle

Different vehicle kinematics could be observed for different impact angles. Figure 46 (a) shows the OMDB and target vehicle after 130 ms for the co-linear  $0^\circ$  impact condition at 90 km/h impact speed. Figure 46 (b) shows the post-crash situation for the most oblique  $20^\circ$  impact configuration. It can be noticed that the vehicle in the co-linear condition experienced yaw motion in the counter-clock wise direction, while the vehicle in the  $20^\circ$  oblique impact experienced yaw motion in clock-wise direction.



**Figure 46. Impact Angle Study – Deformed Shape: (a)  $0^\circ$  Impact; (b)  $20^\circ$  Impact.**

Occupant compartment, brake-pedal, and IP intrusion decreased with increasing impact angle. For the 90 km/h impact velocity, maximum toe-pan intrusion ranged from 166 mm for the  $0^\circ$  impact to 127 mm for the  $20^\circ$  impact, as documented in **Appendix 13**. Similar trends could be observed for the 80 km/h impact velocity with maximum toe-pan intrusion values ranging from 122 mm to 101 mm. Intrusions on the far-side were significantly smaller than on the driver side. Maximum values ranged between 14 mm and 27 mm and between 6 mm and 9 mm for the 90 km/h and 80 km/h studies, respectively.

Figure 47 (a) depicts the delta-v in x- and y-direction, as recorded by an accelerometer at the far-side rear sill location. Values for the 90 km/h impacts are shown using a solid line and 80 km/h simulation results using a dashed line. It can be noticed that higher delta-v values in y-direction correlate with more oblique impact angles. Delta-v values in longitudinal vehicle x-direction are the highest for impact angles of  $5^\circ$  to  $15^\circ$  and are marginally lower for the co-linear  $0^\circ$  and most oblique  $20^\circ$  impacts.

Differences in vehicle yaw motion, i.e., rotation around the z-axis could be observed, as recorded at the vehicle CG. The  $0^\circ$  co-linear impact showed the highest positive vehicle yaw motion in counter-clockwise direction and the  $20^\circ$  oblique condition showed the highest negative vehicle yaw motion in clock-wise direction, when viewed from the top, as shown in Figure 47 (b). A  $10^\circ$  impact angle resulted in close to  $0^\circ$  yaw motion for both impact velocities. Values were taken 100 milliseconds after initial impact.

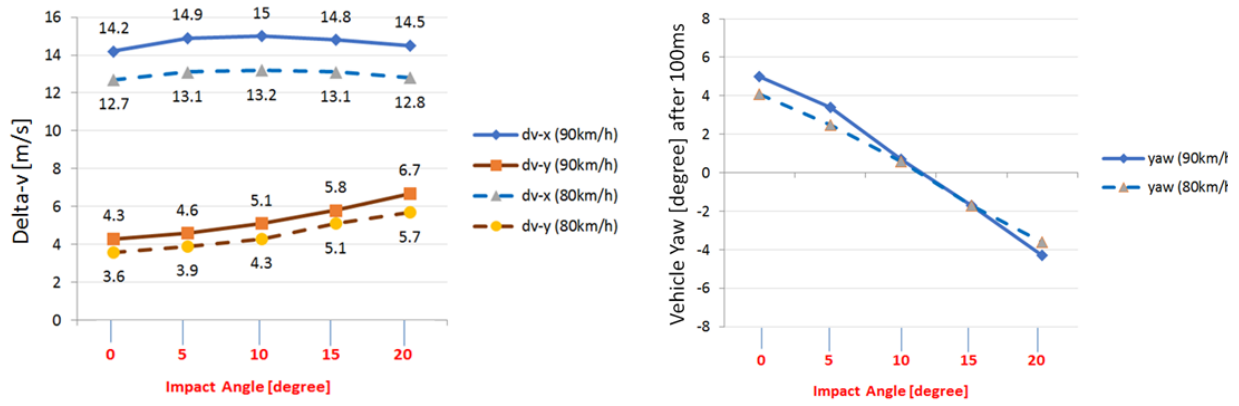


Figure 47. Impact Angle Study: (a) Delta-V; (b) Vehicle Yaw.

### 5.3 Results – Driver

In the impact angle study, the effect of varying parameters within a wider range compared to full-scale test tolerances, as described in Chapter 5.1, was evaluated by analyzing occupant kinematics and injury metrics for a 50 percent THOR in the driver seat. Figure 48 (a) shows the head trajectory of the simulation with the smallest head excursion in y-direction. Figure 48 (b) shows the head trajectory of the simulation with the largest head excursion in y-direction. The near-side occupant was well restrained by the seat belt, driver air bag and side curtain air bag for all analyzed cases and no contact with the A-pillar of the vehicle was observed. Bottoming out of the air bag was observed for the 0° co-linear configuration at 90 km/h, resulting in contact with the steering wheel and higher head injury criteria. No bottoming out was observed for any other impact configurations.

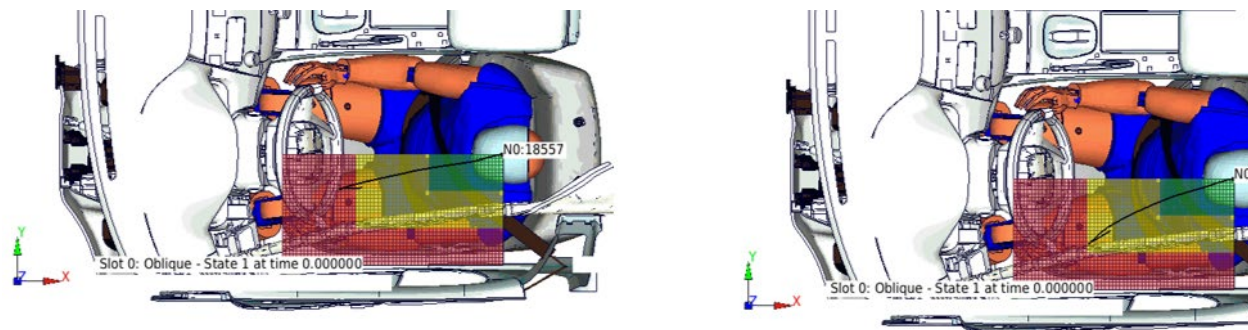


Figure 48. Driver Head Trajectory y-Excursion: (a) Lowest Value; (b) Highest Value.

Maximum head excursion ranged from 381 mm to 445 mm in x-direction and from 99 mm to 180 mm in y-direction, as documented in **Appendix A14**. More head movement in y-direction towards the curtain bag correlated with more oblique impact conditions, as shown in Figure 49 (a). Values for the 90 km/h impacts showed about 20 mm more head movement when compared to the respective 80 km/h simulations. Larger head forward displacement in x-direction correlated with smaller impact angles, as shown in Figure 49 (b). The driver in the 0° co-linear impact experienced the largest value, resulting in increased injury risk measured by HIC and BrIC criteria, due to a bottoming out effect of the driver air bag.

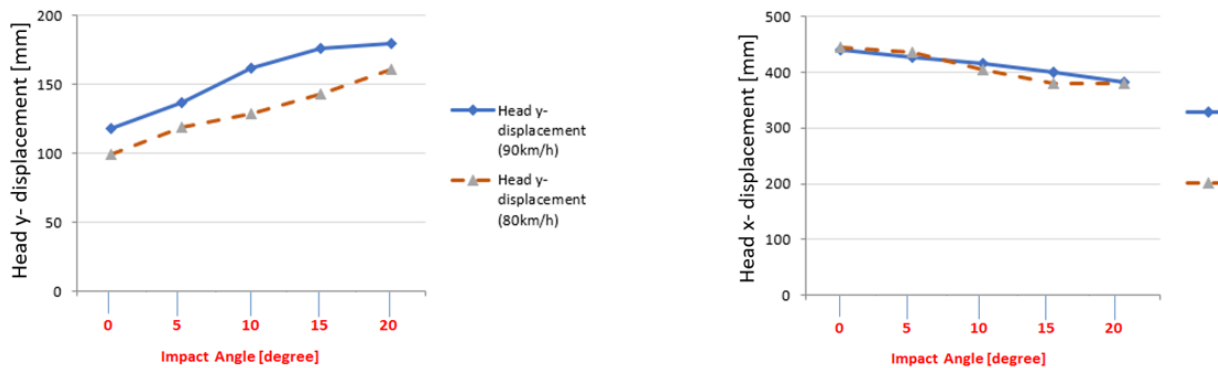


Figure 49. Driver Head Motion: (a) y-Direction; (b) x-Direction.

Injury risk was analyzed using upper and lower thresholds. For example, BrIC values below 0.71 would be considered low risk of injury and no points for the overall rating would be deducted. BrIC values above 1.05 would be considered high risk of injury and 0 points would be given for the Head. Linear interpolation is used to calculate the amount of points for head values between the lower and upper boundary. A total of 100 points can be achieved, resulting from the maximum 25 points for each of the body regions, head, neck, chest, and lower extremities. A star rating was calculated based on the overall points.

Lower overall injury risk was observed for the 80 km/h simulations compared to higher impact velocity cases, as shown in Figure 50 (a). Points for the near-side occupant ranged from 49 (2.5 stars) to 64 (3.5 stars) and from 69 (3.5 stars) to 75 (4.0 stars), respectively. When excluding the bottoming out effect, 74 points would be achieved in the 0° condition at 90 km/h. When excluding this case with increased head injury risk from the analysis, no clear trend between impact angle and overall injury risk could be observed. Similar amount of points (between 62 and 68) were observed for the 5° to 20° impact angles at 90 km/h. Points ranged from 69 to 75 for the 0° to 20° impact angles at 80 km/h.

BrIC values tended to be higher for more oblique impact conditions, when not considering the 0° impact at 90 km/h, where air bag bottoming out occurred, as shown in Figure 50 (b). It was observed that BrIC values were higher for the lower impact velocities in some cases. A similar observation was made for the near-side occupant in two full-scale crash tests with different impact speeds. A near-side occupant in a Malibu test at 108 km/h impact speed experienced a BrIC of 1.4, while the THOR in the same vehicle at the lower 90 km/h impact velocity experienced a BrIC of 1.59.

Higher BRIC values for lower impact velocities, as seen in the current simulation study and the full-scale tests, are non-intuitive at first look. Therefore, time history data for the head angular velocities around the head local x-axis ( $w_x$ ), the local y-axis ( $w_y$ ), the local z-axis ( $w_z$ ), and the maximum chest deflection at the upper right location (chest UR) are shown in **Appendix A19**. It can be noticed that higher impact speed correlated with higher maximum chest deflection. Chest deflection has a less steep slope for the 80km/h simulation and significant lower maximum peak deflection. The head angular velocity around the local y-axis ( $w_y$ ) starts the upward slope later for the 80km/h impact velocity and reaches a higher peak value than for the 90km/h impact velocity at a later point in time. In the used mid-size sedan vehicle environment with the specific restraint system components, more pitch motion of the head was observed for the lower impact speed. Having the same seat belt air bag characteristics, lower impact speed resulted in lower chest deflection and chest forward motion, which allowed the head to experience more y-rotation moving forward in-between the driver and side curtain air bag. The increased angular velocity around the head y-axis was the main reason for the higher BRIC values observed for the lower velocity impact.

Despite the fact that higher BRIC values for the near-side occupant correlated with lower impact speed for the 10° and 15° configurations, it is believed, that BRIC values in the oblique configuration are highly dependent on the specific restraint systems of a vehicle and the resulting head kinematics. It can therefore not be generalized that higher BRIC values correlate with lower impact speeds and further research is suggested.

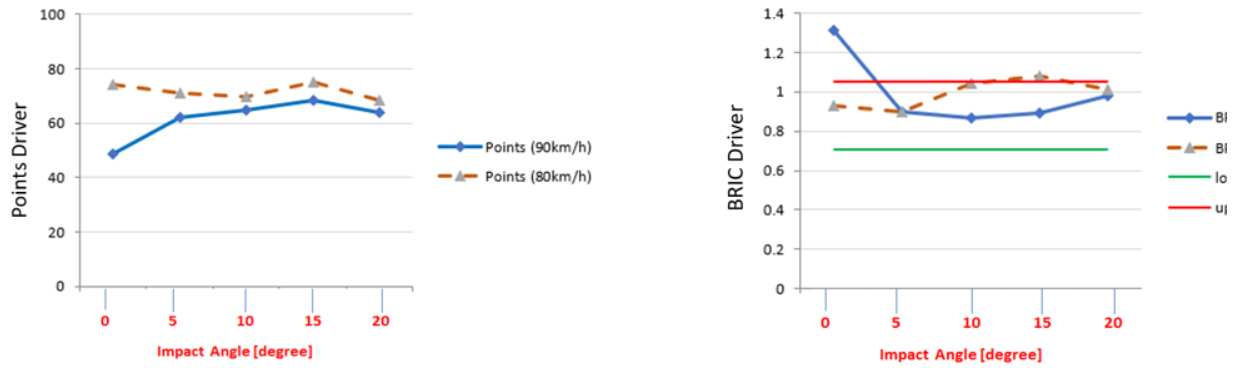


**Figure 50. Impact Angle Study: (a) Points Driver; (b) BrIC Driver.**

Chest deflection was similar for all impact angles at 90 km/h, ranging from 46 mm to 49 mm. More oblique impacts correlated with lower maximum chest deflection. Maximum femur loads tended to be higher for less oblique impact conditions. No clear trend could be observed for maximum tibia axial forces, showing the highest values for 0° and 20° impact conditions, compared to lower values for the 5° to 15° impact angles. Local effects, such as interaction with the pedals and vehicle interior, were found to be responsible for different lower extremity injury risk.

## 5.4 Results – Passenger

In the impact angle study, the effect of varying parameters within a wider range compared to full-scale test tolerances, as described in Chapter 5.1, was evaluated by analyzing occupant kinematics and injury metrics for a 50 percent THOR in the far-side seat. Figure 51 (a) shows the head trajectory of the simulation with the smallest head excursion in y-direction. Figure 51 (b) shows the head trajectory of the simulation with the largest head excursion in y-direction. The far-side occupant was not as well restrained as the near-side driver, especially in the more oblique impact conditions.

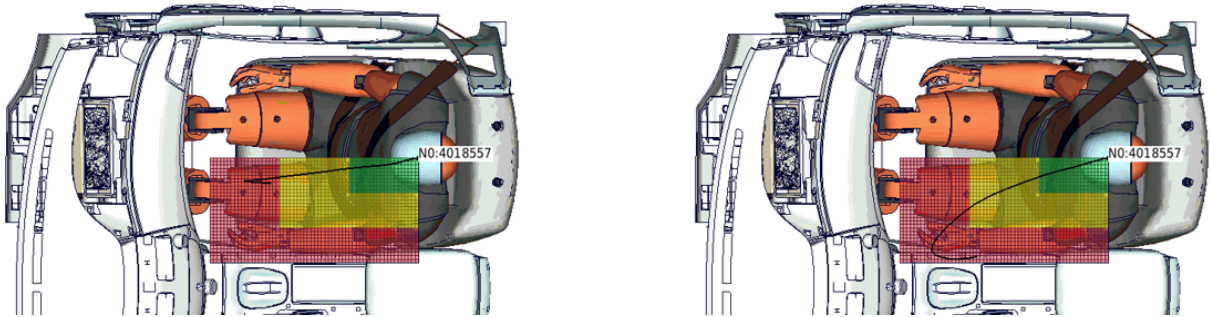


**Figure 51. Impact Angle Study Head Excursion: (a) Best Case; (b) Worst Case.**

Maximum head excursion ranged from 78 mm to 298 mm in y-directions, as shown in Figure 52 (a). Larger head movement in y-direction correlated with more oblique impact angles. Values for the 90 km/h impacts showed about 40 mm more head y-movement when compared to the respective 80 km/h simulations, except for the 0° co-linear impact condition, which showed similar values for the different impact speeds. Head forward displacement in x-direction was similar for the 0° to 15° impact cases where more oblique cases tended to generate marginally lower x-displacement. The 20° impact condition showed the lowest values for both impact speeds, as shown in Figure 52 (b). Head movement was larger in both x- and y-direction when compared to the respective values for the driver side. The combination of curtain air bag and steering wheel with driver air bag were able to control kinematics of the THOR better on the near-side. Lack of interaction with the curtain air bag on the passenger side in the left oblique impact and slipping out of the shoulder-belt in more oblique impact conditions were the reason for the larger movements at the far-side seating position.

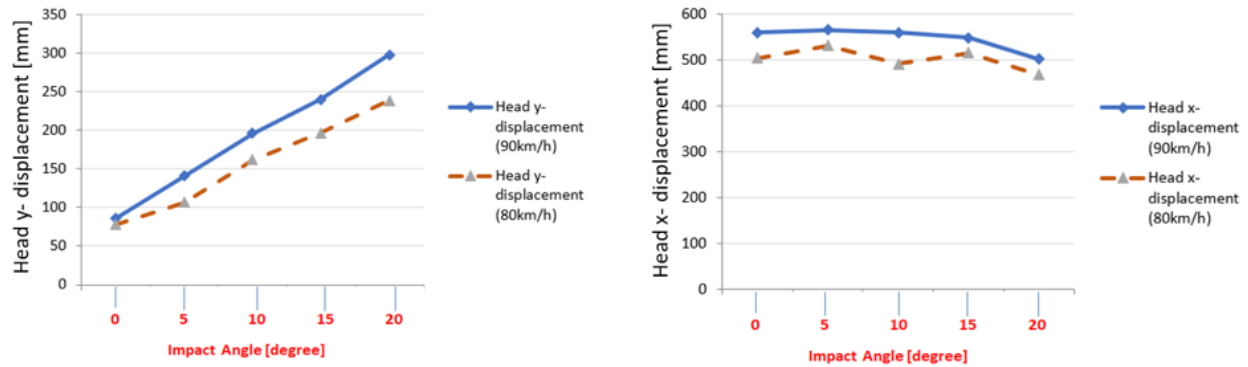


Figure 52. Passenger Head Motion: (a) y-Direction; (b) x-Direction.

Injury risk was analyzed using upper and lower thresholds, as defined in **Appendix A15**. For example, Neck  $N_{ij}$  values below 0.39 would be considered low risk of injury and no points for the overall rating would be deducted.  $N_{ij}$  values above 0.85 would be considered high risk of injury and 0 points would be given for the neck. Linear interpolation is used to calculate the amount of points for head values between the lower and upper boundary. A total of 100 points can be achieved, resulting from the maximum 25 points for each of the body regions, head, neck, chest, and legs. A star rating was calculated based on the overall points.

Lower overall injury risk was observed for the 80 km/h simulations compared to higher impact velocity cases, as shown in Figure 53 (a). Points for the far-side occupant ranged from 57 (3 stars) to 76 (4 stars) for 90 km/h impact speed and from 68 (3.5 stars) to 84 (4.5 stars) for 80 km/h cases. More oblique impact conditions correlated with less points, i.e., higher overall injury risk.

BrIC values tended to be higher for more oblique impact conditions, as shown in Figure 53 (b). Higher impact velocity (90 km/h) correlated with higher BrIC values for the THOR in the passenger side. A similar observation was made for the far-side occupant in two full-scale crash tests with different impact speeds. A far-side occupant in a Malibu test at 90 km/h impact speed experienced a BrIC of 1.59, while the THOR in the same vehicle at the higher 108 km/h impact velocity experienced a BrIC of 2.01.

In contrast to the near-side occupant, where the curtain-air bag has significant effect in controlling the head yaw motion, i.e., the angular velocity around the local z-axis, the head motion is mainly affected by the interaction with the passenger air bag for the far-side occupant. The correlation of BRIC values and impact speed is more intuitive than for the near-side occupant. Higher BRIC values were observed for higher impact speeds in the current simulation study and analyzed full-scale tests for the far-side occupant. Higher impact speed correlated in more forward motion and higher contact normal forces between the head and the air bag. Due to the oblique nature of the evaluated impact configuration, these higher normal forces resulted in higher frictional forces that caused more head yaw motion, i.e., higher angular velocities around the local head z-axis ( $w_z$ ). Higher  $w_z$  values significantly contributed to higher BRIC values for higher impact speeds.

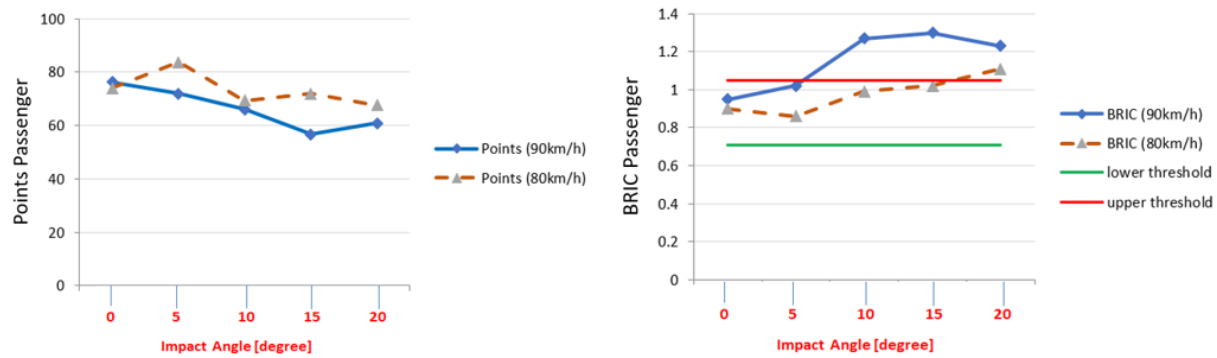


**Figure 53. Impact Angle Study: (a) Passenger Points; (b) Passenger BrIC.**

Chest deflection was smaller than on the driver side due to the reduced interaction with the shoulder-belt. All impact angles at 90 km/h showed similar values, ranging from 38 mm to 39 mm. More oblique angles correlated with lower maximum chest deflection for the 80 km/h study, ranging from 41 mm to 35 mm. Maximum femur load was the highest for the 10° impact angle at 90 km/h due to the interaction with the instrument panel.

Higher tibia resultant moments correlated with more oblique impact angles for 80 km/h and 90 km/h impact speeds, as shown in Figure 54. This occurred in the absence of significant toe-pan intrusion at the far-side occupant compartment. It can also be noticed that values for the 90 km/h cases were only marginally higher than for the lower 80 km/h speed configurations.

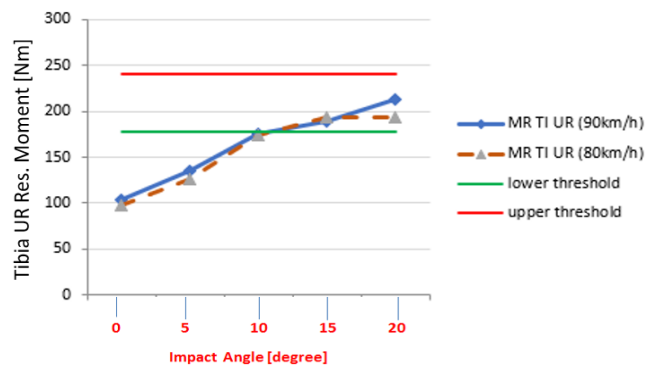


**Figure 54. Impact Angle Study – Maximum Tibia Moment Passenger.**

Time history data showed more differences between simulations with varying parameters and the baseline simulation than for the repeatability study. Overall CORA scores for 90 km/h simulations ranged between 0.63 and 0.83 for the driver and between 0.67 and 0.83 for the passenger.

## 6. Test Procedure Study Summary

A baseline simulation for NHTSA left oblique impact condition was conducted with an FE model of a mid-size sedan vehicle with a THOR occupant in the driver and front passenger seat. Vehicle kinematics, vehicle pulse, occupant kinematics, and occupant injury criteria were compared with results from a full-scale test of the same vehicle. All evaluated criteria were in a range that has been seen in many full-scale tests of sedan vehicles and compared reasonably well with the specific test results for all body regions.

The integrated occupant-vehicle model with all relevant restraints was used to conduct parametric studies to understand the effect of different parameters relevant for the oblique test procedure. Parameters included the impact angle, OMDB vertical misalignment, OMDB overlap, OMDB mass, and impact speed.

Three studies were conducted to understand the importance of the different parameters and their effect on the vehicle and occupants. (1) In the Repeatability Study parameters were varied within a typical range for test tolerances when conducting full-scale tests. (2) In the Sensitivity Study parameters were varied within a range that is beyond defined test tolerances. (3) In the Impact Angle Study configurations within an even wider range of impact angles from co-linear 0° to 20° oblique were analyzed. Characteristic results are summarized in **Appendix A16, A17, and A18**.

Good test repeatability was found when changing parameters within the small ranges used as test tolerances. Vehicle delta-v varied by less than 1 m/s and maximum intrusion varied by less than 30 mm when taking all combinations of parameters into account. Impact speed was the most important factor for the vehicle pulse in x-direction and impact angle was most dominant for the vehicle y-pulse. The overall CORA score for time-history data of the THOR in the driver seat and front passenger seat ranged from 0.86 to 0.94 and 0.81 to 0.94, respectively, when compared to the baseline simulation.

More significant effects were seen when evaluating wider ranges of parameters in the Sensitivity Study. Vehicle delta-v in x- and y-direction varied by more than 3 m/s and 2 m/s, respectively. Maximum toe-pan intrusion varied by about 60 mm, when taking all combinations of parameters into account. The overall CORA score for time-history data of the THOR in the driver seat and front passenger seat ranged from 0.71 to 0.87 and 0.73 to 0.90 respectively, when compared to the baseline simulations. Impact speed was the most important factor for the driver and passenger. Impact angle was found to be especially relevant for far-side occupant results.

Differences were even more significant in the Impact Angle Study with CORA values between 0.63 to 0.83. Different vehicle yaw motion, ranging from counter clock-wise yaw for the 0° co-linear impact to clock-wise yaw of similar extent for the 20° oblique condition, was observed. The combination of vehicle yaw motion and noticeable difference in vehicle y-pulse caused different occupant kinematics with a larger extent of y-motion, especially for the far-side occupant. Overall injury risk was similar for the driver for the different impact angles, while higher overall injury risk was observed for more oblique impact conditions for the passenger in the far-side seating position.

The conducted studies, using integrated occupant vehicle simulations with relevant restraints, enabled valuable insight into the effect of different test parameters for NHTSA's oblique impact condition.

In summary, NHTSA's oblique frontal offset impact test showed overall good repeatability with respect to vehicle kinematics and injury risk, when relevant parameters were changed within defined test tolerances.

## 7. THOR Position Study

The validated integrated occupant-vehicle model was used to conduct parametric studies to understand the effect of different parameters relevant for positioning the THOR. Parameters included the H-point x-, y-, and z-coordinate, the head/torso angle, and the position of the lower extremities. The effect of these parameters on the occupant kinematics and injury risk was evaluated for the driver and front passenger. It was determined which parameter was most important for the respective outcomes, and what effect each parameter had.

### 7.1 Parameters and Ranges

For the THOR position repeatability study, parameters were varied within defined test tolerances for the occupant on the driver seat, as shown in Figure 55. The H-point position was varied by  $\pm 5$  mm in x-, y-, and z- direction. The head angle was varied by  $\pm 1^\circ$ . The lower legs were evaluated for a knee-to-knee distance that varied between +10 mm and -10 mm relative to the baseline model.

The occupant on the front passenger seat was used to conduct a THOR position sensitivity study. In this case, parameters were changed beyond defined seating procedure tolerances. The passenger H-point was changed by  $\pm 20$  mm relative to the baseline position. The H-point y-position was varied by  $\pm 5$  mm. The head and torso angles were changed by  $\pm 5^\circ$ . The knee-to-knee distance was evaluated for the baseline value and for positions with +30 mm and +60 mm larger knee-to-knee distances.

The H-point z-coordinate was evaluated for the baseline value, +10 mm, and +20 mm. The designated seating position H-point coordinates are determined by car manufacturers using CAD data and seat travel diagrams. According to the latest seating procedure protocol, the seat is positioned in the mid fore-aft, lowest height at mid seat cushion angle position. Due to variances in seat cushion thickness, the theoretical H-point z-coordinate can practically not be achieved. Typically, the dummy's actual H-point matches the designated position or is higher. Seat cushions are typically thicker or more firm, which can result in a higher seating position, even if the seat is positioned at lowest height. Therefore, the baseline H-point z-value, +10 mm, and +20 mm values were used for this study. The seat in the simulation was positioned accordingly. The rationale for the range of this parameter was to evaluate the sensitivity of known manufacturing tolerances, the seat cushion height in this case. The seat cushion angle was kept unchanged for the different seating heights.

The OMDB test configuration was kept unchanged for this study, i.e., the barrier impacted the stationary vehicle with 90 km/h with a 35 percent overlap and a  $15^\circ$  oblique angle.

Repeatability Study	Range (Driver)			
H-Point (x)	-5	BL	+5	
H-Point (Y)	-5	BL	+5	
H-Point (Z)	-5	BL	+5	
Head Angle	-1	BL	+1	
Knee/Heel Position	-10	BL	+10	

Sensitivity Study	Range (Passenger)			
H-Point (x)	-20	BL	+20	
H-Point (y)	-5	BL	+5	
H-Point (z)		BL	+10	+20
Head Angle	-5	BL	+5	
Knee/Heel Position		BL	+30	+60

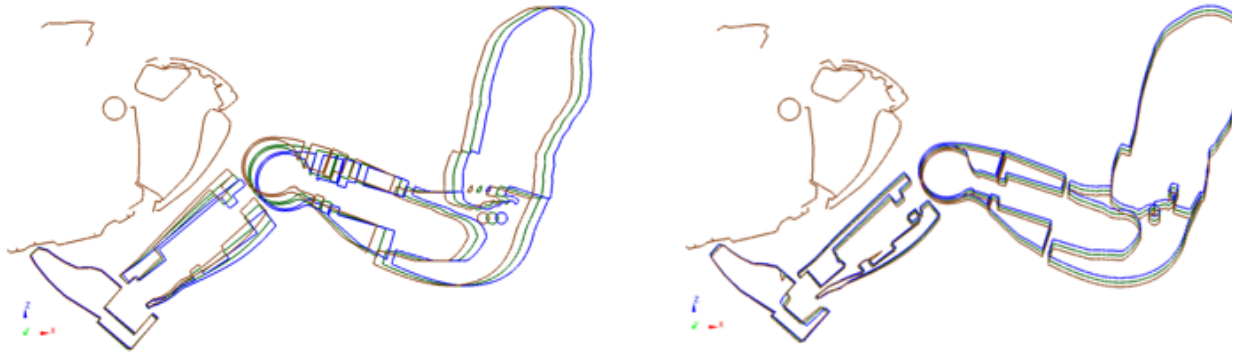
  


**Figure 55. THOR Position Repeatability Study Parameters and Ranges.**

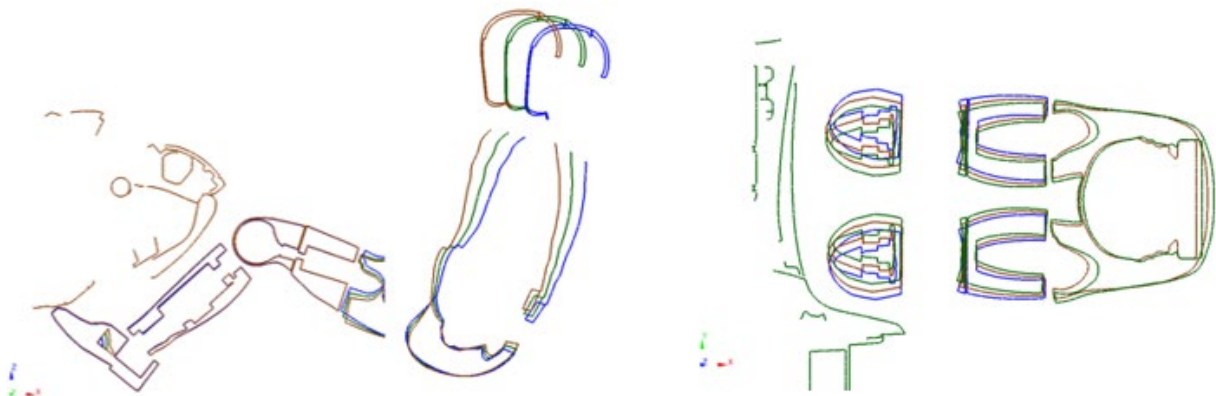
Using a Box-Behnken DoE method with five parameters and three levels, a total of 41 simulations were run to determine the effect and importance of the different parameters. The simulation matrix can be found in **Appendix B1**.

Figure 56 (a) depicts a cross-sectional view of the THOR in the passenger seat at different H-point (HP) x-positions. The THOR shown in brown represents the occupant in a 20 mm more forward seating position. Since the positive direction of the vehicle coordinate system points from front to rear, the most forward position is represented by the value  $x = -20$  mm. The baseline model is represented by green color. The THOR shown in blue represents the occupant in +20 mm more rearward seating position. It can be noticed that while changing the H-point of the occupant, the heel and foot positions were kept unchanged. This was achieved by changing the angle between the pelvis and the upper legs, the angle between the upper and lower leg, and the angle between the tibia and foot. When changing the x-position of the occupants, the longitudinal position of the seat was adjusted accordingly. Similarly, the seat belt was adjusted to fit the new seating position.

Figure 56 (b) shows the THOR in the front passenger seating position for three different H-point z- coordinates, representing the baseline position, +10 mm, and +20 mm higher seating positions. Again, the foot and heel positions were kept unchanged by adjusting the leg angles. The seat and seat belt were adjusted accordingly.



**Figure 56. (a) HP-x -20/0/+20mm; (b)HP-z 0/+10/+20mm.**



**Figure 56. (c) Head Angle - 5/0/+5°; (d) Knee-to-Knee Distance 0/+30/+60 mm**

Figure 56 (c) shows the THOR in the passenger seat for different head/torso angles. The occupant shown in green represents the baseline position with a 0° head angle. Rather than creating different head angles by rotating the head around the neck and keeping the upper torso the same, it was decided to change head and torso angles in tandem and keeping the relative position of the head to the chest. The occupant shown in brown represents a -5° head and torso angle, resulting in a more upright sitting posture. The THOR shown in blue represents a +5° head and torso angle, resulting in a more reclined sitting posture.

Figure 56 (d) shows the passenger with different leg positions. The THOR shown in green represents the baseline model with a knee-to-knee distance according to the latest NHTSA seating procedure protocol and the CMM data provided by the VRTC. The models shown in brown and blue represent a seating position where the knee-to-knee distance was increased by 30 mm and 60 mm, respectively. When changing the knee-to-knee distance, the ankle-to-ankle distance was changed as well. When changing the limbs of the occupants, pre-simulations were conducted to avoid penetrations of the femur bone with the pelvis flesh, for example. “Seat squash” simulations, i.e., integration of the occupant into the seat was conducted for different seating positions and postures.

Knee-to-knee distance for the passenger side is set to 270mm according to the latest THOR passenger seating procedure protocol.<sup>10</sup> When determining the range of knee-to-knee distance for the THOR position sensitivity study, 64 frontal oblique full-scale tests conducted by NHTSA were analyzed. It was found that most tests were conducted used the nominal knee-to-knee distance of 270mm for the front passenger THOR. Larger differences in knee-to-knee distance were found for the driver, as shown in **Appendix B2**. It was found that most tests were conducted using a knee-to-knee distance between 300mm and 350mm, i.e., larger than the nominal distance for the passenger. It is noted that the THOR on the driver seat would be the far-side occupant in a right oblique impact. It was concluded that a reasonable range of knee-to-knee distance for the sensitivity study was to use the baseline value and distances increased by 30mm and 60mm.

---

<sup>10</sup> THOR Seating Procedure Protocol Front Driver and Passenger, Draft 2015, [www.nhtsa.gov](http://www.nhtsa.gov).

## 8. THOR Position Repeatability Study (Driver)

### 8.1 Driver Simulation Results Overview

The THOR on the driver seat was used to conduct the repeatability study.” The driver results, where parameters were changed within a small range according to defined test tolerances, are shown in **Appendix B3, B4, and B5**. The simulations, which were conducted according to the defined DoE matrix, were analyzed with respect to occupant kinematics and interaction with the vehicle interior and restraints. 41 simulations were found to be enough to build reliable response surfaces for the different injury criteria. For each of the simulations, injury values for the head, neck, chest, and lower extremities were extracted. For example, HIC and BrIC values were calculated for the head and the more critical value of the two was used to calculate the points for the head, as described in Chapter 1.2. Color coding was used in **Appendix B2 - B4** to visualize if a value was below the critical lower boundary (green), above the critical upper boundary (red), or in between the two boundary values (yellow) for the respective injury criteria.

In addition to the injury values for the different criteria, the overall point score, the resulting star rating, and the points per body region are shown in **Appendix B3 – B5**. Furthermore, the overall CORA rating, which represents how the time history data of a simulation compared to the baseline simulation is shown. Finally, for each simulation it was measured how far the head center of gravity moved in x-, y-, and z-direction relative to the vehicle.

It can be noticed that 35 out of 41 conducted simulations obtained the same overall 3.5-star rating, which is equivalent to 85 percent of the simulations. The overall CORA rating was between 0.81 and 0.93, i.e., time history data showed “GOOD” correlation when compared to the baseline simulation. It can therefore be stated that good test repeatability was observed in the conducted study for the driver side, when relevant parameters were changed within a small range, i.e., defined tolerances in the THOR seating procedure protocol.

### 8.2 Driver Star Rating

Positioning of the lower extremities was the most important parameter with respect to the overall star rating, represented by a 36 percent importance index, as shown in Figure 57 (a). Knee-to-knee distance was changed by +/-10 mm relative to the baseline simulation and affected the position of the feet and interaction with the footrest and acceleration pedal. H-point x-position, which was modified by +/-5 mm relative to the baseline model, was the least important factor for the overall star rating, represented by a 9 percent importance index.

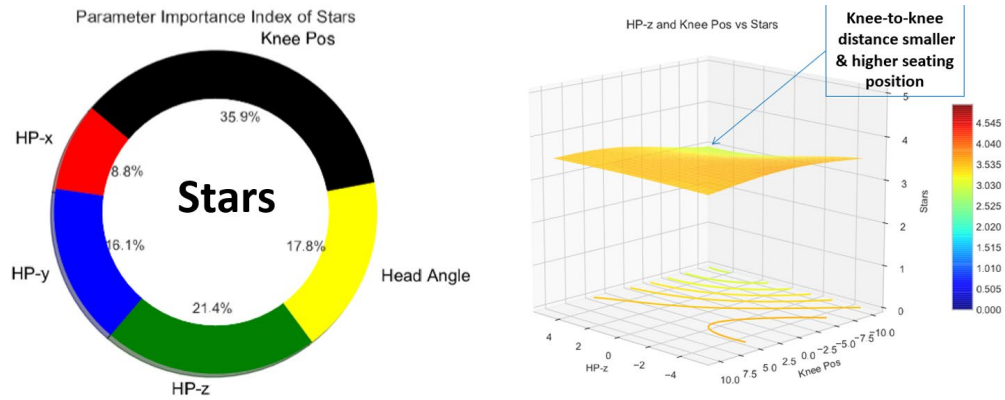


**Figure 57. Driver Star Rating: (a) Importance Index; (b) Response Surface.**

Higher seating position and smaller knee-to-knee distance correlated with a lower star rating, as shown in Figure 57 (b). The select response surface depicts the effect of the H-point z-coordinate and the knee-to-knee distance, when taking all combination of parameters into account.

The effect of individual parameters, when keeping all other parameters at their baseline value, can be found in **Appendix B6**.

### 8.3 Driver Head

The head motion of the driver in the oblique frontal offset condition is mainly controlled by the driver air bag and side curtain air bag. The trajectory of the head center of gravity, as shown in Figure 58 (b), was analyzed. The head moves forward and outward towards the A-pillar. The color-coded scale in the picture on the right was used to visualize differences in head trajectory between simulation runs. The H-point y-coordinate was found to be by far the most important factor with respect to Head y-movement, documented by a 72 percent importance index in Figure 58 (a). While the initial H-point ranged from +/- 5 mm relative to the baseline simulation, the maximum head trajectory in y-direction varied by almost 20 mm, i.e., between 168 mm and 187 mm. More inward seating position correlated with larger head motion in the lateral direction. All other analyzed parameters were of small importance and had no significant effect on the head's y-motion

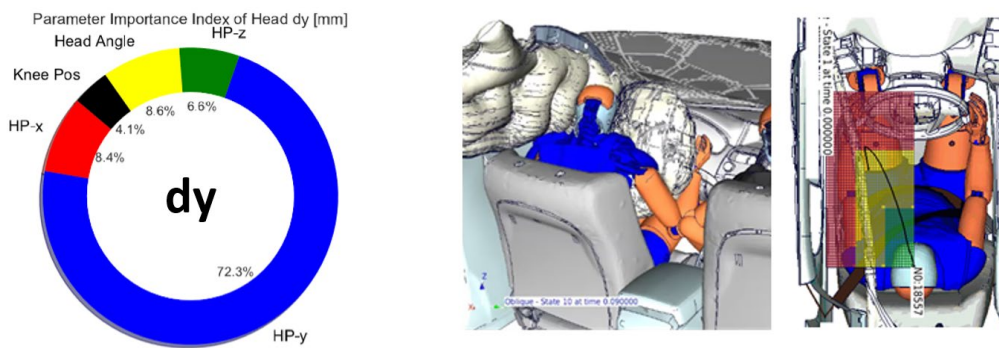


Figure 58. Driver Head y-Trajectory: (a) Importance Index; (b) Kinematics.

The initial head angle, which was directly linked to the torso angle, was found to be the most important parameter for the driver's HIC criteria. The importance index for the head angle was 37 percent, as shown in Figure 59 (a). The second most important parameter for HIC was the H-point y-coordinate with a 22 percent importance index.

More upright and more outward seating position correlated with smaller HIC values, as shown in Figure 59 (b) and **Appendix B7**, due to earlier coupling of the head with the driver and side curtain air bag.

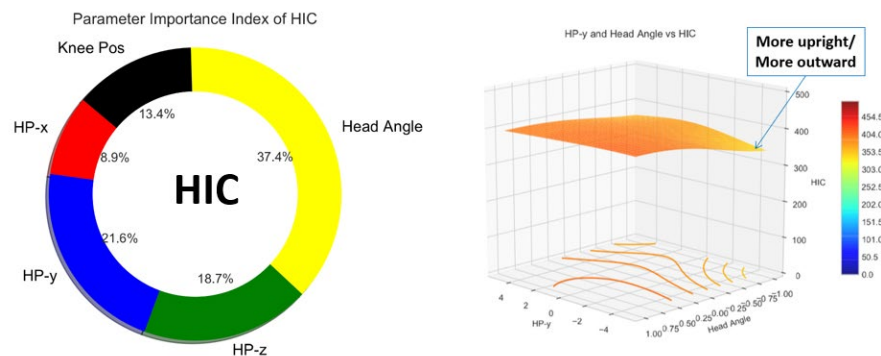
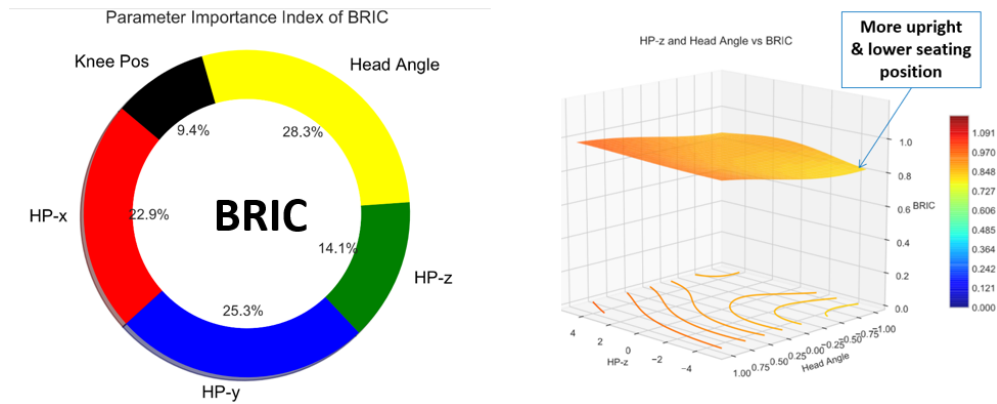


Figure 59. Driver HIC: (a) Importance Index; (b) Response Surface.

Head/torso angle was the most important parameter for BrIC, represented a 28 percent importance index, as shown in Figure 60 (a). More upright and lower seating position correlated with lower BrIC, as shown in Figure 60 (b) and **Appendix B8**, due to earlier coupling of the head with the driver air bag.



**Figure 60. Driver BrIC: (a) Importance Index; (b) Response Surface.**

## 8.4 Driver Neck

Neck tension extension (Nte) was the most critical Nij component used to calculate the neck injury risk. H-point x-position and head/torso angle were the most important parameters with a 44 percent and 32 percent importance index, respectively, as shown in Figure 61 (a). The combination of more upright and more rearward seating position resulted in the highest Nte values, as shown in Figure 61 (b) and **Appendix B9**. Values ranged between 0.34 and 0.41 for all simulations. The lower and upper boundary values for the neck, used for calculating the overall injury risk and star rating, are 0.39 and 0.85, respectively. Hence, no points were deducted for the neck in most cases.

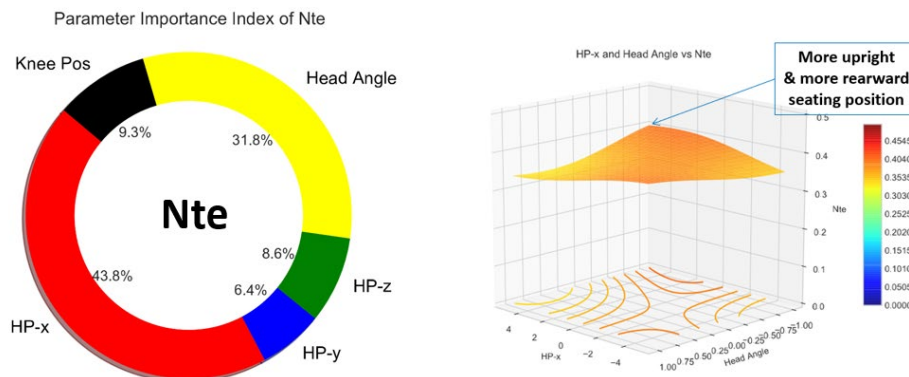
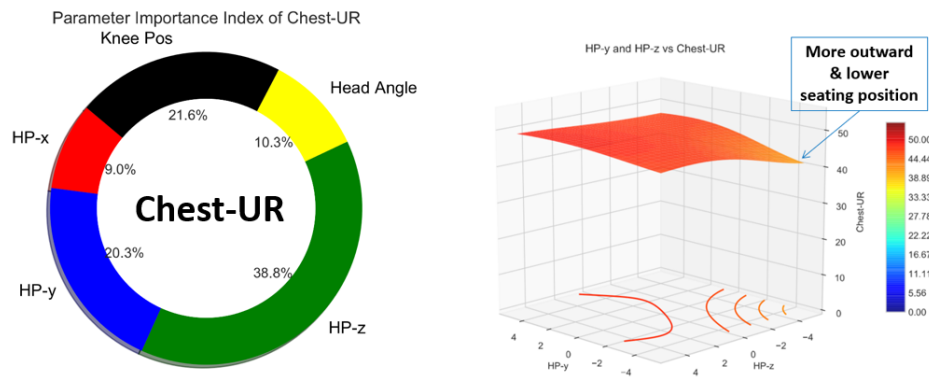


Figure 61. Driver Neck: (a) Importance Index; (b) Response Surface.

## 8.5 Driver Chest and Abdomen

The upper right chest measurement point showed the highest values in all simulations when compared to the other chest locations due to interaction with the shoulder-belt. Although the belt routing is initially closer to the upper left measurement location, maximum deflection occurs at a later stage of the impact, when the occupant has moved forward and outward, resulting in a belt location closer to the upper right chest.

H-point z-coordinate was found to be the most important parameter, represented by a 39 percent index, as shown in Figure 62 (a). The combination of lower and more outward seating position correlated with lower chest deflection, as shown in Figure 62 (b) and **Appendix B10**. 38 of the 41 simulations showed chest maximum chest deflections between 46 mm and 49 mm, i.e., 3 mm difference at most, which documents good test repeatability when seating parameters were changed within defined tolerances.



**Figure 62. Driver Chest: (a) Importance Index; (b) Response Surface.**

H-point y-coordinate was the most important parameter for the maximum abdomen deflection, represented by a 29 percent index, as shown in Figure 63 (a). Values ranged from 49 mm to 55 mm for all simulations, which is well below the critical pass/fail criteria of 89 mm. Abdomen deflection is caused by the interaction with the pelvis-belt. Since the location of the pelvis-belt changes little relative to the pelvis and abdomen when seating postures are varied within small ranges, little effect of any of the evaluated parameters was observed, as shown in Figure 63 (b) and **Appendix B11**.

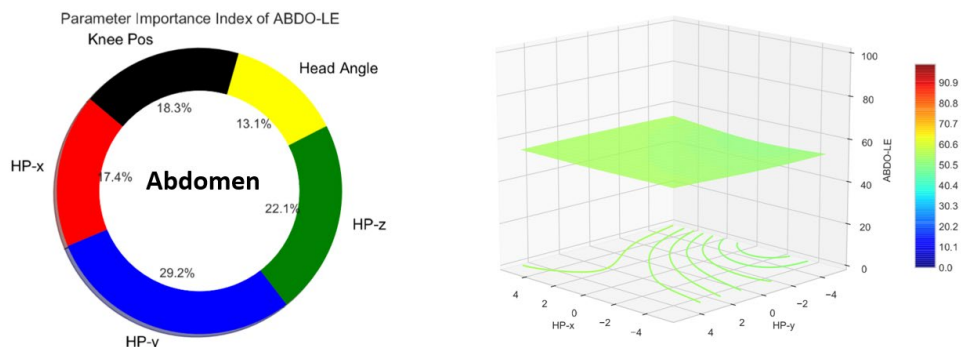


**Figure 63. Driver Abdomen: (a) Importance Index; (b) Response Surface.**

## 8.6 Driver Acetabulum and Femur

H-point x-coordinate was the most important factor for the acetabulum force, documented by a 28 percent index, as shown in Figure 64 (a). More forward and more outward seating position correlated with higher acetabulum forces, as shown in Figure 64 (b) and **Appendix B12**.

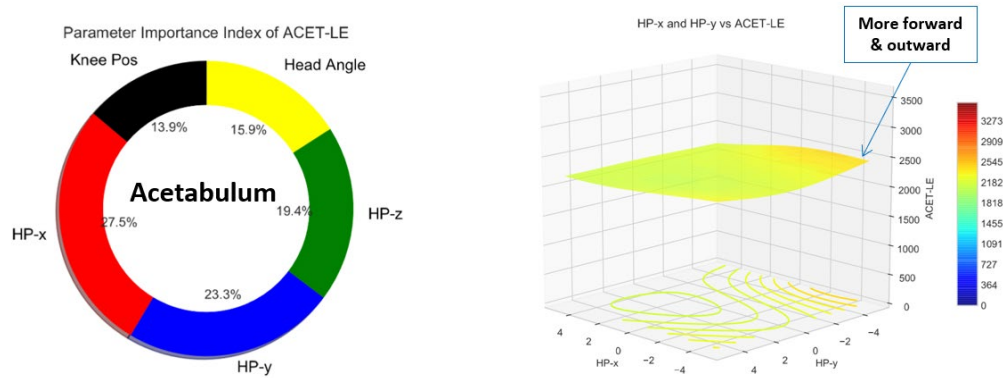


Figure 64. Driver Acetabulum: (a) Importance Index; (b) Response Surface.

H-point z-coordinate was the most important factor for the femur force, documented by a 27 percent index, as shown in Figure 65 (a). Lower seating position correlated with higher femur forces, as shown in Figure 65 (b) and **Appendix B13**.

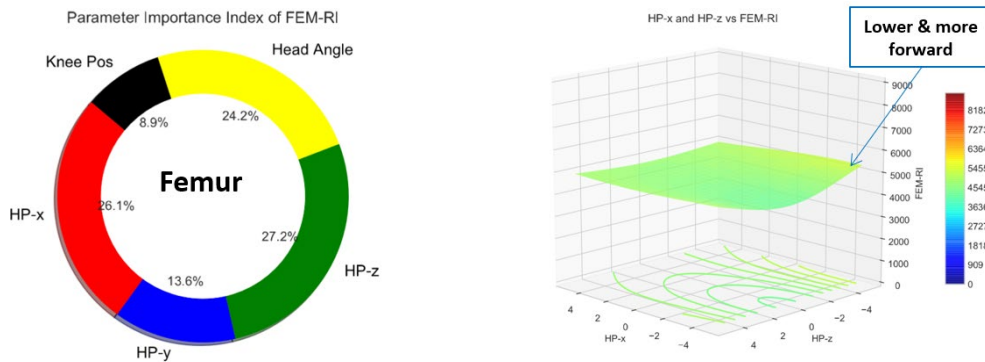
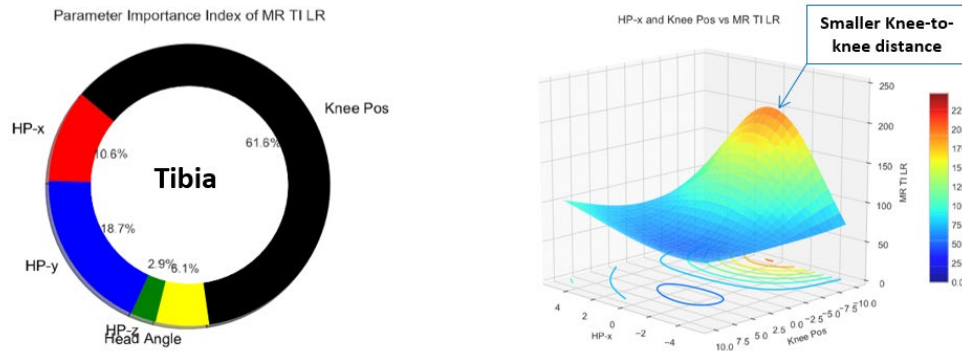


Figure 65. Driver Femur: (a) Importance Index; (b) Response Surface.

## 8.7 Driver Tibia

Knee-to-knee distance was by far the most important parameter for the tibia index, as shown in Figure 66 (a). Resultant moment of the lower right tibia was the most critical component. Changing the distance of the knees affected the position of the feet. Lower leg kinematics were found to be sensitive due to interaction with the acceleration pedal. Smaller knee-to-knee distance tended to lead to kinematics that resulted in larger foot eversion and consequently higher tibia moments, as shown in Figure 66 (b) and **Appendix B14**. When analyzing all conducted simulations, it can be noticed that 37 out of the 41 cases had tibia moments that were below the lower boundary value of 178 Nm, indicating an overall good test repeatability. However, it was found that small differences in positioning the foot on the acceleration pedal can cause significant differences in lower leg kinematics and tibia moments. Hence, positioning of the feet and legs according to an unambiguous protocol seems critical for achieving consistent injury values for the lower legs.



**Figure 66. Driver Tibia: (a) Importance Index; (b) Response Surface.**

## 8.8 THOR Position Repeatability Study Summary (Driver)

Five parameters relevant for seating the THOR on the driver seat in NHTSA's frontal left oblique impact configuration were identified. A DoE analysis was defined to analyze what effect the parameters have on the occupant kinematics and injury criteria. In total, 41 simulations were conducted. Parameters were changed within the tolerances defined in the respective THOR seating procedure protocol. Three parameters related to the dummy's H-point, i.e., the x-, y-, and z-coordinates, were changed by  $\pm 5$  mm relative to the baseline simulation. The THOR in the baseline simulation was positioned using CMM data, which was recorded after a physical dummy has been positioned in the mid-size sedan vehicle. The head angle was changed by  $\pm 1^\circ$  relative to the baseline simulation. Different head angles were realized by rotating the upper body accordingly. The knee-to-knee distance was used as the fifth parameter. Knee-to-knee distance was changed by  $\pm 10$  mm relative to the baseline simulation. When changing the knee-to-knee distance, ankle-to-ankle distance of the feet was changed accordingly.

The ANOVA analysis was used to determine the importance of each parameter for the observed occupant kinematics and injury risks of the different body regions. Graphs and response surfaces were used to visualize the effect of individual parameters and combination of parameters.

Knee-to-knee distance was found to be the most important factor for the tibia loads and the overall star rating. Smaller knee-to-knee distance resulted in interaction with the acceleration pedal that caused high tibia moments due to significant foot excursion in some instances.

The y-coordinate of the H-point was found to be the most important parameter for the head y-trajectory. More inward seating position correlated with higher head excursion.

Head/torso angle was the most important factor for HIC and BrIC. A more upright seating posture correlated with lower injury values due to earlier coupling with the driver air bag. HIC values for all simulations were below the lower boundary. BrIC values varied within a larger range and influenced the overall point score used for calculating the star rating.

The THOR's H-point x-coordinate was the most important parameter for the neck injury criteria. A more forward seating position correlated with higher neck tension extension (Nte) values.

The z-coordinate of the THOR in the driver seat was found to be the most important parameter for the chest deflection. The upper right chest deflection location showed the highest values in all simulations, caused by interaction with the shoulder-belt. Lower seating position correlated with lower maximum chest deflection.

Differences for most injury criteria were small. Tibia loads were found to be the most sensitive with respect to THOR positioning on the driver seat due to interaction with the acceleration pedal.

Thirty-five of the 41 simulations showed the same star rating. The overall CORA score for the conducted simulations with small differences in seating position ranged from 0.81 to 0.94, when compared to the baseline run. A value above 0.8 was considered a "GOOD" correlation.

It was concluded that NHTSA's frontal oblique test configuration showed good test repeatability when relevant parameters for positioning the THOR on the driver seat were changed within small tolerances, as defined in the seating procedure protocol.

## 9. THOR Position Sensitivity Study (Passenger)

### 9.1 Passenger Simulation Results Overview

To determine the “sensitivity” of occupant kinematics and injury criteria with respect to positioning the occupant in NHTSA’s oblique impact configuration, five relevant parameters were changed within ranges that were beyond those defined in the THOR positioning protocol for the passenger side. The THOR position in longitudinal direction was varied by +/-20 mm relative to the designated seating position. The H-point y-coordinate was varied by +/- 5 mm, and H-point z-coordinate was evaluated for +10 mm and +20 mm higher seating positions, in addition to the baseline simulation. Head and torso angle were changed in tandem and ranged from -5°, i.e., more upright, to +5°, i.e., more reclined. The knee-to-knee distance was evaluated for the +30 mm and +60 mm cases, in addition to the baseline position. The simulations, which were conducted according to a defined DoE matrix, were analyzed with respect to occupant kinematics, injury risk, and interaction with the vehicle interior and restraints.

The results of the sensitivity study are documented in **Appendix B15, B16, and B17**. 41 simulations were found to be enough to build reliable response surfaces for the different injury criteria. For each of the simulations, injury values for the head, neck, chest, and lower extremities were extracted. For example, HIC and BrIC values were calculated for the head and the more critical value of the two was used to calculate the points for the head, as described in Chapter 1.2. Color coding was used in **Appendix B15 - B17** to visualize if a value was below the critical lower boundary (green), above the critical upper boundary (red), or in between the two boundary values (yellow) for the respective injury criteria. In addition to the injury values for the different body regions, the overall point score, the resulting star rating and the points per body region were determined. Furthermore, the overall CORA rating, which represents how the time history data of a simulation with modified seating position compared to the baseline simulation, is shown. Finally, how far the head center of gravity moved in x-, y-, and z-direction relative to the vehicle was measured.

Thirty-seven out of 41 conducted simulations obtained an overall star rating of 2.5 or 3-stars, three cases received 2.0-stars, and one case received 1.5-stars. The overall CORA rating was between 0.7 and 0.9, i.e., time history data showed “GOOD” to “FAIR” correlation when compared to the baseline simulation. The results indicate a higher sensitivity than the results obtained from the repeatability study conducted for the THOR on the driver side. This is partly because of the wider range of respective parameters evaluated and the fact that the far-side occupant slides out of the shoulder-belt and experiences less controlled kinematics. The kinematics of the near-side occupant, in contrast, are better controlled by the seat belt, driver and side curtain air bag. The motion of the THOR on the passenger seat is mainly controlled by the pelvis-belt and the passenger air bag in the later phase of the impact.

## 9.2 Passenger Overall Score

Positioning of the lower extremities was the most important parameter with respect to the overall point score, documented by a 32 percent importance index, as shown in Figure 67 (a). Knee-to-knee distance was changed by +30 mm and +60 mm relative to the baseline simulation and affected the kinematics of the THOR on the passenger seat. Smaller knee-to-knee distance correlated with a higher point score, i.e., better star rating, as shown in Figure 67 (b). The trend lines shown below are extracted from calculated response surfaces and reflect the effect a parameter, when the baseline value was used for the other parameters. When evaluating the effect of combination of parameters, it was found that the combination of more upright and more forward seating position correlated with a higher overall score, i.e., a better star rating, as shown in **Appendix B18**. Earlier coupling of the far-side occupant with the passenger air bag was the reason for the observed effect.

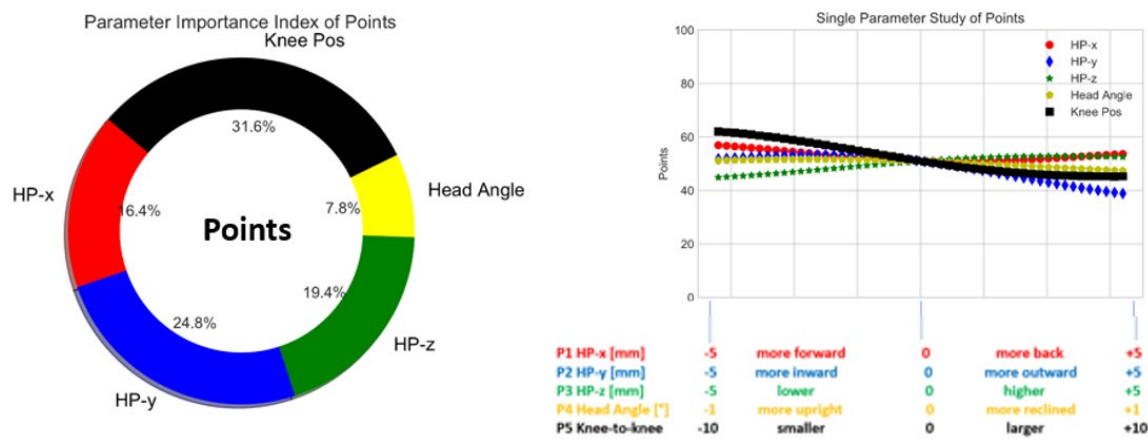
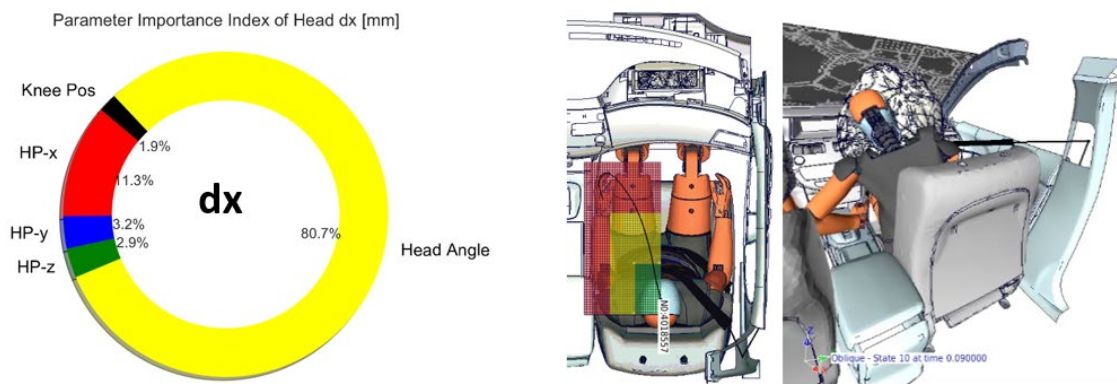


Figure 67. Passenger Overall Score: (a) Importance Index; (b) Effect of Parameters.

### 9.3 Passenger Head

The head motion of the passenger in the left oblique frontal offset condition is mainly controlled by vehicle kinematics and the passenger air bag. The trajectory of the head center of gravity, as shown in Figure 68 (b), was analyzed. The head moves forward and inward towards the middle of the vehicle. The color-coded scale in the picture was used to visualize differences in head trajectory between simulation runs. The head/torso angle was found to be by far the most important factor for the head x-movement, documented by a 81 percent importance index in Figure 68 (a). A more reclined seating position correlated with a larger head motion in the longitudinal direction. All other analyzed parameters were of small importance and had no significant effect on the head's x-motion. The amount of forward motion is relevant for a potential interaction with the instrument panel.



**Figure 68. Passenger Head x-Trajectory: (a) Importance Index; (b) Kinematics.**

The initial head angle, which was directly linked to the torso angle, was found to be the most important parameter for the driver's HIC criteria. The importance index for the head angle was 61 percent, as shown in Figure 69 (a). A more reclined initial seating position correlated with higher HIC value, as shown in Figure 69 (b), due to later coupling with the passenger air bag and larger forward motion, which resulted in contact with the instrument panel in some cases. This agrees with the observation that a more reclined seating position resulted in a larger longitudinal head trajectory.

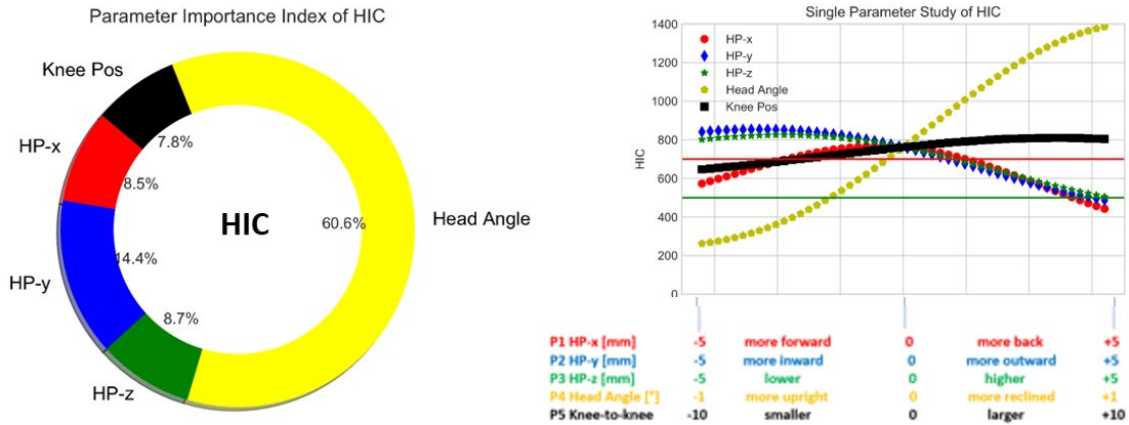


**Figure 69. Passenger HIC: (a) Importance Index; (b) Effect of Parameters.**

H-point y-coordinate was the most important parameter for BrIC, represented by a 35 percent importance index, as shown in Figure 70 (a). A more outward initial seating position correlated with the highest BrIC values, as shown in Figure 70 (b). Different injury mechanisms caused high BRIC values. Cases where the head contacted the instrument panel showed high HIC and high BrIC values. If no contact with the instrument panel occurred, interaction of the head with the passenger air bag influenced the BrIC of the far-side THOR. Knee-to-knee distance was the second most important parameter for BrIC, with a 26 percent index. Larger knee-to-knee distance correlated with higher BrIC, as shown in Figure 70 (b) and **Appendix B19**. Leg position influenced occupant kinematics and resulted in an interaction of the head with the passenger air bag that produced a higher rotational yaw velocity of the head, i.e., rotation of the head around the local z-axis, while rolling off the air bag.

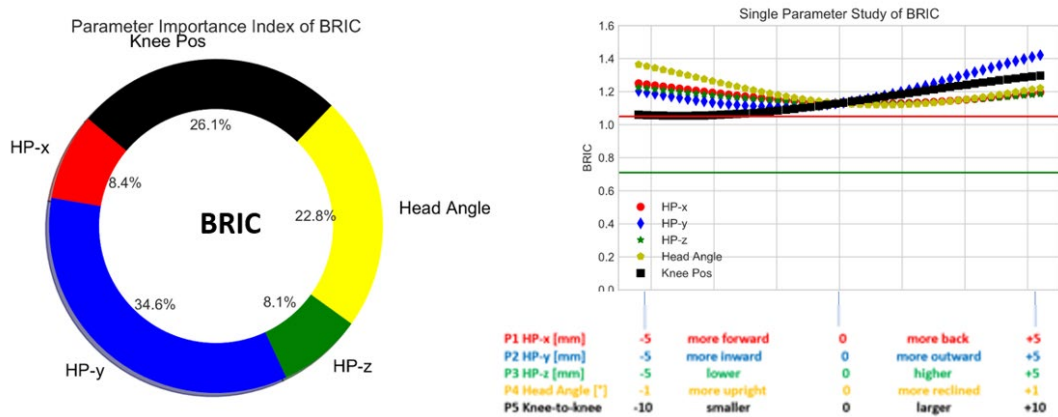


**Figure 70. Passenger BrIC: (a) Importance Index; (b) Effect of parameters.**

## 9.4 Passenger Neck

Neck tension flexion (Ntf) was the most critical Nij component used to calculate the neck injury risk. H-point y-position was the most important parameter, with a 37 percent importance index, as shown in Figure 71 (a). More outward seating position resulted in the highest Nte values, as shown in Figure 71 (b) and **Appendix B20**. A similar correlation was observed for the BrIC analysis. Again, interaction of the head with the passenger air bag was found to be the reason for the higher neck injury risk values.

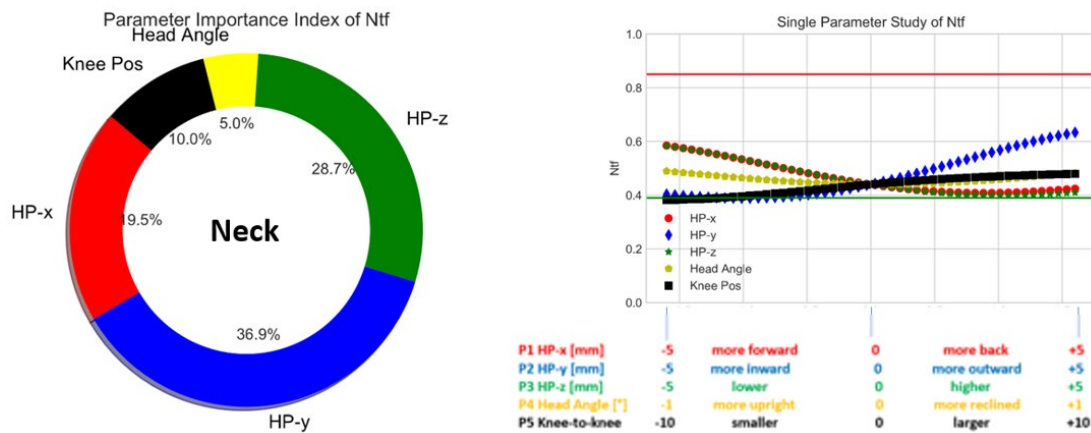


Figure 71. Passenger Neck: (a) Importance Index; (b) Effect of Parameters.

## 9.5 Passenger Chest and Abdomen

Chest values were lower than for the THOR on the driver seat, because the shoulder-belt slides off and has no significant effect on the upper chest measurement points. Consequently, the lower left chest location showed the highest values for the THOR on the far-side passenger seat. Values were below or just above the lower boundary value of 38 mm.

Knee position was the most important parameter, represented by a 37 percent index, as shown in Figure 72 (a). Smaller knee-to-knee distance correlated with smaller maximum chest deflection, as shown in Figure 72 (b) and **Appendix B21**. The pelvis was kept further back, when knees were closer together due to the interaction of the knees with the instrument panel and resulted in smaller lower chest deflection. It can also be seen from Figure 72 (b) that a more reclined seating posture correlated with higher chest deflection. When more reclined, air bag coupling occurs later in the impact and the upper torso gains more momentum which results in a higher force between the belt and the lower chest area and in higher chest deflection.

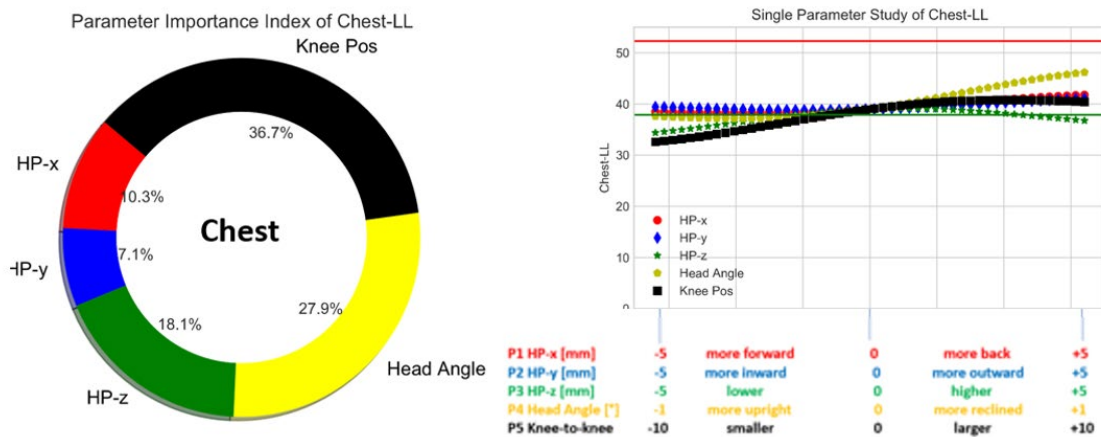


Figure 72. Passenger Chest: (a) Importance Index; (b) Effect of Parameters.

Head/torso angle was the most important parameter for the maximum abdomen deflection, represented by a 28 percent index, as shown in Figure 73 (a). Values ranged from 51 mm to 66 mm for all simulations, which is well below the critical pass/fail criteria of 89 mm. Abdomen deflection is caused by the interaction with the pelvis-belt. Higher values correlated with a more rearward and more reclined seating position, as shown in Figure 73 (b) and **Appendix B22**. The same mechanism as described for the maximum chest deflection was the reason for these effects.

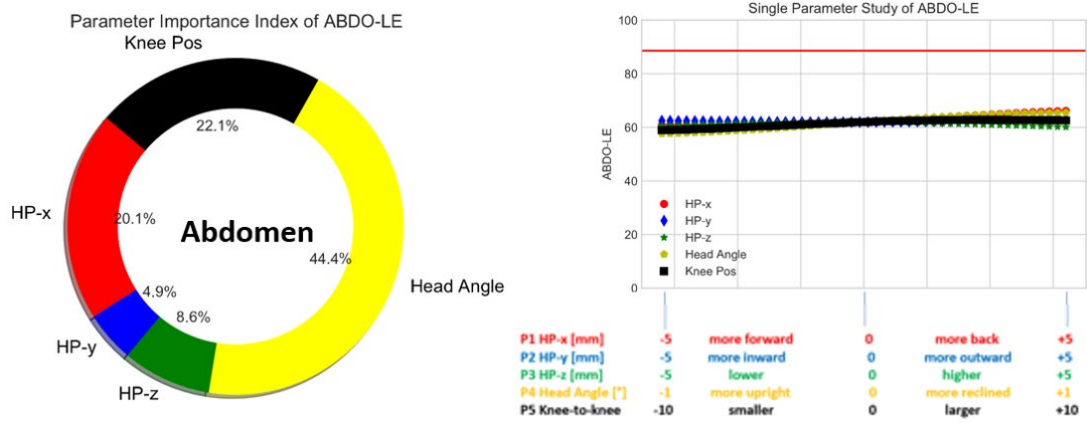


Figure 73. Passenger Abdomen: (a) Importance Index; (b) Effect of Parameters.

## 9.6 Passenger Acetabulum and Femur

The head/thorax angle of the THOR on the passenger seat, was the most important parameter for the acetabulum force loads. The importance index was 26 percent, as shown in Figure 74 (a). More upright seating position correlated with higher acetabulum loads, as shown in Figure 74 (b). A more forward seating position also correlated with a higher acetabulum force, due to more sever interaction with the instrument panel.

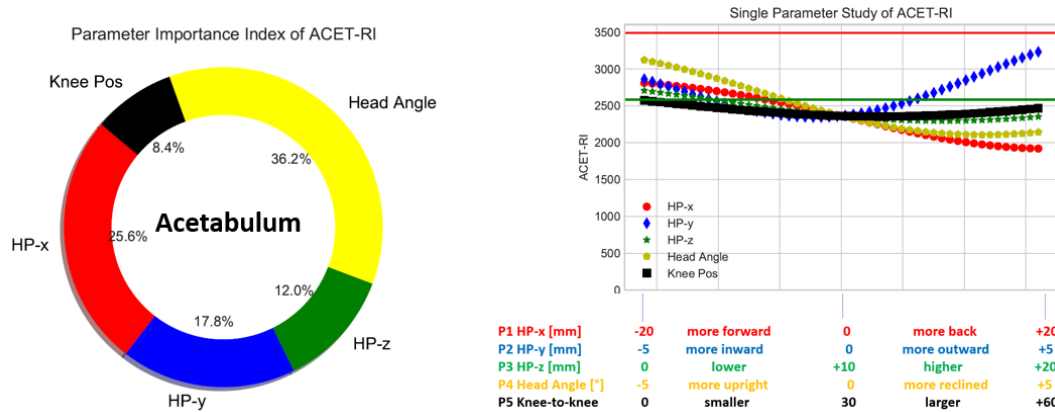


Figure 74. Passenger Acetabulum: (a) Importance Index; (b) Effect of Parameters.

The longitudinal seating position, i.e., the x-coordinate of the THOR on the passenger seat, was the most important parameter for the femur loads. The importance index was 76 percent, as shown in Figure 75 (a). More forward seating position correlated with higher femur loads, as shown in Figure 75 (b) and **Appendix B23**. More severe interaction of the femur with the instrument panel correlated with a more forward seating position. A more forward seating position also correlated with a higher acetabulum force.

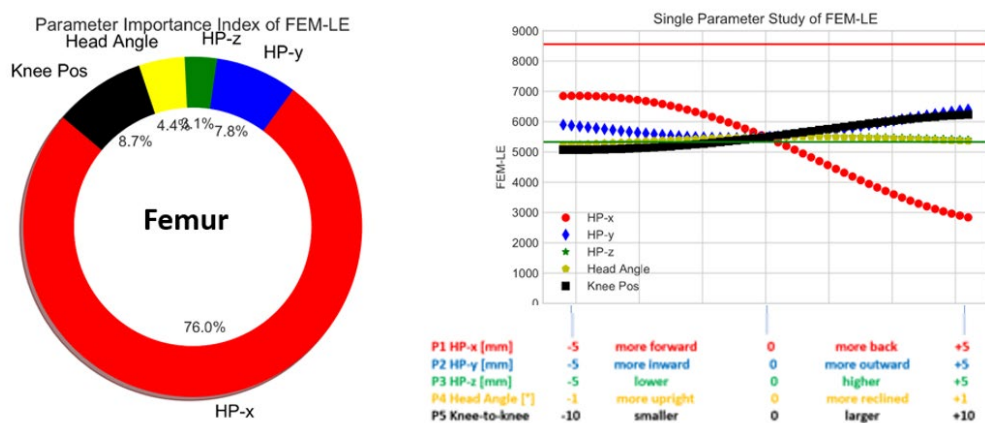


Figure 75. Passenger Femur: (a) Importance Index; (b) Effect of Parameters.

## 9.7 Passenger Tibia

H-point x-coordinate and knee-to-knee distance were by far the most important parameters for the tibia criteria, represented by a 53 percent and 39 percent importance index, as shown in Figure 76 (a). More rearward seating position and larger knee-to-knee distance correlated with higher upper tibia moments due to interaction of the lower legs with the toe-pan and instrument panel, as shown in Figure 76 (b) and **Appendix B24**. Tibia loads showed the highest sensitivity compared to other injury criteria. No significant toe-pan intrusion was observed on the passenger side. Since there are also no pedals existent, differences in lower leg kinematics and interaction with the floor pan and instrument panel were the reason for the observed sensitivity.

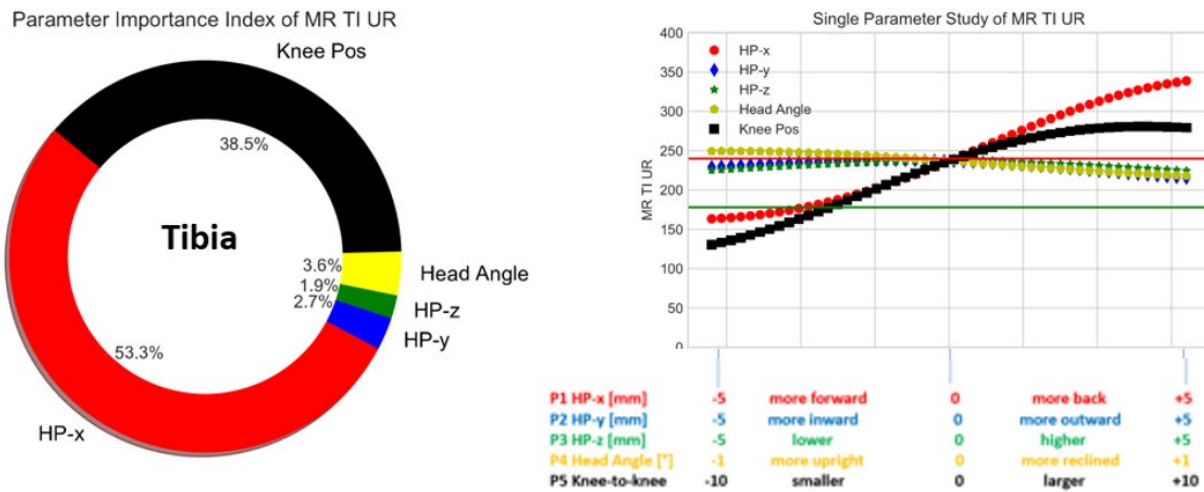


Figure 76. Passenger Tibia: (a) Importance Index; (b) Effect of Parameters.

## 9.8 THOR Position Sensitivity Study Summary (Passenger)

Five relevant parameters for positioning the THOR on the front passenger seat in NHTSA's left frontal offset oblique impact configuration were identified. A DoE analysis was defined to determine what effect the parameters have on occupant kinematics and injury criteria. In total, 41 simulations were conducted. Parameters were changed beyond tolerances defined in the respective THOR seating procedure protocol. Three parameters related to the dummy's H-point, i.e., the x-, y-, and z-coordinates, were changed. The H-point x-location was changed by  $\pm 20$  mm relative to the designated seating position. The H-point y-position was changed by  $\pm 5$  mm, and the H-point z-coordinate was evaluated for +10 mm and +20 mm higher seating positions. The THOR in the baseline simulation was positioned using CMM data, which was recorded after a physical dummy has been positioned in the mid-size sedan vehicle according to the latest THOR positioning protocol. The head angle, defined as the fourth parameter, was changed by  $\pm 5^\circ$  relative to the position in the baseline simulation. Different head angles were realized by rotating the upper body accordingly. A head and torso angle of  $+5^\circ$  represents a more reclined seating posture, and a  $-5^\circ$  angle correlates with a more upright seating position. The knee-to-knee distance was identified as the fifth relevant parameter. Knee-to-knee distance was changed by +30 mm and +60 mm relative to the baseline simulation. When changing the knee-to-knee distance, ankle-to-ankle distance was changed accordingly.

The most important parameter for the passengers HIC criteria was the head/torso angle. A more reclined seating posture correlated with more overall forward motion and increased the likelihood of impacting the instrument panel in the analyzed vehicle environment, which resulted in higher HIC values. A more reclined seating posture also correlated with higher chest and abdomen deflection.

BrIC criteria were mostly affected by the occupant's initial y-position. A more outward seating position resulted in higher BrIC values due to higher head yaw motion caused by the interaction with the passenger air bag. Similarly, a higher combination of neck tension and flexion was observed for a more outward seating position due to the interaction with the passenger air bag.

A more reclined seating posture and larger knee-to-knee distance allowed the far-side occupant to gain more momentum and resulted in higher forces between the pelvis-belt and the abdomen. Since the seat belt slid off the shoulder of THOR on the passenger seat, maximum chest deflection occurred for the lower chest locations and was caused by interaction with the seat belt.

Femur and acetabulum forces were mostly affected by the initial longitudinal seating position. A more forward seating position correlated with higher forces due to a more severe interaction with instrument panel. The most important parameters for the maximum tibia loads were the H-point x-coordinate and the knee-to-knee distance. A more rearward seating position and more spread out upper legs correlated with higher tibia loads, specifically upper tibia moments, due to differences in lower extremity kinematics.

Knee-to-knee distance showed the most influence for the chest deflection (37%) and the second-most influence for the BrIC (26%) for the THOR on the passenger seat. More spread out legs allowed the occupant to move more forward resulting in higher forces between the belt and the lower chest area. Similarly, more spread out legs allowed the occupant to gain more momentum.

With the seat belt sliding off the shoulder, differences in upper body kinematics resulted in higher contact forces between the head and the passenger air bag, resulting in higher BrIC values, to higher head angular velocities around the local z-axis.

Differences in occupant kinematics and injury criteria for the THOR on the passenger seat were larger than for the near-side occupant, as documented in **Appendix B25**. Changing relevant THOR positioning parameters beyond tolerances, as defined in the seating procedure protocol, resulted in a more significant effect on the occupant kinematics and injury criteria. The more sensitive outcome can be partly contributed to the larger range of respective parameters and partly to the far-side seating position. The near-side occupant's motion on the driver seat in the oblique impact configuration was well controlled by the seat belt, driver air bag, and side curtain air bag. The far-side THOR on the passenger seat moved towards the middle of the vehicle, the seat belt slid off the shoulder, and the head rolled off the passenger air bag and hit the instrument panel in some cases.

Despite these observations it was found that 37 out of 41 conducted simulations obtained an overall star rating of 2.5-stars or 3-stars. The overall CORA rating was between 0.7 and 0.9, i.e., time history data showed "GOOD" to "ACCEPTABLE/FAIR" correlation, when compared to the designated seating position used in the baseline simulation.

## **10. Limitations**

The documented results and conclusions are based on finite element simulations with a validated FE model of a mid-size sedan vehicle and existing THOR occupant models. Findings do not necessarily apply to other vehicle structures and restraint systems.

DoE immanent limitations apply. Validated response surfaces and trend-lines were used to determine the relationship between factors affecting NHTSA's oblique impact test procedure and the output represented by vehicle and occupant injury metrics. A Box-Behnken DoE approach was used to generate surrogate models, which are based on fewer design points, i.e., simulation runs, than full factorial methods.

## 11. Conclusion

A baseline simulation for NHTSA's left oblique impact condition was conducted with an FE model of a 2014 Honda Accord mid-size sedan vehicle and a THOR dummy in the driver and front passenger seat. Vehicle kinematics, vehicle pulse, occupant kinematics, and occupant injury criteria were compared with results from a full-scale test of the same vehicle. All evaluated criteria compared reasonably well with the specific test results for all body regions. The integrated occupant-vehicle model with all relevant restraints was used to conduct parametric studies to understand the effect of different parameters. ANOVA analysis was used to determine the importance of each parameter. Graphs and response surfaces were used to visualize the effect of individual parameters and combination of parameters.

In the first part of this research, the Test Procedure Study, relevant parameters for setting up NHTSA's oblique frontal impact test and their effect on vehicle and occupant criteria were determined. Parameters included the OMDB impact angle, vertical misalignment, overlap, mass, and impact speed.

Three studies were conducted within the test procedure analysis to understand the importance of the different parameters: (1) In the Repeatability Study, parameters were varied within defined full-scale test tolerances. (2) In the Sensitivity Study, parameters were beyond defined test tolerances. (3) In the Impact Angle Study, OMDB impact angles from co-linear  $0^\circ$  to  $20^\circ$  oblique were analyzed.

Good test repeatability was found when changing parameters within the small ranges used as test tolerances. Vehicle delta-v varied by less than 1 m/s and maximum intrusion varied by less than 30 mm when taking all combinations of parameters into account. The overall CORA score for time-history data ranged from 0.86 to 0.94 for the driver and 0.81 to 0.94 for the passenger, when compared to the baseline simulation. Impact speed was the most important factor for vehicle pulse in x-direction and impact angle was most dominant for vehicle y-pulse.

More significant effects were observed when evaluating a wider range of parameters in the Sensitivity Study. Vehicle delta-v in x- and y-direction varied by more than 3 m/s and 2 m/s, respectively. Maximum toe-pan intrusion varied by about 60 mm. The overall CORA score for time-history data ranged from 0.71 to 0.87 for the driver and 0.73 to 0.90 for the passenger. BrIC increased with higher delta-v for the far-side occupant. Impact speed was the most important factor for the driver. Impact angle was found to be more relevant for far-side occupant results.

Differences were even more significant in the Impact Angle Study with CORA values between 0.63 to 0.83. Different vehicle yaw motion, ranging from counter clock-wise yaw for  $0^\circ$  co-linear impact to clock-wise yaw of similar extent for  $20^\circ$  oblique conditions, was observed. Substantial differences in vehicle yaw motion and y-pulse resulted in different occupant kinematics, especially for the far-side THOR.

BrIC increased (due to more head rotational motion) and HIC decreased (due to marginally smaller head translational motion) with increased principle direction of force (PDOF), i.e., a more oblique or angled impact. Differences were larger for the passenger due to the absence of

side curtain interaction compared to the driver side. Higher overall injury risk was observed for more oblique impact conditions for the passenger in the far-side seating position. A similar overall injury risk of the near-side occupant was found when comparing the 20° and 0° configurations. The oblique impact showed higher BRIC values but lower chest deflection when compared to the co-linear condition for the driver.

In the second part of this research, the THOR Position Study,” the integrated occupant-vehicle model was used to conduct parametric studies to understand the effect of different parameters relevant for positioning the THOR. Parameters included the H-point x-, y-, and z-coordinate, the head/torso angle, and the position of the lower extremities. The effect of these parameters on the occupant kinematics and injury risk was evaluated. It was determined which parameter was most important for the respective outcomes, and what effect each parameter had.

The THOR on the driver seat was used to conduct a repeatability study.” Parameters were changed within defined tolerances. E.g., head and torso angle were varied by  $\pm 1^\circ$ . The overall CORA score ranged between 0.81 and 0.94 when compared to the baseline condition. A value above 0.8 was considered a “GOOD” correlation. It was concluded that NHTSA’s frontal oblique test configuration showed good test repeatability when relevant parameters for positioning the THOR on the driver seat were changed within small tolerances, as defined in the seating procedure protocol.

The THOR on the passenger seat was used to conduct a sensitivity study.” Parameters were changed within ranges that are beyond defined test protocol tolerances. E.g. head and torso angle were varied by  $\pm 5^\circ$ . Differences in occupant kinematics and injury risk were larger than for the driver side, which can be partly ascribed to the larger range for respective parameters and partly to the less controlled kinematics of the far-side occupant. The overall CORA rating was between 0.7 and 0.9, i.e., time history data showed “GOOD” to “ACCEPTABLE/FAIR” correlation, when compared to the designated seating position used in the baseline simulation.

An overview of the most important parameters and their effect of respective body regions is documented in **Appendix B26**.

The conducted studies using integrated occupant vehicle simulations with relevant restraints allowed valuable insight into the effect of different THOR positioning parameters for NHTSA’s oblique impact condition.

In summary, NHTSA’s oblique frontal offset impact test showed overall good repeatability with respect to vehicle kinematics and injury risk, when relevant parameters were changed within defined tolerances.

## **APPENDIX A: Test Procedure Study Additional Graphs**

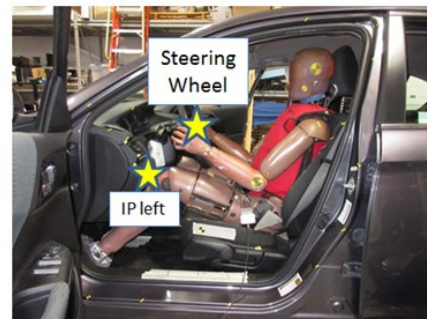
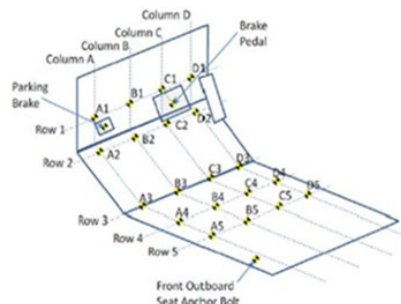
### A1. Test Versus Simulation for Driver and Passenger

Test	Criteria (THOR)		BL Simulation			Test	Criteria (THOR)		BL Sim.
Driver	LWR	UPR	Driver	Driver*		Passenger	LWR	UPR	Passenger
186	500	700	353	353	HIC	859	500	700	606
0.61	0.71	1.05	0.89	0.61	BRIC	1.48	0.71	1.05	1.3
0.19	0.39	0.85	0.32	0.32	Ntf	0.12	0.39	0.85	0.68
0.03	0.39	0.85	0.22	0.22	Ncf	0.01	0.39	0.85	0.09
0.24	0.39	0.85	0.3	0.3	Nte	0.41	0.39	0.85	0.47
0.01	0.39	0.85	0.07	0.07	Nce	0.05	0.39	0.85	0.08
25	37.9	52.3	27	27	Chest-UL	31	37.9	52.3	28
49	37.9	52.3	47	47	Chest-UR	27	37.9	52.3	30
1	37.9	52.3	9	9	Chest-LL	39	37.9	52.3	38
37	37.9	52.3	32	32	Chest-LL	6	37.9	52.3	12
50	NA	88.6	54	54	ABDO-LE	66	NA	88.6	62
62	NA	88.6	54	54	ABDO-RI	59	NA	88.6	62
1733	2583	3486	1996	1996	ACET-LE	4456	2583	3486	2183
2075	2583	3486	981	981	ACET-RI	2537	2583	3486	2466
3372	5331	8558	4461	4461	FEM-LE	5194	5331	8558	4788
2010	5331	8558	4361	4361	FEM-RI	5516	5331	8558	1279
945	4235	5577	638	638	FZ TI UL	1660	4235	5577	877
1515	4235	5577	1164	1164	FZ TI UR	1420	4235	5577	828
2921	3573	5861	1615	1615	FZ TI LL	1421	3573	5861	3202
3188	3573	5861	3243	3243	FZ TI LR	936	3573	5861	2884
113	178	240	94	94	MR TI UL	69	178	240	164
83	178	240	106	106	MR TI UR	42	178	240	189
80	178	240	70	70	MR TI LL	174	178	240	108
101	178	240	84	84	MR TI LR	82	178	240	97
81			68	84	Points	60			57
4.5★			3.5★	4.5★	Stars	3.0★			3.0★
25			9	25	Head	0			0
25			25	25	Neck	24			9.25
5.75			9.25	9.25	Chest	23			24.8
25			25	25	Legs	12.5			22.8

Calculation of overall score without considering BRIC (using test value)

## A2. Test Versus Simulation for Vehicle Intrusion and Pulse

	Driver-Side			Passenger-Side	
	Test	BL Sim.		Test	BL Sim.
	x [mm]	x [mm]		x [mm]	x [mm]
A1	100	102	A1	6	19
B1	142	128	B1	5	15
C1	133	150	C1	4	12
D1	103	101	D1	1	8
A2	76	82	A2	2	15
B2	84	104	B2	1	13
C2	96	110	C2	3	10
D2	71	83	D2	2	6
A3	37	52	A3	0	20
B3	46	62	B3	2	13
C3	50	88	C3	3	9
D3	39	64	D3	2	7
A4	0	26	A4	0	17
B4	2	29	B4	2	10
C4	3	31	C4	1	8
D4	4	26	D4	2	4
A5	1	26	A5	0	17
B5	1	27	B5	1	10
C5	0	29	C5	3	9
D5	0	24	D5	1	6
Break Pedal	171	156			
IP left	14	36	IP left	20	14
IP right	2	29	IP right	10	5
Steering Column	1	19			
Max. Toe Pan	142	150	Max. TP	6	20
dv(x) [m/s]	15.5	14.8			
dv(y) [m/s]	5.3*	5.5*			
	* at 90ms				



### A3. Test Procedure Repeatability Study – Simulation Matrix

	P1	P2	P3	P4	P5
DOE #	Impact Angle	Vert. Misall. (z)	Horiz. Misall. (y)	OMDB Mass	Impact Speed
1	16	50	0	2486	90
2	16	-50			
3	14	50			
4	14	-50			
5	16	0	50	2486	90
6	16		-50		
7	14		50		
8	14		-50		
9	16	0	0	2436	90
10	16			2536	
11	14			2436	
12	14			2536	
13	16	0	0	2486	91
14	16				89
15	14				91
16	14				89
17	15	50	50	2486	90
18		50	-50		
19		-50	50		
20		-50	-50		
21	15	50	0	2436	90
22		50		2536	
23		-50		2436	
24		-50		2536	
25	15	50	0	2486	91
26		50			89
27		-50			91
28		-50			89
29	15	0	50	2436	90
30			50	2536	
31			-50	2436	
32			-50	2536	
33	15	0	50	2486	91
34			50		89
35			-50		91
36			-50		89
37	15	0	0	2436	91
38				2536	89
39				2436	91
40				2536	89
41	15	0	0	2486	90

#### A4. Repeatability Study – Vehicle Results Near-Side

DOE #	1	2	3	4	5	6	7	8	9	10	11	12	13	14	15	16	17	18	19	20
Impact Angle	16	16	14	14	16	16	14	14	16	16	14	14	16	16	14	14	15	15	15	15
Vert. Misal. (z)	50	-50	50	-50	0	0	0	0	0	0	0	0	0	0	0	0	50	50	-50	-50
Horiz. Misal. (y)	0	0	0	0	50	-50	50	-50	0	0	0	0	0	0	0	0	50	-50	50	-50
OMDB Mass	2486	2486	2486	2486	2486	2486	2486	2486	2436	2536	2436	2536	2486	2486	2486	2486	2486	2486	2486	2486
Impact Speed	90	90	90	90	90	90	90	90	90	90	90	90	91	89	91	89	90	90	90	90
A1	91	100	104	99	101	107	94	112	94	97	98	107	102	89	104	96	89	100	103	107
B1	110	127	130	128	132	129	119	136	118	122	121	129	126	111	122	121	111	124	127	132
C1	131	148	151	149	153	149	138	157	138	141	143	150	150	132	142	144	129	148	143	155
D1	83	104	102	101	105	105	92	114	89	91	95	100	98	86	96	98	83	95	99	112
A2	74	81	84	80	82	90	77	94	76	78	79	84	82	74	82	78	71	80	88	88
B2	89	103	105	103	107	105	97	111	95	97	100	104	102	90	99	99	88	101	101	109
C2	91	110	110	111	111	109	102	116	99	102	104	108	107	94	103	105	91	108	101	116
D2	68	86	83	84	83	87	74	95	72	74	77	80	82	71	79	80	65	81	79	95
A3	46	51	53	53	51	57	50	60	48	50	51	54	52	46	54	51	44	52	55	57
B3	54	62	64	63	63	65	59	69	57	59	61	64	63	54	63	60	52	62	62	68
C3	76	88	88	92	88	88	83	94	80	82	84	88	88	77	86	85	72	90	81	94
D3	58	65	64	69	63	67	61	74	58	59	61	64	67	58	66	63	51	68	60	73
A4	24	26	28	29	26	30	27	33	24	26	28	29	27	24	31	27	21	28	28	32
B4	27	29	31	32	29	33	29	37	27	29	31	32	31	26	34	30	23	32	30	35
C4	30	31	32	35	31	35	31	39	29	30	32	34	34	29	36	32	24	36	32	38
D4	25	27	28	31	27	30	27	35	25	26	27	30	29	24	32	28	20	30	27	33
A5	24	26	29	29	26	30	27	33	25	26	28	29	28	24	32	27	21	29	28	32
B5	25	27	29	30	27	30	27	34	25	27	29	30	29	24	32	28	21	30	28	33
C5	27	29	30	32	28	32	29	36	27	28	30	32	31	26	34	29	22	32	30	35
D5	23	25	26	29	25	28	26	32	23	24	26	28	27	23	29	26	19	29	24	30
Break Pedal	152	135	156	164	158	156	148	163	154	140	155	181	164	139	165	162	150	127	151	157
IP left	31	35	38	37	33	41	36	42	35	36	35	40	40	33	39	36	33	35	38	43
IP right	24	26	29	30	27	32	26	34	25	25	26	32	31	24	31	28	23	26	29	31
Steering Column	15	20	21	19	20	23	20	27	21	19	22	23	21	16	22	18	17	17	24	22
Max. Toe Pan	131	148	151	149	153	149	138	157	138	141	143	150	150	132	142	144	129	148	143	155
	[m/s]	[m/s]	[m/s]	[m/s]	[m/s]	[m/s]	[m/s]	[m/s]	[m/s]	[m/s]	[m/s]	[m/s]	[m/s]	[m/s]	[m/s]	[m/s]	[m/s]	[m/s]	[m/s]	[m/s]
dv(x)	14.8	14.7	14.6	14.9	14.9	14.7	15	14.6	14.6	14.9	14.8	15	14.9	14.6	15	14.7	14.9	14.9	14.6	14.7
dv(y)	5.9	6.2	5.6	5.7	5.8	6.1	5.7	5.8	5.8	6.1	5.5	5.5	6.1	5.9	5.7	5.4	5.9	5.8	5.8	5.8

DOE #	21	22	23	24	25	26	27	28	29	30	31	32	33	34	35	36	37	38	39	40	41
Impact Angle	15	15	15	15	15	15	15	15	15	15	15	15	15	15	15	15	15	15	15	15	15
Vert. Misal. (z)	50	50	-50	-50	50	50	-50	-50	0	0	0	0	0	0	0	0	0	0	0	0	0
Horiz. Misal. (y)	0	0	0	0	0	0	0	0	50	50	-50	-50	50	50	-50	-50	0	0	0	0	0
OMDB Mass	2436	2536	2436	2536	2486	2486	2486	2486	2436	2536	2436	2536	2486	2486	2486	2486	2436	2536	2436	2536	2486
Impact Speed	90	90	90	90	91	89	91	89	90	90	90	90	91	89	91	89	91	89	91	89	90
A1	88	94	89	104	100	90	106	99	90	92	104	110	95	87	114	102	104	89	108	98	102
B1	107	114	111	125	121	110	132	122	115	117	123	134	117	114	137	124	126	111	130	121	128
C1	128	135	129	143	141	130	157	139	136	144	143	154	135	136	157	144	147	130	149	143	150
D1	78	90	83	99	95	85	108	93	91	93	100	112	92	90	112	101	99	86	100	96	101
A2	68	76	71	82	80	70	88	78	73	76	86	91	77	70	92	83	84	72	85	79	82
B2	84	91	88	101	96	86	110	98	94	96	101	110	95	93	111	100	103	89	105	99	104
C2	87	94	91	107	99	89	118	104	99	102	105	115	100	98	116	104	107	93	109	104	110
D2	63	73	65	82	76	67	90	78	73	77	83	93	73	73	93	83	82	71	81	77	83
A3	43	48	44	53	51	43	58	50	45	48	55	61	50	44	59	52	54	45	55	49	52
B3	51	56	52	63	59	51	68	60	54	58	63	70	59	54	69	61	64	54	65	59	62
C3	73	77	72	88	81	72	97	85	78	85	86	94	82	78	93	84	88	77	89	83	88
D3	55	58	51	66	61	54	72	63	56	64	65	72	61	57	71	64	66	58	65	61	64
A4	22	25	21	30	27	21	33	28	21	25	30	35	28	20	32	27	30	24	30	25	26
B4	25	28	23	33	30	24	36	30	24	28	33	38	31	23	35	30	33	27	33	28	29
C4	28	30	24	35	31	26	38	33	25	32	35	40	32	25	37	32	35	29	34	30	31
D4	23	25	20	30	27	21	33	28	21	27	29	36	28	22	32	27	30	25	29	25	26
A5	22	25	21	30	27	21	33	28	21	25	30	35	29	21	33	27	30	24	30	26	26
B5	23	26	21	31	28	22	34	28	22	26	31	36	29	21	33	28	31	25	31	26	27
C5	25	27	22	32	29	23	35	30	23	29	32	37	30	23	35	30	32	26	32	27	29
D5	21	23	19	28	25	20	31	27	20	26	27	32	27	20	30	25	28	23	28	24	24
Break Pedal	148	153	150	164	159	147	165	131	138	155	153	152	128	139	164	157	168	143	174	153	156
IP left	31	34	33	40	38	30	41	35	27	33	38	44	38	28	45	35	39	34	44	33	36
IP right	22	27	23	29	29	24	32	25	20	26	29	34	26	21	34	28	30	25	33	26	29
Steering Column	13	18	17	20	21	15	23	18	15	18	21	27	21	11	28	21	22	18	23	19	19
Max. Toe Pan	128	135	129	143	141	130	157	139	136	144	143	154	135	136	157	144	147	130	149	143	150
	[m/s]	[m/s]	[m/s]	[m/s]	[m/s]	[m/s]	[m/s]	[m/s]	[m/s]	[m/s]	[m/s]	[m/s]	[m/s]	[m/s]	[m/s]	[m/s]	[m/s]	[m/s]	[m/s]	[m/s]	[m/s]
dv(x)	14.6	14.8	14.7	14.8	14.9	14.6	15	14.6	14.7	15	14.5	14.8	15.1	14.6	14.8	14.5	15	14.5	15.1	14.7	14.8
dv(y)	5.8	5.8	5.9	5.9	5.8	5.7	6.2	5.8	5.7	6	5.8	5.9	5.9	5.8	6	5.8	5.8	5.6	5.8	5.7	5.8

## A5. Repeatability Study – Vehicle Results Far-side

DOE #	1	2	3	4	5	6	7	8	9	10	11	12	13	14	15	16	17	18	19	20
	41	42	43	44	45	46	47	48	49	50	51	52	53	54	55	56	16	17	18	19
Impact Angle	16	16	14	14	16	16	14	14	16	16	14	14	16	16	14	14	15	15	15	15
Vert. Misal. (z)	50	-50	50	-50	0	0	0	0	0	0	0	0	0	0	0	0	50	50	-50	-50
Horiz. Misal. (y)	0	0	0	0	50	-50	50	-50	0	0	0	0	0	0	0	0	50	-50	50	-50
OMDB Mass	2486	2486	2486	2486	2486	2486	2486	2486	2436	2536	2436	2536	2486	2486	2486	2486	2486	2486	2486	2486
Impact Speed	90	90	90	90	90	90	90	90	90	90	90	90	91	89	91	89	90	90	90	90
A1	14	18	21	22	20	16	22	20	17	17	21	21	17	15	22	19	18	19	15	20
B1	15	13	15	18	15	12	18	14	13	14	18	18	15	13	19	15	15	16	12	14
C1	13	9	12	13	10	8	15	10	10	11	14	14	12	10	15	12	12	12	9	9
D1	9	7	8	8	6	6	10	7	7	7	9	9	8	7	9	7	8	8	6	6
A2	14	18	15	20	17	17	19	18	15	16	18	19	16	14	20	16	13	19	13	19
B2	13	15	14	17	14	14	17	17	12	13	16	17	13	12	18	14	13	15	11	16
C2	11	9	10	12	9	8	13	10	9	10	13	13	11	9	13	10	11	11	8	9
D2	8	5	6	7	5	5	9	5	5	6	8	8	7	6	8	6	7	6	5	5
A3	17	22	20	23	21	22	21	24	19	20	21	23	20	18	23	20	16	22	18	25
B3	12	14	14	16	14	13	16	16	13	13	16	17	13	12	17	14	12	14	11	15
C3	9	8	9	10	8	8	11	9	8	9	10	11	9	8	11	9	8	9	7	9
D3	8	6	7	8	7	6	8	7	7	7	8	8	7	7	8	7	7	7	6	6
A4	16	19	17	20	18	20	19	22	16	17	19	20	18	16	21	18	14	20	16	22
B4	10	11	10	12	11	11	12	13	10	11	12	13	11	10	13	11	10	12	9	12
C4	8	8	8	9	8	8	9	9	8	8	9	10	8	7	10	8	7	8	7	9
D4	4	4	5	5	5	5	5	6	4	5	5	6	5	4	6	5	4	5	4	5
A5	15	19	17	20	18	19	19	22	16	17	19	20	18	16	21	18	13	20	16	22
B5	10	10	10	11	11	10	12	12	10	10	11	12	10	9	12	10	9	11	9	11
C5	8	9	9	10	9	9	10	11	9	9	10	11	9	8	11	9	8	9	8	10
D5	6	6	6	6	6	6	6	7	5	6	6	7	6	5	7	6	5	6	5	7
IP left	11	12	12	20	13	16	12	16	12	12	11	14	16	12	14	13	11	13	13	15
IP right	4	4	5	9	3	5	4	5	4	3	4	6	5	5	6	5	3	6	5	5
Max. Toe Pan	17	22	21	23	21	22	22	24	19	20	21	23	20	18	23	20	18	22	18	25

DOE #	21	22	23	24	25	26	27	28	29	30	31	32	33	34	35	36	37	38	39	40	41
	57	58	59	60	20	21	22	23	61	62	63	64	24	25	26	27	65	66	67	68	2
Impact Angle	15	15	15	15	15	15	15	15	15	15	15	15	15	15	15	15	15	15	15	15	15
Vert. Misal. (z)	50	50	-50	-50	50	50	-50	-50	0	0	0	0	0	0	0	0	0	0	0	0	0
Horiz. Misal. (y)	0	0	0	0	0	0	0	0	50	50	-50	-50	50	50	-50	-50	0	0	0	0	0
OMDB Mass	2436	2536	2436	2536	2486	2486	2486	2486	2436	2536	2436	2536	2486	2486	2486	2486	2536	2436	2536	2486	2486
Impact Speed	90	90	90	90	91	89	91	89	90	90	90	90	91	89	91	89	91	89	91	89	90
A1	12	16	21	22	19	14	22	17	17	17	18	21	22	16	20	14	23	15	22	18	19
B1	12	13	16	17	15	13	17	15	13	16	12	14	18	13	14	11	18	13	17	13	15
C1	11	11	12	12	12	11	12	12	10	14	9	9	15	11	10	8	14	11	13	10	12
D1	7	8	8	8	8	7	8	8	7	9	6	7	10	8	7	6	9	7	9	7	8
A2	11	13	19	19	15	11	21	18	12	16	15	17	19	12	17	12	19	14	18	14	15
B2	10	11	16	16	13	11	16	14	11	14	14	16	17	12	16	10	17	12	16	12	13
C2	9	9	11	11	11	9	11	11	9	12	8	9	13	10	10	7	13	10	12	9	10
D2	6	6	6	7	7	6	6	7	6	8	5	5	9	7	5	4	8	6	7	6	6
A3	14	18	23	23	19	15	25	21	16	19	20	24	22	16	23	18	23	18	23	19	20
B3	9	11	15	15	13	10	16	14	11	13	13	15	16	11	16	11	16	12	16	13	13
C3	7	8	10	10	9	7	10	9	7	10	8	9	11	8	9	7	11	8	10	8	9
D3	6	7	8	8	7	6	7	7	6	7	6	7	8	7	7	5	8	7	8	6	7
A4	13	15	21	21	17	13	22	19	13	17	18	22	20	14	21	16	20	16	20	17	17
B4	8	9	12	11	10	8	13	11	8	10	10	13	12	9	13	9	13	10	12	10	10
C4	6	7	9	9	8	6	10	8	6	8	8	10	9	6	9	7	9	7	9	8	8
D4	3	4	5	5	5	3	6	5	4	4	5	6	5	4	6	4	5	4	5	5	4
A5	13	15	21	21	17	13	22	18	13	17	18	21	19	13	20	16	20	16	20	16	17
B5	7	9	12	11	10	8	12	10	8	10	10	12	12	8	12	8	12	9	12	10	10
C5	6	8	10	10	9	7	11	9	7	9	9	11	10	7	10	8	11	8	11	9	9
D5	4	5	7	6	6	5	7	6	5	5	6	7	7	4	7	5	7	5	7	6	6
IP left	9	12	14	14	14	9	15	10	9	12	16	18	13	9	16	14	14	14	16	12	14
IP right	3	5	6	5	6	4	7	5	5	5	6	6	4	3	6	6	4	5	6	4	5
Max. Toe Pan	14	18	23	23	19	15	25	21	17	19	20	24	22	16	23	18	23	18	23	19	20

## A6. Repeatability Study – Driver Results

DOE #			1	2	3	4	5	6	7	8	9	10	11	12	13	14	15	16	17	18	19	20
Impact Angle			16	16	14	14	16	16	14	14	16	16	14	14	16	16	14	14	15	15	15	15
Vert. Misall. (z)			50	-50	50	-50	0	0	0	0	0	0	0	0	0	0	0	0	50	50	-50	-50
Horiz. Misall. (y)			0	0	0	0	50	-50	50	-50	0	0	0	0	0	0	0	0	50	-50	50	-50
OMDB Mass			2486	2486	2486	2486	2486	2486	2486	2486	2436	2536	2436	2536	2486	2486	2486	2486	2486	2486	2486	2486
Impact Speed			90	90	90	90	90	90	90	90	90	90	90	90	91	89	91	89	90	90	90	90
HIC	500	700	381	373	370	385	369	362	370	366	369	384	378	370	393	391	381	366	366	378	375	379
BRIC	0.71	1.05	0.96	0.91	0.9	0.85	0.9	0.93	0.88	0.85	0.93	0.93	0.93	0.88	0.9	0.94	0.93	0.89	0.95	0.9	0.92	0.91
Ntf	0.39	0.85	0.28	0.1	0.31	0.09	0.01	0.31	0.05	0.33	0.11	0.14	0.07	0.32	0.32	0.13	0.32	0.3	0.32	0.27	0.29	0.3
Ncf	0.39	0.85	0.19	0.22	0.12	0.21	0.07	0.23	0.13	0.22	0.21	0.21	0.18	0.14	0.21	0.2	0.18	0.24	0.19	0.15	0.13	0.22
Nte	0.39	0.85	0.37	0.38	0.35	0.37	0.35	0.36	0.37	0.37	0.37	0.36	0.35	0.36	0.4	0.37	0.4	0.36	0.4	0.37	0.36	0.38
Nce	0.39	0.85	0.1	0.13	0.19	0.09	0.1	0.09	0.16	0.09	0.09	0.13	0.09	0.09	0.09	0.1	0.09	0.09	0.17	0.13	0.16	0.09
Chest-UL	37.9	52.3	27	28	28	29	28	25	28	28	27	27	27	27	28	26	27	26	27	28	27	28
Chest-UR	37.9	52.3	48	47	48	47	48	47	48	48	48	48	47	48	48	47	48	47	46	49	48	48
Chest-LL	37.9	52.3	16	15	19	16	15	17	17	18	15	16	17	18	16	13	17	17	18	15	20	18
Chest-LR	37.9	52.3	33	33	34	34	35	32	35	33	32	33	33	33	32	33	33	32	33	35	33	33
ABDO-LE	NA	88.6	55	55	52	56	53	54	53	53	53	52	55	55	55	53	54	54	53	54	52	55
ABDO-RI	NA	88.6	56	54	51	54	52	53	52	53	53	51	55	54	56	53	54	54	53	54	50	54
ACET-LE	2583	3486	1923	1919	2035	2385	2145	1832	2236	2014	2027	2068	2234	2250	2068	1897	2215	2245	2059	2260	1791	2008
ACET-RI	2583	3486	873	939	832	972	937	1051	923	1047	910	883	979	1014	1123	929	899	988	895	984	1007	1042
FEM-LE	5331	8558	3724	3987	4285	4212	3875	4549	3937	4594	4646	4474	3953	4448	4709	3502	4505	3876	4469	3519	4640	5324
FEM-RI	5331	8558	4474	4104	5179	4551	4435	4739	4390	5064	4324	4434	4602	5333	4474	4122	5171	4872	4842	4426	4798	4974
FZ TI UL	4235	5577	598	654	648	631	646	735	682	570	688	647	650	622	622	723	638	641	665	667	682	614
FZ TI UR	4235	5577	1265	1150	1121	1219	1171	1027	1140	1138	1061	1044	1085	1065	1266	1141	1126	1133	1056	1456	988	1087
FZ TI LL	3573	5861	1523	1596	1412	1572	1639	1805	1618	1749	1641	1624	1642	1712	1634	1620	1795	1582	1622	1640	1541	1666
FZ TI LR	3573	5861	3080	3949	2873	3721	3489	3474	3311	3278	3371	3321	2983	3092	3581	3381	3123	2940	2968	4054	2934	3872
MR TI UL	178	240	70	99	82	91	84	80	68	74	79	88	80	82	101	78	82	91	88	74	89	113
MR TI UR	178	240	100	98	130	98	108	107	103	106	98	96	94	97	108	89	96	95	89	102	108	105
MR TI LL	178	240	71	105	237	76	86	190	69	104	74	80	67	73	79	67	80	66	65	191	194	114
MR TI LR	178	240	78	97	129	77	109	83	93	98	83	78	71	60	82	75	70	73	69	101	104	86
Points			63	65	54	70	66	64	67	69	64	64	66	67	66	66	64	68	66	62	62	64
Stars			3.5★	3.5★	3.0★	3.5★	3.5★	3.5★	3.5★	3.5★	3.5★	3.5★	3.5★	3.5★	3.5★	3.5★	3.5★	3.5★	3.5★	3.5★	3.5★	3.5★
CORA			0.91	0.94	0.88	0.93	0.91	0.93	0.91	0.88	0.94	0.93	0.94	0.91	0.92	0.92	0.94	0.92	0.93	0.90	0.86	0.92

DOE #			21	22	23	24	25	26	27	28	29	30	31	32	33	34	35	36	37	38	39	40	41	
Impact Angle			15	15	15	15	15	15	15	15	15	15	15	15	15	15	15	15	15	15	15	15	15	
Vert. Misall. (z)			50	50	-50	-50	50	50	-50	-50	0	0	0	0	0	0	0	0	0	0	0	0	0	
Horiz. Misall. (y)			0	0	0	0	0	0	0	0	50	50	-50	-50	50	50	-50	-50	0	0	0	0	0	
OMDB Mass			2436	2536	2436	2536	2486	2486	2486	2486	2436	2536	2436	2536	2486	2486	2486	2486	2436	2536	2436	2536	2486	
Impact Speed			90	90	90	90	91	89	91	89	90	90	90	90	91	89	91	89	91	89	91	89	90	
HIC	500	700	384	412	355	352	406	376	377	349	362	378	340	382	385	360	368	356	384	372	368	379	353	
BRIC	0.71	1.05	0.93	0.96	0.89	0.91	0.92	0.94	0.85	0.92	0.93	0.91	0.9	0.89	0.9	0.9	0.95	0.89	0.92	0.88	0.96	0.89		
Ntf	0.39	0.85	0.12	0.33	0.27	0.25	0.06	0.3	0.12	0.08	0.07	0.27	0.09	0.3	0.1	0.26	0.28	0.09	0.08	0.13	0.3	0.33	0.29	
Ncf	0.39	0.85	0.19	0.19	0.2	0.18	0.21	0.2	0.16	0.19	0.2	0.2	0.19	0.14	0.2	0.22	0.21	0.27	0.14	0.2	0.16	0.19	0.22	
Nte	0.39	0.85	0.36	0.36	0.36	0.39	0.38	0.35	0.37	0.37	0.36	0.38	0.35	0.36	0.37	0.38	0.36	0.35	0.37	0.38	0.37	0.37	0.37	
Nce	0.39	0.85	0.19	0.16	0.13	0.09	0.09	0.09	0.09	0.14	0.09	0.09	0.09	0.09	0.09	0.09	0.09	0.1	0.1	0.1	0.09	0.09	0.09	
Chest-UL	37.9	52.3	28	27	28	29	28	28	28	27	28	28	26	27	28	28	28	27	27	27	27	27	27	
Chest-UR	37.9	52.3	48	47	49	49	48	46	49	47	47	49	46	47	49	47	48	47	48	47	48	47	47	
Chest-LL	37.9	52.3	17	19	17	17	19	16	18	16	16	16	17	18	18	15	18	15	17	15	19	16	16	
Chest-LR	37.9	52.3	34	33	35	33	34	34	33	34	34	35	31	33	35	34	33	34	33	34	33	32	32	
ABDO-LE	NA	88.6	54	55	51	55	54	52	55	54	53	54	56	55	54	55	55	52	56	53	54	55	54	
ABDO-RI	NA	88.6	54	55	50	54	53	53	53	53	53	55	54	53	51	53	54	50	54	53	53	55	54	
ACET-LE	2583	3486	2043	1983	2110	2208	1880	2043	2350	2191	2259	2253	2003	1857	2210	2146	1773	1906	2239	2102	2135	2038	1996	
ACET-RI	2583	3486	1004	1027	940	983	948	1020	992	1061	908	985	1061	1036	1012	942	933	1076	914	1012	1057	942	981	
FEM-LE	5331	8558	5185	4318	4815	5216	5211	4709	4416	4228	2767	3776	4627	5220	4909	3421	5073	4576	4648	4593	5237	3494	4461	
FEM-RI	5331	8558	4549	4942	4333	4562	5344	4598	4598	4146	4657	4126	5232	5031	4428	4210	5444	4640	4996	4436	5602	4187	4361	
FZ TI UL	4235	5577	614	651	588	593	620	641	666	583	762	702	782	820	657	658	657	602	638	648	613	659	638	
FZ TI UR	4235	5577	1276	1069	1127	1137	1078	1102	1217	1146	1044	1362	1044	1094	1078	1244	1027	1167	1167	1104	1120	1125	1164	
FZ TI LL	3573	5861	1605	1736	1564	1559	1629	1671	1605	1553	1610	1615	1749	1797	1644	1630	1684	1772	1732	1601	1602	1560	1615	
FZ TI LR	3573	5861	3043	3096	3814	3685	2968	2949	3853	3649	3268	3294	3566	3477	3431	3227	3531	3359	3373	3246	3313	3137	3243	
MR TI UL	178	240	70	78	69	83	90	73	103	83	78	74	83	100	95	79	103	76	81	83	112	78	94	
MR TI UR	178	240	87	96	104	100	102	93	112	111	97	92	104	106	96	96	118	106	93	105	100	97	106	
MR TI LL	178	240	66	81	82	69	80	71	173	74	85	72	228	151	77	71	218	85	102	64	77	75	70	
MR TI LR	178	240	78	74	87	87	82	85	96	93	87	85	91	125	87	80	77	99	73	85	83	80	84	
Points			64	64	63	63	65	67	66	66	66	64	60	68	64	68	58	65	67	67	66	64	68	
Stars			3.5★	3.5★	3.5★	3.5★	3.5★	3.5★	3.5★	3.5★	3.5★	3.5★	3.5★	3.5★	3.5★	3.5★	3.5★	3.5★	3.5★	3.5★	3.5★	3.5★	3.5★	
CORA			0.91	0.91	0.94	0.94	0.92	0.91	0.92	0.93	0.91	0.91	0.91	0.91	0.90	0.91	0.94	0.91	0.89	0.95	0.94	0.92	0.94	1.00

## A7. Repeatability Study – Passenger Results

DOE #			1	2	3	4	5	6	7	8	9	10	11	12	13	14	15	16	17	18	19	20
Impact Angle			16	16	14	14	16	16	14	14	16	16	14	14	16	16	14	14	15	15	15	15
Vert. Misall. (z)			50	-50	50	-50	0	0	0	0	0	0	0	0	0	0	0	0	50	50	-50	-50
Horiz. Misall. (y)			0	0	0	0	50	-50	50	-50	0	0	0	0	0	0	0	0	50	-50	50	-50
OMDB Mass			2486	2486	2486	2486	2486	2486	2486	2486	2436	2536	2436	2536	2486	2486	2486	2486	2486	2486	2486	2486
Impact Speed			90	90	90	90	90	90	90	90	90	90	90	90	91	89	91	89	90	90	90	90
HIC	500	700	512	500	373	896	460	612	468	446	340	409	409	347	421	351	771	405	466	457	376	390
BRIC	0.71	1.05	1.49	1.31	1.24	1.14	1.11	1.42	1.45	1.34	1.5	1.29	1.57	1.52	1.3	1.35	1.2	1.14	1.57	1.4	1.24	1.35
Ntf	0.39	0.85	0.7	0.5	0.45	0.49	0.46	0.73	0.66	0.65	0.57	0.46	0.63	0.56	0.51	0.47	0.61	0.52	0.71	0.54	0.51	0.67
Ncf	0.39	0.85	0.08	0.08	0.08	0.08	0.08	0.17	0.08	0.08	0.08	0.08	0.12	0.08	0.08	0.08	0.08	0.08	0.08	0.08	0.08	0.08
Nte	0.39	0.85	0.44	0.5	0.48	0.46	0.47	0.46	0.49	0.48	0.42	0.39	0.51	0.44	0.51	0.43	0.53	0.48	0.49	0.52	0.5	0.49
Nce	0.39	0.85	0.08	0.08	0.08	0.21	0.08	0.08	0.08	0.08	0.08	0.08	0.08	0.08	0.08	0.08	0.12	0.08	0.08	0.08	0.08	0.08
Chest-UL	37.9	52.3	30	27	29	30	28	29	30	30	29	29	29	29	29	28	30	29	29	28	30	29
Chest-UR	37.9	52.3	31	30	31	30	30	30	30	31	30	30	30	30	31	30	31	30	30	30	31	30
Chest-LL	37.9	52.3	39	37	39	38	39	38	39	39	38	38	39	38	39	37	39	39	39	41	39	39
Chest-LL	37.9	52.3	13	11	14	15	10	13	13	14	12	12	14	12	13	12	14	13	13	11	14	12
ABDO-LE	NA	88.6	62	61	62	65	62	63	64	63	63	62	64	63	64	63	63	63	63	62	62	62
ABDO-RI	NA	88.6	64	63	63	65	65	64	65	63	63	64	64	63	64	63	64	63	65	63	62	62
ACET-LE	2583	3486	2273	3518	1946	2611	2784	2517	2402	2607	2109	2082	2372	2255	2337	2199	2338	2136	2257	3212	2062	2388
ACET-RI	2583	3486	2588	3418	2289	2432	3095	2330	2691	2537	2407	2390	2568	2561	2616	2348	2740	2434	2650	3455	2248	2449
FEM-LE	5331	8558	3847	4897	4627	4599	5301	4261	4740	4058	4501	5020	4396	4665	4546	4273	5196	4193	5054	4819	4439	4924
FEM-RI	5331	8558	1199	1129	1118	1092	1256	1246	1074	1260	1057	1280	1077	1277	993	1004	1323	1306	1378	1310	1281	1176
FZ TI UL	4235	5577	869	1020	857	940	896	853	953	895	853	823	933	952	848	808	910	876	915	1024	822	962
FZ TI UR	4235	5577	847	957	860	873	905	873	906	918	717	846	836	882	876	791	939	865	835	947	821	823
FZ TI LL	3573	5861	3213	2717	3328	3528	2935	3086	3497	3641	3071	3337	3095	3362	3227	2711	2978	2913	2973	3063	3157	3174
FZ TI LR	3573	5861	2931	2995	3327	3066	3322	2974	3237	3977	2770	2940	3202	3164	3066	2665	3398	3155	2847	3003	3113	3177
MR TI UL	178	240	157	159	187	169	174	161	152	162	165	168	166	168	158	192	164	149	184	158	199	169
MR TI UR	178	240	204	200	198	199	202	199	188	193	201	201	204	201	207	216	204	201	174	211	195	192
MR TI LL	178	240	101	89	100	107	102	102	99	97	102	106	96	101	112	95	98	97	96	100	101	104
MR TI LR	178	240	95	101	99	103	102	100	96	107	96	97	96	101	103	104	98	90	80	105	100	105
Points			51	52	64	65	57	52	55	55	60	67	55	61	60	63	54	61	53	43	62	55
Stars			3.0★	3.0★	3.5★	3.5★	3.0★	3.0★	3.0★	3.0★	3.5★	3.5★	3.0★	3.5★	3.5★	3.5★	3.0★	3.5★	3.0★	2.5★	3.5★	3.0★
CORA			0.91	0.83	0.87	0.91	0.88	0.90	0.90	0.86	0.87	0.90	0.91	0.88	0.90	0.89	0.94	0.90	0.91	0.81	0.84	0.90

DOE #			21	22	23	24	25	26	27	28	29	30	31	32	33	34	35	36	37	38	39	40	41
Impact Angle			15	15	15	15	15	15	15	15	15	15	15	15	15	15	15	15	15	15	15	15	15
Vert. Misall. (z)			50	50	-50	-50	50	50	-50	-50	0	0	0	0	0	0	0	0	0	0	0	0	0
Horiz. Misall. (y)			0	0	0	0	0	0	0	0	50	50	-50	-50	50	50	-50	-50	0	0	0	0	0
OMDB Mass			2436	2536	2436	2536	2486	2486	2486	2486	2436	2536	2436	2536	2486	2486	2486	2486	2436	2536	2436	2536	2486
Impact Speed			90	90	90	90	91	89	91	89	90	90	90	90	91	89	91	89	91	89	91	89	90
HIC	500	700	359	382	473	378	832	380	463	376	419	619	397	421	413	399	445	421	506	375	1002	401	606
BRIC	0.71	1.05	1.39	1.43	1.43	1.29	1.21	1.5	1.39	1.3	1.38	1.47	1.49	1.39	1.35	1.31	1.42	1.44	1.35	1.38	1.3	1.44	1.3
Ntf	0.39	0.85	0.6	0.64	0.54	0.5	0.62	0.68	0.58	0.43	0.65	0.71	0.71	0.64	0.61	0.52	0.63	0.7	0.71	0.59	0.63	0.66	0.68
Ncf	0.39	0.85	0.08	0.08	0.08	0.08	0.08	0.22	0.08	0.08	0.08	0.27	0.08	0.08	0.08	0.08	0.08	0.08	0.08	0.08	0.08	0.08	0.09
Nte	0.39	0.85	0.47	0.43	0.47	0.47	0.53	0.48	0.46	0.45	0.45	0.46	0.49	0.44	0.5	0.45	0.45	0.51	0.51	0.51	0.52	0.46	0.47
Nce	0.39	0.85	0.08	0.08	0.08	0.08	0.16	0.08	0.08	0.08	0.08	0.08	0.08	0.08	0.08	0.08	0.08	0.08	0.08	0.08	0.22	0.08	0.08
Chest-UL	37.9	52.3	30	30	29	29	30	30	29	29	29	28	29	29	29	28	29	29	29	29	29	29	28
Chest-UR	37.9	52.3	30	30	29	30	31	30	30	30	30	30	30	31	30	30	30	30	31	29	30	30	30
Chest-LL	37.9	52.3	39	39	38	38	39	39	39	38	38	40	38	38	39	39	38	38	39	38	38	38	38
Chest-LL	37.9	52.3	14	14	13	12	14	14	13	14	12	13	14	15	12	13	15	13	14	12	13	11	12
ABDO-LE	NA	88.6	62	62	61	63	62	62	61	64	61	63	64	62	61	62	62	62	63	61	64	63	62
ABDO-RI	NA	88.6	62	63	62	63	62	63	63	63	63	64	63	63	64	62	63	63	62	62	64	63	62
ACET-LE	2583	3486	2219	2223	2772	2182	2255	2107	2669	2226	2494	2837	2384	2698	2637	2454	2526	2431	2428	2235	2237	2108	2183
ACET-RI	2583	3486	2643	2463	2920	2454	2565	2335	3157	2568	2797	3258	2360	2583	3041	2758	2506	2291	2615	2487	2635	2326	2466
FEM-LE	5331	8558	4707	4777	5131	4822	5518	4574	5623	4438	4330	5096	4418	4656	5537	4662	4861	4218	5050	4606	5356	4443	4788
FEM-RI	5331	8558	1151	1303	1160	1093	1386	1161	950	1060	1097	1454	1225	1321	1164	990	1229	993	936	1171	1444	1236	1279
FZ TI UL	4235	5577	835	978	930	778	947	828	967	791	994	926	828	888	1041	904	877	835	878	839	933	891	877
FZ TI UR	4235	5577	823	878	914	875	911	824	837	808	922	867	893	875	945	949	865	815	952	835	955	852	828
FZ TI LL	3573	5861	2911	3212	2971	3247	3182	3131	3038	3020	3224	3171	3308	3282	3240	2944	3268	3026	3283	3200	3383	3124	3202
FZ TI LR	3573	5861	2876	3169	2884	3134	3291	2998	3121	2780	3117	3448	3426	3285	3473	3310	3197	3205	3110	2850	3341	3217	2884
MR TI UL	178	240	188	185	183	161	183	203	177	175	165	156	163	167	166	172	161	172	162	159	159	157	164
MR TI UR	178	240	199	187	219	223	201	194	231	218	187	200	205	192	185	196	201	198	208	198	221	192	189
MR TI LL	178	240	101	105	110	116	110	105	116	110	103	106	107	103	104	97	105	99	104	98	104	100	108
MR TI LR	178	240	99	74	106	112	92	92	112	111	95	100	117	109	90	98	108	105	96	97	98	98	97
Points			56	58	54	60	55	52	44	64	56	40	52	57	53	60	57	54	49	60	52	57	57
Stars			3.0★	3.0★	3.0★	3.0★	3.0★	3.0★	2.5★	3.5★	3.0★	2.5★	3.0★	3.0★	3.0★	3.5★	3.0★	3.0★	2.5★	3.0★	3.0★	3.0★	3.0★
CORA			0.89	0.90	0.85	0.88	0.93	0.89	0.85	0.87	0.88	0.84	0.88	0.89	0.86	0.88	0.89	0.87	0.93	0.92	0.92	0.91	1.00

### A8. Sensitivity Study – Simulation Matrix

	Angle	Overlap	Mass	Speed
DOE #	P1	P2	P3	P4
1	20	40	2250	85
2	20	30		
3	10	40		
4	10	30		
5	20	35	2500	85
6	20		2000	
7	10		2500	
8	10		2000	
9	20	35	2250	90
10	20			80
11	10			90
12	10			80
13	15	40	2500	85
14		40	2000	
15		30	2500	
16		30	2000	
17	15	40	2250	90
18		40		80
19		30		90
20		30		80
21	15	35	2500	90
22			2500	80
23			2000	90
24			2000	80
25	15	35	2250	85

## A9. Sensitivity Study – Vehicle Results Near-Side

DOE #	1	2	3	4	5	6	7	8	9	10	11	12	13	14	15	16	17	18	19	20	21	22	23
Impact Angle	20	20	10	10	20	20	10	10	20	20	10	10	15				15				15		
Overlap	40	30	40	30	35				35				40	40	30	30	40	40	30	30	35		
OMDB Mass	2250				2500	2000	2500	2000	2250				2500	2000	2500	2000	2250				2500	2500	2000
Impact Speed	85				85				90	80	90	80	85				90	80	90	80	90	80	90
A1	64	76	71	84	71	53	85	63	82	52	90	58	73	64	91	67	80	55	101	63	102	64	76
B1	89	97	97	105	95	76	114	88	105	75	121	80	97	90	111	86	105	78	124	84	128	88	99
C1	108	117	120	124	115	96	137	112	125	92	146	103	117	111	126	103	125	98	141	101	150	108	120
D1	77	84	76	87	76	63	94	70	84	60	97	62	75	72	88	69	81	59	99	64	101	68	79
A2	55	63	58	68	60	45	67	49	69	43	74	46	59	54	75	54	64	44	85	51	82	50	61
B2	73	78	78	84	76	61	92	71	85	60	100	64	79	75	89	69	85	63	99	67	104	71	81
C2	77	80	84	89	80	64	98	77	87	63	108	71	84	81	93	73	90	70	104	72	110	76	86
D2	57	60	59	72	61	47	74	52	65	45	79	47	59	56	72	54	64	47	78	51	83	53	63
A3	33	35	34	42	35	25	43	28	39	23	48	26	36	32	45	31	39	24	51	28	52	28	37
B3	41	43	42	50	43	33	53	37	49	31	60	33	44	41	52	38	49	32	58	35	62	37	45
C3	63	62	66	71	65	52	78	60	69	50	88	56	67	65	74	58	72	56	80	56	88	60	69
D3	45	43	45	50	48	36	56	40	50	34	63	36	46	46	55	42	51	38	56	38	64	40	49
A4	15	14	12	20	16	9	21	9	18	7	26	8	15	13	21	12	18	6	25	9	26	9	16
B4	17	16	15	23	18	11	24	12	20	9	30	10	18	16	24	15	20	9	27	11	29	12	19
C4	19	17	17	24	20	13	26	13	22	10	32	12	19	19	26	16	22	11	27	13	31	13	21
D4	15	13	14	19	16	10	22	10	18	8	27	9	16	16	21	12	19	9	23	9	26	10	17
A5	15	14	12	20	16	9	21	9	18	7	27	7	15	13	21	13	18	6	25	9	26	9	16
B5	16	14	13	21	16	9	22	10	19	7	27	8	16	14	22	13	19	7	24	10	27	10	17
C5	17	15	14	22	18	11	24	11	20	8	29	10	17	16	24	14	20	9	26	11	29	11	18
D5	14	11	13	17	15	9	21	9	16	6	26	8	15	14	18	11	17	8	20	7	24	9	15
Break Pedal	81	93	107	130	97	65	138	103	104	55	153	72	95	53	97	77	118	41	114	60	156	89	109
IP left	18	19	15	30	22	14	26	13	24	12	31	11	22	13	27	18	22	7	31	13	36	13	21
IP right	12	14	10	20	15	10	20	9	18	8	24	7	14	10	19	12	15	6	22	9	29	8	14
Steering Column	9	12	9	21	10	8	19	8	16	5	19	7	12	8	16	9	12	2	18	7	19	5	9
Max. Toe Pan	108	117	120	124	115	96	137	112	125	92	146	103	117	111	126	103	125	98	141	101	150	108	120
dv-x [m/s]	13.1	12.9	13.6	13	13.7	12.3	14.1	12.5	13.8	12.2	14.2	12.7	14.3	12.9	13.7	12.2	14.4	12.6	13.5	12.2	14.8	13.1	13.2
dv-y [m/s]	5.9	6	4.5	4.8	6.2	5.5	4.5	4.2	6.4	5.3	4.8	4.2	5.4	4.9	5.7	5	5.6	4.8	5.6	5	5.8	5.1	5.3
DOE #	1	2	3	4	5	6	7	8	9	10	11	12	13	14	15	16	17	18	19	20	21	22	23
Impact Angle	20	20	10	10	20	20	10	10	20	20	10	10	15				15				15		
Overlap	40	30	40	30	35				35				40	40	30	30	40	40	30	30	35		
OMDB Mass	2250				2500	2000	2500	2000	2250				2500	2000	2500	2000	2250				2500	2500	2000
Impact Speed	85				85				90	80	90	80	85				90	80	90	80	90	80	90

### A10. Sensitivity Study – Vehicle Results Far-Side

DOE #	1	2	3	4	5	6	7	8	9	10	11	12	13	14	15	16	17	18	19	20	21	22	23
Impact Angle	20	20	10	10	20	20	10	10	20	20	10	10	15				15				15		
Overlap	40	30	40	30	35				35				40	40	30	30	40	40	30	30	35		
OMDB Mass	2250				2500	2000	2500	2000	2250				2500	2000	2500	2000	2250				2500	2500	2000
Impact Speed	85				85				90	80	90	80	85				90	80	90	80	90	80	90
A1	13	3	15	4	9	2	17	7	11	1	19	6	15	11	5	-1	19	7	11	-1	19	6	9
B1	9	-1	14	2	6	2	15	7	7	0	16	6	13	11	3	-1	15	8	5	-1	15	5	8
C1	8	-1	12	1	4	2	11	5	5	1	12	5	11	10	2	-1	13	7	3	0	12	4	6
D1	6	0	7	1	4	2	7	4	4	2	8	3	7	6	2	0	9	5	3	0	8	3	4
A2	9	1	11	4	6	3	14	5	8	0	17	4	12	9	7	0	14	5	10	-1	15	4	7
B2	9	2	12	4	7	3	13	6	9	1	15	5	12	10	6	0	14	6	9	-1	13	4	7
C2	8	-1	10	1	4	1	10	4	5	1	11	4	9	8	2	-1	11	6	3	0	10	3	5
D2	5	-1	7	1	2	1	6	3	2	1	7	3	6	6	1	-1	7	4	1	0	6	2	3
A3	11	7	13	10	11	6	17	6	13	4	19	5	13	11	12	6	15	5	17	2	20	7	11
B3	9	2	10	3	7	3	12	5	9	1	14	4	10	9	5	1	13	5	7	0	13	5	7
C3	6	0	7	2	4	2	8	3	5	1	9	2	7	6	2	0	8	4	3	0	9	3	5
D3	5	0	7	1	2	1	7	3	3	0	8	2	6	6	1	0	7	4	2	0	7	2	4
A4	9	6	9	9	10	5	14	5	12	3	17	4	11	10	11	5	13	4	14	2	17	5	9
B4	7	2	7	4	6	3	9	3	7	2	11	3	8	7	5	2	9	4	5	1	10	4	6
C4	5	1	5	2	4	2	6	2	5	1	8	2	6	5	3	1	7	2	4	0	8	3	4
D4	3	1	2	1	2	1	3	1	3	0	5	1	3	3	2	0	4	1	2	0	4	1	2
A5	9	5	9	8	9	5	14	4	11	3	17	4	10	10	10	5	12	4	14	2	17	5	9
B5	6	2	6	3	5	3	8	3	6	2	10	3	7	6	4	1	8	3	5	1	10	4	5
C5	6	2	6	2	5	2	7	2	6	1	9	2	6	6	4	1	7	3	5	1	9	3	5
D5	3	0	3	1	3	1	5	1	4	0	6	1	4	3	2	0	5	1	3	0	6	1	3
IP left	4	5	3	8	7	4	9	5	9	6	11	5	6	4	9	6	4	4	9	4	14	5	4
IP right	3	2	3	5	3	2	4	3	3	4	4	4	3	2	5	3	2	3	4	3	5	4	2
bolt	1	0	1	0	1	0	1	0	1	0	1	0	1	1	1	0	1	1	1	0	2	0	1
Max. Toepan	13	7	15	10	11	6	17	7	13	4	19	6	15	11	12	6	19	8	17	2	20	7	11

## A11. Sensitivity Study – Driver Results

DOE #		1	2	3	4	5	6	7	8	9	10	11	12	13	14	15	16	17	18	19	20	21	22	23	24	25	
Impact Angle		20	20	10	10	20	20	10	10	20	20	10	10			15			15				15			15	
Overlap		40	30	40	30			35				35		40	40	30	30	40	40	30	30		35			35	
OMDB Mass			2250			2500	2000	2500	2000			2250		2500	2000	2500	2000			2250		2500	2500	2000	2000	2250	
Impact Speed			85				85			90	80	90	80		85			90	80	90	80	90	80	90	80	85	
HIC	500	700	290	270	293	303	318	251	317	315	339	241	359	359	339	303	305	249	345	279	298	234	353	369	295	312	361
BRIC	0.71	1.05	1	1.07	0.9	0.89	0.99	0.96	0.85	0.98	0.99	0.97	0.87	1.04	0.98	1.03	1.06	1.03	0.95	1.02	0.99	0.98	0.89	1.08	0.94	1.04	1.07
Nif	0.39	0.85	0.13	0.15	0.06	0.09	0.17	0.09	0.27	0.09	0.11	0.1	0.32	0.33	0.08	0.07	0.01	0.09	0.06	0.08	0.11	0.09	0.29	0.33	0.24	0.06	0.12
Ncf	0.39	0.85	0.12	0.2	0.16	0.12	0.14	0.11	0.08	0.17	0.17	0.1	0.15	0.15	0.2	0.17	0.1	0.11	0.19	0.15	0.17	0.14	0.22	0.12	0.2	0.09	0.14
Nte	0.39	0.85	0.36	0.36	0.37	0.34	0.35	0.33	0.34	0.38	0.38	0.32	0.36	0.36	0.36	0.34	0.33	0.31	0.36	0.36	0.38	0.33	0.37	0.36	0.35	0.33	0.35
Nce	0.39	0.85	0.13	0.17	0.11	0.21	0.22	0.16	0.16	0.1	0.16	0.11	0.09	0.09	0.1	0.09	0.14	0.09	0.09	0.1	0.09	0.12	0.09	0.09	0.09	0.1	0.1
Chest-UL	37.9	52.3	28	26	27	26	26	25	27	22	27	25	27	21	27	24	27	25	27	22	28	24	27	21	25	21	23
Chest-UR	37.9	52.3	46	40	47	45	45	42	46	36	46	42	46	30	45	40	44	42	46	36	46	40	47	32	44	29	37
Chest-LL	37.9	52.3	9	10	12	15	9	8	14	7	11	10	16	12	11	7	13	10	12	6	16	10	16	11	12	12	9
Chest-LR	37.9	52.3	35	31	35	31	32	31	36	35	31	31	34	30	35	39	30	30	34	35	34	31	32	31	31	31	36
ABDO-LE	NA	88.6	50	50	50	49	52	47	48	49	54	49	51	52	51	50	50	49	52	50	50	48	54	53	51	50	50
ABDO-RI	NA	88.6	52	51	49	49	53	48	48	48	55	52	51	53	52	52	51	49	53	52	47	48	54	55	51	52	49
ACET-LE	2583	3486	1691	1640	1838	1878	1734	1526	2020	2099	1735	1546	2136	2747	2019	2208	1751	1775	2067	2055	1600	1493	1996	2465	2059	2068	2426
ACET-RI	2583	3486	1129	1095	942	1017	989	1174	856	930	923	1166	829	1157	966	925	816	807	932	1184	1018	808	981	988	1000	1040	923
FEM-LE	5331	8558	2372	1923	2167	4698	2297	2346	2959	2073	2894	2138	3477	1816	2701	2249	3100	2314	2684	1689	3872	2015	4461	1469	3071	1520	2310
FEM-RI	5331	8558	4220	3871	3594	4636	3926	3743	4579	3821	4330	3519	4268	3154	3709	3640	3481	3240	4407	3160	4369	3035	4361	3156	3776	2643	3551
FZ TI UL	4235	5577	764	728	723	770	758	815	566	709	839	802	565	669	699	769	641	663	708	767	777	634	658	672	671	785	634
FZ TI UR	4235	5577	1257	1009	1094	957	1086	1032	1072	1092	1086	1023	1145	1087	1117	1189	940	927	1188	1128	1115	886	1164	952	1129	919	1005
FZ TI LL	3573	5861	1718	1309	1778	1560	1719	1563	1357	1390	1584	1576	1372	1373	1632	1661	1486	1410	1725	1765	1588	1274	1615	1526	1556	1490	1526
FZ TI LR	3573	5861	4042	3294	3281	2700	3771	3580	3054	2994	3961	3234	3054	2909	3231	3236	3083	2899	3434	3081	3473	2598	3243	3023	3077	2993	3093
MR TI UL	178	240	87	88	69	109	87	82	66	73	92	90	72	68	75	83	68	70	73	84	71	59	94	79	73	62	71
MR TI UR	178	240	106	92	70	80	98	90	80	79	105	80	91	87	82	81	93	86	89	74	113	83	106	89	92	85	94
MR TI LL	178	240	71	65	72	72	66	68	64	71	74	70	61	65	71	69	76	61	71	73	217	67	70	60	66	59	62
MR TI LR	178	240	134	90	52	77	94	81	59	61	123	73	71	41	80	102	93	73	88	61	119	51	84	80	73	57	70
Points			61	71	68	72	65	73	72	79	62	73	71	73	67	73	65	69	67	77	57	75	68	75	71	76	75
Stars			3.5★	4.0★	3.5★	4.0★	3.5★	4.0★	4.0★	4.0★	3.5★	4.0★	4.0★	4.0★	3.5★	4.0★	3.5★	3.5★	3.5★	4.0★	3.0★	4.0★	3.5★	4.0★	4.0★	4.0★	4.0★
CORA			0.78	0.80	0.83	0.71	0.81	0.82	0.78	0.87	0.77	0.83	0.78	0.75	0.84	0.84	0.80	0.81	0.78	0.87	0.79	0.78	0.76	0.87	0.84	0.83	1.00
Head			2.75	0	8.5	9	3.5	5	11.25	4	3.5	4.5	10.25	0.5	4	1.25	0	1.25	5.75	1.75	3.5	4	9	0	6.25	0.5	0
Neck			25	25	25	25	25	25	25	25	25	25	25	25	25	25	25	25	25	25	25	25	25	25	25	25	25
Chest			11	21.25	9.25	12.75	12.75	18	11	25	11	18	11	25	12.75	21.25	14.5	18	11	25	11	21.25	9.25	25	14.5	25	25
Legs			22.5	25	25	25	25	23.88	25	25	25	22.88	25	25	22.75	25	25	25	25	25	25	17	25	25	25	25	25
Head rx [*°s]			16	18	8	8	16	15	8	8	14	15	8	13	12	16	17	17	13	15	17	16	11	13	14	12	13
Head ry [*°s]			46	43	46	47	46	45	46	51	46	44	46	50	48	46	46	45	46	48	45	46	45	54	45	52	51
Head rz [*°s]			22	30	16	11	22	21	10	16	22	23	12	23	20	22	27	26	19	22	23	22	16	21	19	20	23
DOE #		1	2	3	4	5	6	7	8	9	10	11	12	13	14	15	16	17	18	19	20	21	22	23	24	25	
Impact Angle		20	20	10	10	20	20	10	10	20	20	10	10			15			15				15			15	
Overlap		40	30	40	30			35				35		40	40	30	30	40	40	30	30		35			35	
OMDB Mass			2250			2500	2000	2500	2000			2250		2500	2000	2500	2000			2250		2500	2500	2000	2000	2250	
Impact Speed			85				85			90	80	90	80		85			90	80	90	80	90	80	90	80	85	
Head dx [mm]			378	383	418	415	383	367	420	397	380	375	416	401	408	389	407	392	402	388	401	396	399	381	391	367	385
Head dy [mm]			164	172	137	165	173	163	140	133	174	158	147	128	160	143	159	154	162	139	163	149	176	143	161	131	150
Head dz [mm]			227	251	236	229	242	235	218	248	239	237	223	260	233	231	247	253	234	232	250	240	246	249	229	233	248

## A12. Sensitivity Study – Passenger Results

DOE #		1	2	3	4	5	6	7	8	9	10	11	12	13	14	15	16	17	18	19	20	21	22	23	24	25
Impact Angle		20	20	10	10	20	20	10	10	20	20	10	10													
Overlap		40	30	40	30									40	40	30	30	40	40	30	30					
OMDB Mass			2250			2500	2000	2500	2000					2500	2000	2500	2000					2500	2500	2000	2000	2250
Impact Speed			85							90	80	90	80					90	80	90	80	90	80	90	80	85
HIC	500 700	323	242	410	290	366	268	316	240	420	274	328	265	420	290	367	249	432	325	364	271	606	265	271	250	431
BRIC	0.7 1.05	1.1	1.1	1.02	0.98	1.23	0.95	1.15	0.89	1.23	1.04	1.25	0.84	1.2	0.99	1.13	1.02	1.26	0.98	1.17	0.89	1.3	1.02	1.4	0.95	1.12
Nlf	0.4 0.85	0.4	0.39	0.41	0.38	0.41	0.36	0.37	0.33	0.47	0.35	0.38	0.35	0.42	0.36	0.42	0.38	0.46	0.37	0.4	0.39	0.68	0.37	0.41	0.37	0.46
Ncf	0.4 0.85	0.08	0.08	0.08	0.07	0.08	0.08	0.08	0.08	0.08	0.08	0.3	0.08	0.24	0.08	0.08	0.08	0.08	0.08	0.08	0.07	0.09	0.08	0.08	0.08	0.08
Nte	0.4 0.85	0.51	0.36	0.5	0.4	0.45	0.36	0.42	0.39	0.43	0.35	0.47	0.38	0.5	0.43	0.43	0.4	0.52	0.48	0.46	0.33	0.47	0.42	0.42	0.35	0.4
Nce	0.4 0.85	0.08	0.08	0.08	0.07	0.08	0.08	0.07	0.07	0.08	0.08	0.07	0.07	0.08	0.08	0.08	0.08	0.08	0.08	0.08	0.08	0.08	0.08	0.08	0.08	0.08
Chest-UL	38 52.3	26	28	28	30	26	25	30	29	26	25	30	30	28	27	30	29	27	26	29	28	28	27	28	26	27
Chest-UR	38 52.3	30	29	29	31	30	30	31	30	30	29	31	30	29	29	31	30	30	28	31	29	30	28	30	28	29
Chest-LL	38 52.3	37	36	39	38	37	35	39	39	36	36	39	40	38	38	38	36	38	37	38	36	38	37	38	37	37
Chest-LR	38 52.3	8	10	8	14	8	8	11	10	7	11	13	8	8	10	14	11	10	9	14	9	12	9	11	11	9
ABDO-LE	NA 88.6	59	59	56	58	60	56	58	54	60	55	60	55	61	58	60	57	61	59	62	55	62	57	57	54	57
ABDO-RI	NA 88.6	61	60	57	58	64	61	58	57	63	57	61	56	63	60	61	58	64	62	63	55	62	56	60	57	60
ACET-LE	### 3486	2099	1575	2554	2024	2791	2407	2221	1768	2692	2316	2418	1828	2602	2436	1982	1706	2724	2527	2175	1673	2183	1959	2529	2301	2467
ACET-RI	### 3486	2769	1840	2873	2161	2728	2326	2235	1972	2958	2053	2565	1870	3198	2826	2304	1797	3058	2650	2164	1739	2466	2108	2202	1887	2611
FEM-LE	### 8558	3580	2412	3622	3138	3058	2006	3277	2212	3462	1904	3849	1740	3946	2750	2996	1996	4142	1833	3432	1296	4788	1909	3361	1241	2868
FEM-RI	### 8558	1018	592	893	727	855	655	1130	785	1005	831	1005	643	1160	614	817	816	1066	789	791	909	1279	794	1081	653	869
FZ TI UL	### 5577	764	663	903	828	808	732	736	623	794	687	874	572	909	809	733	639	906	745	851	533	877	645	788	656	781
FZ TI UR	### 5577	870	672	949	686	884	687	816	752	866	662	927	727	929	867	810	647	931	757	736	566	828	748	866	670	901
FZ TI LL	### 5861	2376	2235	3204	2497	2406	2504	2906	2579	2222	2233	3245	2502	3255	3153	2663	2125	3031	2634	3111	1769	3202	2999	2518	2757	2834
FZ TI LR	### 5861	2898	2372	3207	2486	2643	2659	2838	3119	2491	2778	3350	2870	2918	2973	2817	2167	2958	2994	3154	2312	2884	3096	2498	2887	2624
MR TI UL	178 240	172	149	145	185	167	155	165	169	213	134	143	165	159	200	208	167	162	172	155	124	164	171	139	123	161
MR TI UR	178 240	183	220	163	172	204	184	169	164	199	197	181	167	200	209	202	191	176	188	220	219	189	193	184	194	197
MR TI LL	178 240	98	80	79	68	84	75	80	59	93	67	85	62	92	93	80	67	98	73	84	67	108	91	93	72	86
MR TI LR	178 240	109	99	79	87	97	87	83	78	106	88	97	74	88	89	107	95	90	81	115	100	97	88	95	86	93
Points		65	67	65	77	64	80	71	82	59	72	68	83	56	66	67	74	61	71	63	76	57	72	72	78	67
Stars		3.5★	3.5★	3.5★	4.0★	3.5★	4.0★	4.0★	4.5★	3.0★	4.0★	3.5★	4.5★	3.0★	3.5★	3.5★	4.0★	3.5★	4.0★	3.5★	4.0★	3.0★	4.0★	4.0★	4.0★	3.5★
CORA		0.79	0.80	0.90	0.74	0.87	0.81	0.83	0.78	0.81	0.83	0.83	0.74	0.83	0.84	0.80	0.78	0.80	0.88	0.80	0.73	0.77	0.81	0.83	0.82	1.00
Head		0	0	1.75	4	0	5.75	0	9	0	0.5	0	12	0	3.5	0	1.75	0	4	0	9	0	1.75	0	5.75	0
Neck		18.5	25	19	24.5	21.75	25	23.25	25	20.75	25	20.75	25	19	22.75	22.75	24.5	18	20	21.25	25	9.25	23.25	23.25	25	21.25
Chest		25	25	25	24.75	25	25	23	23	25	25	23	21.25	24.75	24.75	24.75	25	24.75	25	24.75	25	24.75	25	24.75	25	25
Legs		21.38	16.5	21	23.5	17	23.75	25	25	12.75	21.13	24.38	25	12	15.38	19	22.38	18.38	22.13	16.5	16.75	22.75	22	23.75	21.75	20.75
Head rx [°s]		39	46	39	39	47	31	45	34	49	35	53	32	48	51	54	45	56	32	54	51	61	44	55	31	42
Head ry [°s]		49	37	41	39	53	44	42	35	51	44	40	35	43	39	36	35	46	44	35	39	39	36	50	42	48
Head rz [°s]		15	24	18	16	16	12	24	16	17	19	27	13	25	25	20	19	20	15	24	25	26	19	29	15	16
DOE #		1	2	3	4	5	6	7	8	9	10	11	12	13	14	15	16	17	18	19	20	21	22	23	24	25
Impact Angle		20	20	10	10	20	20	10	10	20	20	10	10													
Overlap		40	30	40	30									40	40	30	30	40	40	30	30					
OMDB Mass			2250			2500	2000	2500	2000					2500	2000	2500	2000					2500	2500	2000	2000	2250
Impact Speed			85							90	80	90	80					90	80	90	80	90	80	90	80	85
Head dx [mm]		470	499	509	524	478	452	539	512	482	457	544	514	511	488	528	497	507	470	526	495	548	515	498	456	488
Head dy [mm]		267	267	181	175	271	253	164	152	275	244	184	146	232	234	228	210	234	204	241	206	240	197	225	191	216
Head dz [mm]		394	387	383	386	406	366	399	363	404	351	391	353	406	392	413	369	420	378	406	369	399	384	391	354	408

### A13. Impact Angle Study – Vehicle Results

31	32	33	34	35	Run #	41	42	43	44	45
0	5	10	15	20	Impact Angle	0	5	10	15	20
35					Overlap	35				
2500					OMDB Mass	2500				
90					Impact Speed	80				
102	106	100	102	88	A1	64	69	64	64	58
133	137	128	128	108	B1	90	93	88	88	83
166	165	152	150	127	C1	122	116	112	108	101
110	112	102	101	83	D1	70	70	70	68	67
85	88	80	82	73	A2	51	54	51	50	49
111	114	106	104	86	B2	74	76	71	71	67
128	122	114	110	88	C2	90	82	77	76	71
97	91	84	83	64	D2	57	54	53	53	51
59	60	53	52	42	A3	29	33	30	28	27
72	73	65	62	51	B3	40	42	38	37	35
107	101	93	88	70	C3	74	66	61	60	56
79	75	68	64	51	D3	49	45	40	40	38
37	37	31	26	20	A4	10	13	11	9	9
41	41	34	29	22	B4	14	16	13	12	11
46	43	36	31	23	C4	20	18	15	13	13
38	39	31	26	20	D4	15	15	12	10	10
37	38	31	26	20	A5	11	13	11	9	9
39	39	32	27	20	B5	12	14	11	10	10
41	41	33	29	21	C5	15	16	13	11	11
36	37	29	24	18	D5	13	14	11	9	9
180	192	177	156	104	Break Pedal	98	101	99	89	59
49	48	44	36	28	IP left	15	18	13	13	14
37	37	32	29	20	IP right	12	13	8	8	10
27	30	26	19	18	Steering Column	11	13	7	5	7
166	165	152	150	127	Max. Toe Pan	122	116	112	108	101
14.2	14.9	15	14.8	14.5	dv-x [m/s]	12.7	13.1	13.2	13.1	12.8
4.3	4.6	5.1	5.8	6.7	dv-y [m/s]	3.6	3.9	4.3	5.1	5.7
5	3.4	0.7	-1.7	-4.3	yaw [deg.]	4.1	2.5	0.6	-1.7	-3.6
31	32	33	34	35	Run #	41	42	43	44	45
0	5	10	15	20	Impact Angle	0	5	10	15	20
35					Overlap	35				
2500					OMDB Mass	2500				
90					Impact Speed	80				

### A14. Impact Angle Study – Driver Results

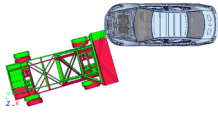
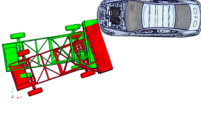
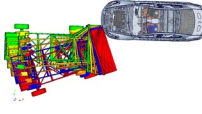
31	32	33	34	35	Run #	41	42	43	44	45
0	5	10	15	20	Impact Angle	0	5	10	15	20
35					Overlap	35				
2500					OMDB Mass	2500				
90					Impact Speed	80				
576	471	409	353	386	HIC	336	300	379	369	265
1.31	0.9	0.87	0.89	0.98	BRIC	0.93	0.9	1.04	1.08	1.01
0.38	0.31	0.33	0.29	0.02	Ntf	0.33	0.33	0.39	0.33	0.13
0.06	0.07	0.12	0.22	0.15	Ncf	0.12	0.06	0.13	0.12	0.14
0.45	0.46	0.44	0.37	0.39	Nte	0.36	0.38	0.41	0.36	0.32
0.43	0.44	0.41	0.09	0.14	Nce	0.43	0.49	0.09	0.09	0.14
29	27	29	27	26	Chest-UL	25	27	21	21	26
49	48	48	47	46	Chest-UR	40	42	31	32	43
19	20	19	16	12	Chest-LL	10	11	12	11	10
32	33	32	32	31	Chest-LL	31	31	32	31	32
51	53	54	54	55	ABDO-LE	48	47	53	53	50
50	53	53	54	57	ABDO-RI	49	49	55	55	52
1901	2285	2019	1996	1639	ACET-LE	1723	1702	2919	2465	1516
1327	1136	1108	981	1011	ACET-RI	816	822	1281	988	1128
5955	5119	5410	4461	3172	FEM-LE	2338	2885	1822	1469	2175
5107	4720	4961	4361	4752	FEM-RI	3069	3897	3671	3156	3422
577	536	556	638	747	FZ TI UL	696	570	713	672	871
1240	1214	1190	1164	1130	FZ TI UR	1222	1096	1037	952	1033
1660	1294	1387	1615	1591	FZ TILL	1555	1372	1593	1526	1523
3868	2997	3051	3243	3762	FZ TILR	3855	2891	2922	3023	3294
114	84	117	94	81	MR TI UL	67	62	71	79	83
148	104	97	106	111	MR TI UR	124	103	74	89	83
72	66	72	70	79	MR TILL	53	59	68	60	67
63	61	74	84	112	MR TILR	55	40	50	80	86
49	62	65	68	64	Points	74	71	70	75	69
2.5★	3.5★	3.5★	3.5★	3.5★	Stars	4.0★	4.0★	3.5★	4.0★	3.5★
0.63	0.73	0.81	1.00	0.83	CORA	0.62	0.68	0.84	1.00	0.78
0	8.5	10.25	9	4	Head	6.75	8.5	0.5	0	2.25
21.75	21.25	22.25	25	25	Neck	22.75	19.5	24	25	25
5.75	7.5	7.5	9.25	11	Chest	21.25	18	25	25	16.25
21	25	24.75	25	24	Legs	23.5	25	20.38	25	25
15	14	11	11	14	Head rx [°/s]	11	9	8	13	15
45	44	45	45	47	Head ry [°/s]	47	47	54	54	45
44	17	13	16	21	Head rz [°/s]	16	14	17	21	25
31	32	33	34	35	Run #	41	42	43	44	45
0	5	10	15	20	Impact Angle	0	5	10	15	20
35					Overlap	35				
2500					OMDB Mass	2500				
90					Impact Speed	80				
440	428	415	399	383	Head dx [mm]	445	435	405	381	381
118	137	162	176	180	Head dy [mm]	99	119	129	143	161
161	176	198	246	239	Head dz [mm]	218	230	260	249	238

### A15. Impact Angle Study – Passenger Results

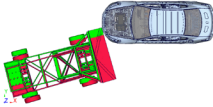
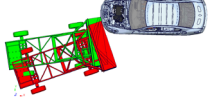
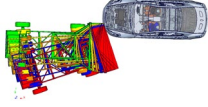
Run #			31	32	33	34	35		41	42	43	44	45
Impact Angle			0	5	10	15	20		0	5	10	15	20
Overlap			35						35				
OMDB Mass			2500						2500				
Impact Speed			90						80				
HIC	500	700	454	439	409	606	328		462	334	425	265	319
BRIC	0.71	1.05	0.95	1.02	1.27	1.3	1.23		0.9	0.86	0.99	1.02	1.11
Ntf	0.39	0.85	0.39	0.44	0.45	0.68	0.44		0.46	0.37	0.42	0.37	0.37
Ncf	0.39	0.85	0.07	0.26	0.26	0.09	0.09		0.19	0.07	0.21	0.08	0.08
Nte	0.39	0.85	0.43	0.41	0.48	0.47	0.47		0.39	0.38	0.37	0.42	0.47
Nce	0.39	0.85	0.07	0.07	0.07	0.08	0.09		0.07	0.07	0.08	0.08	0.08
Chest-UL	37.9	52.3	31	31	30	28	27		30	30	27	27	25
Chest-UR	37.9	52.3	32	32	31	30	30		31	31	29	28	29
Chest-LL	37.9	52.3	39	39	39	38	38		41	39	37	37	35
Chest-LL	37.9	52.3	13	13	15	12	11		7	8	9	9	7
ABDO-LE	NA	88.6	58	61	62	62	64		53	55	53	57	58
ABDO-RI	NA	88.6	60	63	63	62	63		54	56	56	56	62
ACET-LE	2583	3486	2599	2350	2549	2183	2768		2551	2136	3118	1959	2277
ACET-RI	2583	3486	2604	2459	2638	2466	2769		2602	2076	2793	2108	2366
FEM-LE	5331	8558	4581	5157	5862	4788	3760		2222	2563	2414	1909	2114
FEM-RI	5331	8558	760	910	809	1279	1285		892	583	839	794	783
FZ TI UL	4235	5577	807	911	959	877	927		699	625	740	645	683
FZ TI UR	4235	5577	793	834	937	828	806		677	683	871	748	732
FZ TI LL	3573	5861	2842	3272	3261	3202	2337		2623	2191	2254	2999	2167
FZ TI LR	3573	5861	2560	3077	3507	2884	2715		2144	2254	2832	3096	2802
MR TI UL	178	240	133	175	159	164	195		161	173	160	171	148
MR TI UR	178	240	104	135	175	189	213		98	127	174	193	194
MR TI LL	178	240	60	75	84	108	90		58	58	54	91	67
MR TI LR	178	240	60	75	88	97	111		64	70	79	88	85
Points			76	72	66	57	61		74	84	69	72	68
Stars			4.0★	4.0★	3.5★	3.0★	3.5★		4.0★	4.5★	3.5★	4.0★	3.5★

CORA			0.67	0.75	0.83	1.00	0.82		0.68	0.79	0.78	1.00	0.80
Head			5.75	1.75	0	0	0		8.5	10.75	3.5	1.75	0
Neck			22.75	22.25	20	9.25	20.75		21.25	25	23.25	23.25	20.75
Chest			23	23	23	24.75	24.75		19.5	23	25	25	25
Legs			24.75	25	23	22.75	15.38		24.75	25	17.63	22	21.88
Head rx [°/s]			35	40	56	61	48		30	33	30	44	43
Head ry [°/s]			38	40	45	39	50		42	35	45	36	45
Head rz [°/s]			18	18	23	26	20		11	13	15	19	18
Run #			31	32	33	34	35		41	42	43	44	45
Impact Angle			0	5	10	15	20		0	5	10	15	20
Overlap			35						35				
OMDB Mass			2500						2500				
Impact Speed			90						80				
Head dx [mm]			559	565	559	548	501		503	530	491	515	467
Head dy [mm]			86	141	196	240	298		78	107	162	197	239
Head dz [mm]			388	394	420	399	408		349	370	378	384	376

### A16. Test Procedure Parametric Study – Overview Vehicle

	<b>Repeatability Study</b> 	<b>Sensitivity Study</b> 	<b>Impact Angle Study</b> 	
Impact Angle [°]	2 14° to 16°	10 10° - 20°	20 0° - 20°	20 0° - 20°
OMDB z-Position [mm]	100 -50 to +50	n/a	n/a	n/a
OMDB overlap [%]	5 33 to 38	10 30 to 40	n/a 35	n/a 35
OMDB mass [kg]	100 2438 to 2538	500 2000 to 2500	n/a 2500	n/a 2500
Impact velocity [km/h]	2 89 to 91	10 80 to 90	90	80
Toe-pan Intrusion Near-Side [mm]	28 129 to 157	59 91 to 150	39 127 to 166	21 101 to 122
Toe-pan Intrusion Far-Side [mm]	11 14 to 25	16 4 to 20	13 14 to 27	3 6 to 9
dv-x [m/s]	0.6 14.5 to 15.1	3.0 11.8 to 14.8	0.8 14.2 to 15.0	0.5 12.7 to 13.2
dv-y [m/s]	0.8 5.4 to 6.2	2.2 4.2 to 6.4	2.4 4.3 to 6.7	2.1 3.6 to 5.7

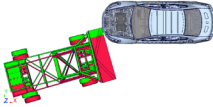
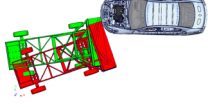
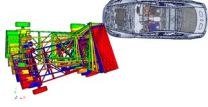
### A17. Test Procedure Parametric Study – Overview Driver

	<b>Repeatability Study</b> 	<b>Sensitivity Study</b> 	<b>Impact Angle Study</b> 	
Impact Angle [°]	2 14° to 16°	10 10° - 20°	20 0° - 20°	20 0° - 20°
OMDB z-Position [mm]	100 -50 to +50	n/a	n/a	n/a
OMDB overlap [%]	5 33 to 38	10 30 to 40	n/a 35	n/a 35
OMDB mass [kg]	100 2438 to 2538	500 2000 to 2500	n/a 2500	n/a 2500
Impact velocity [km/h]	2 89 to 91	10 80 to 90	90	80
Stars Driver	0.5 3 to 3.5	1.5 3 to 4.5	1 2.5 to 3.5	0.5 3.5 to 4
Points Driver	14 54 to 68	22 57 to 79	6 68 to 74*	5 69 to 74
CORA Driver	0.86 0.86 to 0.94	0.71 0.71 to 0.87	0.63 0.63 to 0.83	0.62 0.62 to 0.84
BrIC Driver	0.12 0.85 to 0.97	0.21 0.87 to 1.08	0.44 0.87 to 1.31	0.18 0.90 to 1.08
Chest Driver [mm]	2 47 to 49	17 30 to 47	3 46 to 49	12 31 to 43
Head x-displacement [mm]	408 396 to 408	420 367 to 420	440 383 to 440	445 381 to 445
Head y-displacement [mm]	188 167 to 188	176 128 to 176	180	161 99 to 161

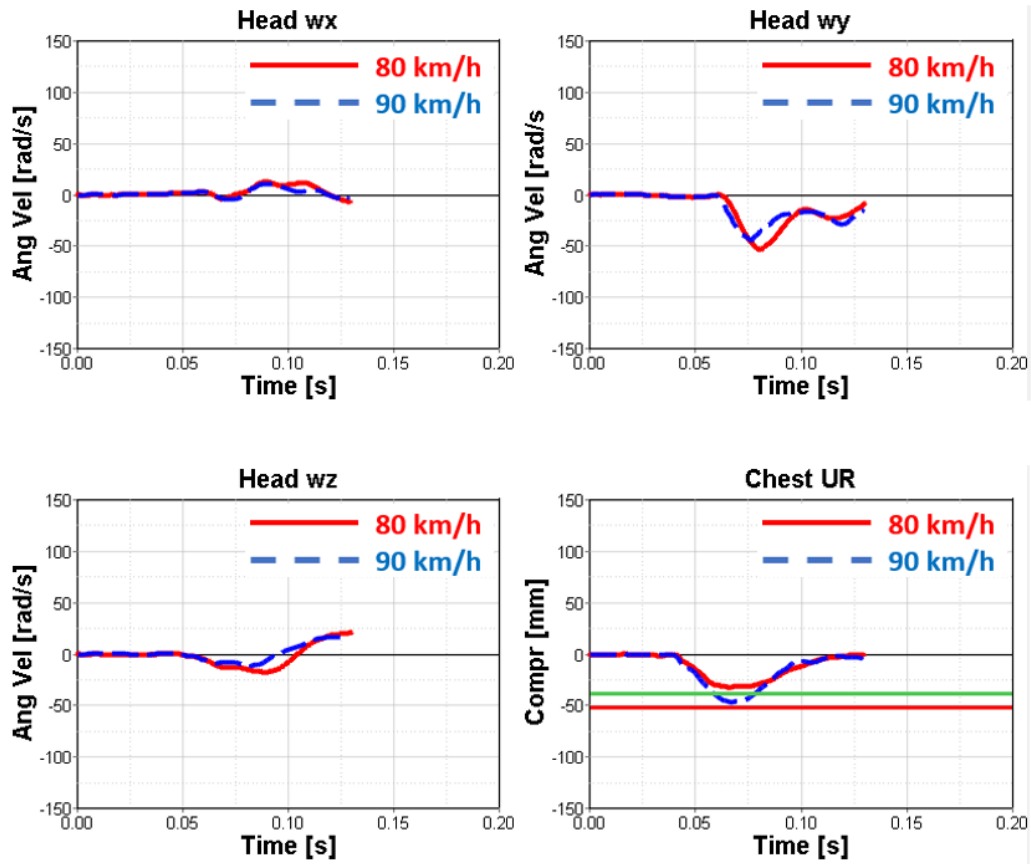
			118 to 180	
--	--	--	---------------	--

\* without bottoming out for 0° impact condition

### A18. Test Procedure Parametric Study – Overview Passenger

	<b>Repeatability Study</b> 	<b>Sensitivity Study</b> 	<b>Impact Angle Study</b> 	
Impact Angle [°]	2 14° to 16°	10 10° - 20°	20 0° - 20°	20 0° - 20°
OMDB z-Position [mm]	100 -50 to +50	n/a	n/a	n/a
OMDB overlap [%]	5 33 to 38	10 30 to 40	n/a 35	n/a 35
OMDB mass [kg]	100 2438 to 2538	500 2000 to 2500	n/a 2500	n/a 2500
Impact velocity [km/h]	2 89 to 91	10 80 to 90	90	80
Stars Passenger	1 2.5 to 3.5	1.5 3 to 4.5	1 3 to 4	1 3.5 to 4.5
Points Passenger	27 40 to 67	27 56 to 83	19 57 to 76	16 68 to 84
CORA Passenger	0.81 0.81 to 0.94	0.73 0.73 to 0.90	0.68 0.68 to 0.80	0.67 0.67 to 0.83
BrIC Passenger	0.21 1.29 to 1.50	0.56 0.84 to 1.40	0.35 0.95 to 1.30	0.25 0.86 to 1.11
Chest Passenger [mm]	4 37 to 41	5 35 to 40	1 38 to 39	6 35 to 41
Head x-displacement [mm]	551 506 to 551	548 452 to 548	559 501 to 559	530 467 to 530
Head y-displacement [mm]	262 224 to 262	271 146 to 271	298 86 to 298	239 78 to 239

### A19. Driver BRIC & Chest – 80km/h Versus. 90km/h

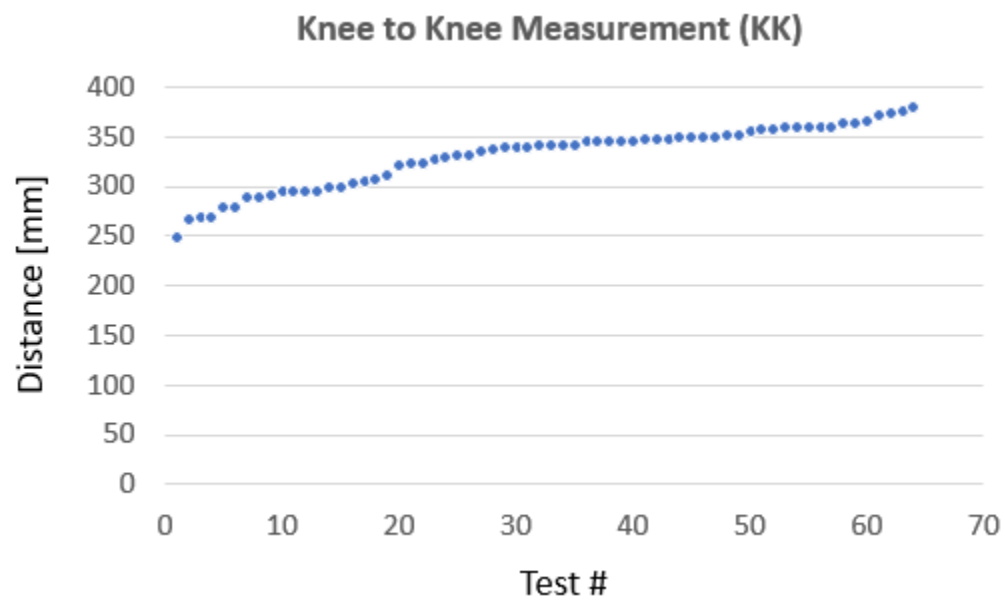
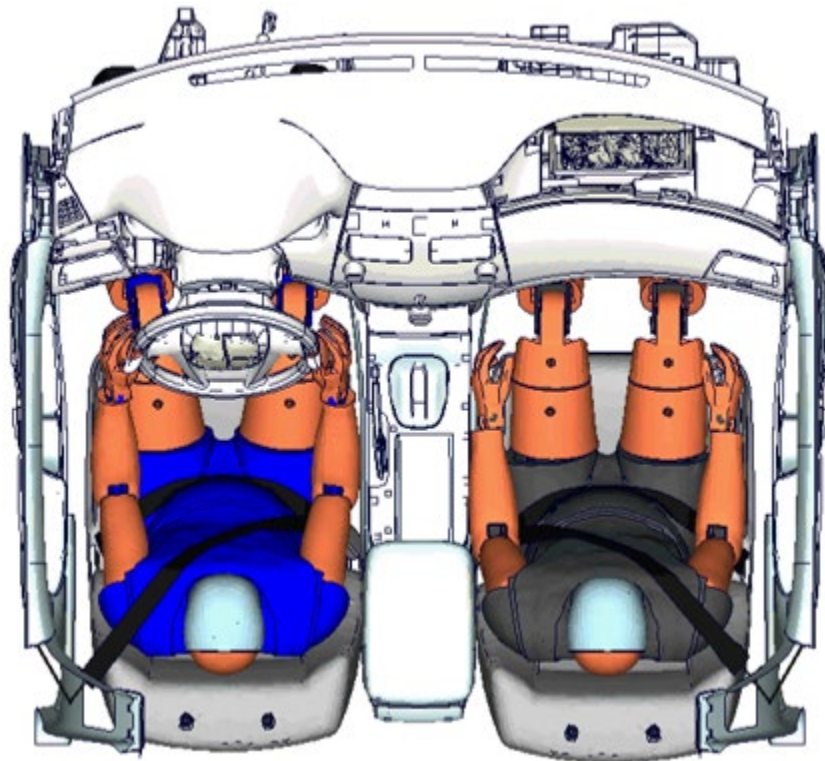


## **APPENDIX B: THOR Position Study Additional Graphs**

## B1. THOR Position Simulation Matrix – Driver & Passenger

Repeatability Study (Driver)						Sensitivity Study (Passenger)					
DOE #	HP-x	HP-y	HP-z	Head Angle	Knee Pos	DOE #	HP-x	HP-y	HP-z	Head Angle	Knee Pos
1	5	5	0	0	0	1	20	5	10	0	30
2	5	-5				2	20	-5			
3	-5	5				3	-20	5			
4	-5	-5				4	-20	-5			
5	5	0	5	0	0	5	20	0	20	0	30
6	5		-5			6	20		0		
7	-5		5			7	-20		20		
8	-5		-5			8	-20		0		
9	5	0	0	1	0	9	20	0	10	5	30
10	5			-1		10	20			-5	
11	-5			1		11	-20			5	
12	-5			-1		12	-20			-5	
13	5	0	0	0	10	13	20	0	10	0	60
14	5				-10	14	20				0
15	-5				10	15	-20				60
16	-5				-10	16	-20				0
17	0	5	5	0	0	17	0	5	20	0	30
18		5	-5			18		5	0		
19		-5	5			19		-5	20		
20		-5	-5			20		-5	0		
21	0	5	0	1	0	21	0	5	10	5	30
22		5		-1		22		5		-5	
23		-5		1		23		-5		5	
24		-5		-1		24		-5		-5	
25	0	5	0	0	10	25	0	5	10	0	60
26		5			-10	26		5			0
27		-5			10	27		-5			60
28		-5			-10	28		-5			0
29	0	0	5	1	0	29	0	0	20	5	30
30			5	-1		30			20	-5	
31			-5	1		31			0	5	
32			-5	-1		32			0	-5	
33	0	0	5	0	10	33	0	0	20	0	60
34			5		-10	34			20		0
35			-5		10	35			0		60
36			-5		-10	36			0		0
37	0	0	0	1	10	37	0	0	10	5	60
38				1	-10	38				5	0
39				-1	10	39				-5	60
40				-1	-10	40				-5	0
41	0	0	0	0	0	41	0	0	10	0	30

## B2. Knee-to-Knee Distance in 64 Full-Scale Tests



### B3. Repeatability Study – Driver Results Runs 1–16

DOE #	1	2	3	4	5	6	7	8	9	10	11	12	13	14	15	16
HP-x	5	5	-5	-5	5	5	-5	-5	5	5	-5	-5	5	5	-5	-5
HP-y	5	-5	5	-5	0				0				0			
HP-z	0				5	-5	5	-5	0				0			
Head Angle	0				0				1	-1	1	-1	0			
Knee Pos	0				0				0				10	-10	10	-10
HIC	382	371	384	380	380	378	387	369	402	428	404	432	408	385	387	388
BRIC	0.88	0.98	0.88	0.94	0.95	0.9	0.93	0.89	0.98	1.08	0.94	1.11	0.93	0.96	0.88	0.93
Ntf	0.31	0.34	0.07	0.3	0.34	0.26	0.34	0.26	0.32	0.33	0.1	0.35	0.35	0.31	0.34	0.33
Ncf	0.24	0.2	0.19	0.19	0.2	0.14	0.18	0.22	0.25	0.18	0.23	0.2	0.19	0.19	0.23	0.15
Nte	0.35	0.34	0.37	0.36	0.34	0.37	0.38	0.37	0.34	0.4	0.4	0.35	0.37	0.34	0.36	0.39
Nce	0.1	0.1	0.09	0.1	0.2	0.14	0.1	0.09	0.11	0.12	0.09	0.12	0.17	0.13	0.17	0.1
Chest-UL	31	26	27	25	29	27	26	26	28	26	27	25	28	27	27	27
Chest-UR	48	48	47	48	48	47	48	48	46	47	47	46	50	47	48	48
Chest-LL	16	19	16	18	18	16	18	18	17	19	10	16	18	19	17	17
Chest-LL	36	35	30	32	34	35	32	33	33	32	30	28	32	31	29	29
ABDO-LE	55	55	55	53	54	55	53	54	54	54	51	53	53	53	52	51
ABDO-RI	55	55	55	51	53	56	52	54	53	53	46	54	52	52	51	52
ACET-LE	2181	2179	2366	2431	2197	2210	2746	2648	2485	2310	1656	2394	2285	2485	2164	2234
ACET-RI	1202	1206	935	820	1248	1186	1042	804	1212	1138	1032	1046	1026	1107	1038	1006
FEM-LE	4718	4471	4202	4378	4257	3678	4776	4320	3831	4104	5253	3820	4714	4478	4067	4617
FEM-RI	4940	5367	4548	4407	4931	4934	5044	5320	4534	4710	5101	4127	5189	4944	4514	4262
FZ TI UL	680	643	615	617	613	619	629	615	617	532	615	659	641	632	589	623
FZ TI UR	1008	1068	1095	1080	1006	1011	1024	1060	988	853	1169	1024	1262	1063	1188	1099
FZ TI LL	1799	1590	1715	1724	1758	1559	1686	1637	1754	1720	1751	1455	1657	1918	1540	1700
FZ TI LR	3271	3447	3070	3226	3211	3315	3052	3335	3209	2940	3056	2988	3259	3288	3153	3267
MR TI UL	92	76	92	82	77	64	84	83	84	94	85	85	98	85	96	103
MR TI UR	110	113	88	112	103	101	97	108	97	108	118	101	108	110	72	75
MR TI LL	127	72	112	68	98	78	79	64	60	73	69	69	64	70	66	75
MR TI LR	101	75	72	101	94	95	102	87	102	101	122	95	103	94	72	72
Points	67	61	69	64	63	68	62	66	65	59	65	61	61	64	67	64
Stars	3.5★	3.5★	3.5★	3.5★	3.5★	3.5★	3.5★	3.5★	3.5★	3.0★	3.5★	3.5★	3.5★	3.5★	3.5★	3.5★
CORA	0.91	0.89	0.92	0.91	0.93	0.90	0.93	0.92	0.88	0.81	0.81	0.84	0.91	0.89	0.92	0.90
DOE #	1	2	3	4	5	6	7	8	9	10	11	12	13	14	15	16
Head	9.8	4.0	9.8	6.3	5.8	8.5	6.8	9.0	4.0	0.0	6.3	0.0	6.8	5.0	9.8	6.8
Neck	25.0	25.0	25.0	25.0	25.0	25.0	25.0	25.0	25.0	24.5	24.5	25.0	25.0	25.0	25.0	25.0
Chest	7.5	7.5	9.3	7.5	7.5	9.3	7.5	7.5	11.0	9.3	9.3	11.0	4.0	9.3	7.5	7.5
Legs	25.0	24.9	25.0	25.0	25.0	25.0	22.8	24.1	25.0	25.0	25.0	25.0	25.0	25.0	25.0	25.0
Head dx [mm]	406	408	396	393	410	406	397	391	421	439	414	431	407	402	401	398
Head dy [mm]	182	168	184	168	173	170	171	175	171	180	170	172	179	175	173	177
Head dz [mm]	243	249	248	237	238	235	234	239	244	234	250	232	253	250	237	235

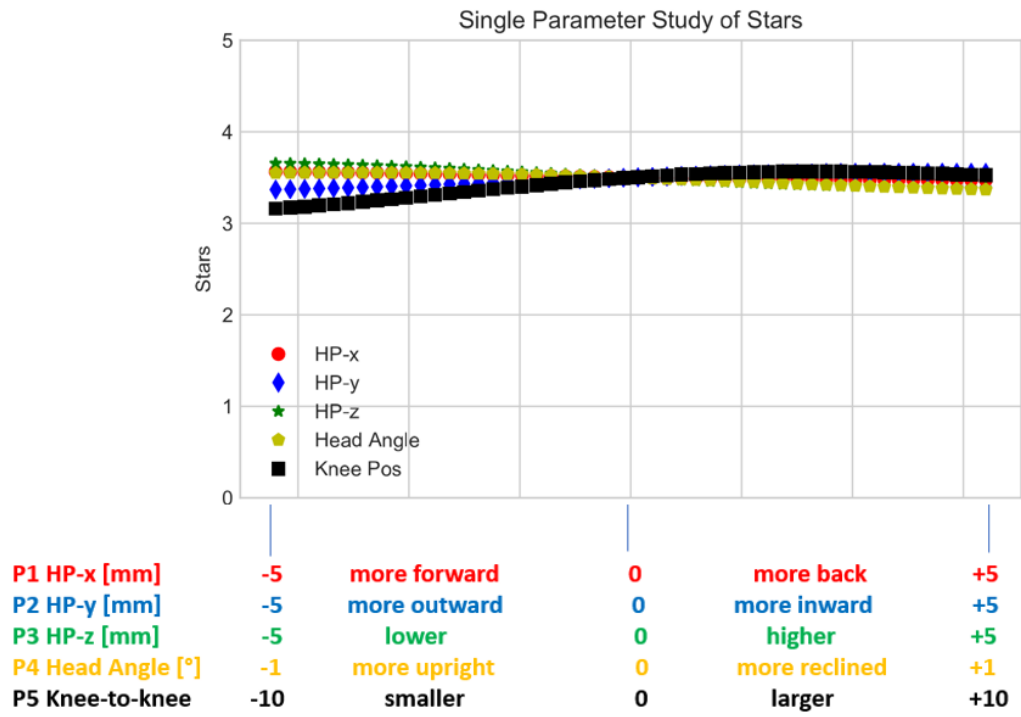
#### B4. Repeatability Study – Driver Results Runs 17–28

DOE #	17	18	19	20	21	22	23	24	25	26	27	28
HP-x	0				0				0			
HP-y	5	5	-5	-5	5	5	-5	-5	5	5	-5	-5
HP-z	5	-5	5	-5	0				0			
Head Angle	0				1	-1	1	-1	0			
Knee Pos	0				0				10	-10	10	-10
HIC	399	381	361	404	394	363	404	340	390	385	374	431
BRIC	0.94	0.87	0.99	0.99	0.94	0.87	1	0.89	0.9	0.92	0.93	1.05
Ntf	0.35	0.33	0.33	0.31	0.33	0.1	0.1	0.28	0.33	0.26	0.1	0.39
Ncf	0.29	0.2	0.23	0.17	0.21	0.27	0.23	0.21	0.22	0.2	0.27	0.23
Nte	0.38	0.4	0.36	0.39	0.37	0.38	0.36	0.38	0.4	0.4	0.39	0.38
Nce	0.09	0.09	0.15	0.09	0.13	0.09	0.1	0.18	0.1	0.08	0.19	0.13
Chest-UL	29	27	26	22	28	29	24	25	30	28	25	22
Chest-UR	49	47	47	41	46	48	47	49	48	47	48	44
Chest-LL	17	17	17	9	16	17	16	19	16	15	19	11
Chest-LL	30	31	33	34	32	31	30	32	31	30	31	36
ABDO-LE	52	54	50	51	54	55	53	51	54	52	53	49
ABDO-RI	51	54	49	52	53	55	52	49	55	53	51	49
ACET-LE	2081	2250	2269	2834	2423	2667	2250	2141	2065	2369	2363	2907
ACET-RI	1039	1018	1090	1185	1059	1051	1172	1146	1139	1167	881	1438
FEM-LE	5325	4613	4750	5072	4406	4162	4322	5488	4804	5313	4360	5891
FEM-RI	4819	5134	4774	5362	4808	5217	4840	5536	4999	4847	4798	5505
FZ TI UL	652	639	639	652	666	634	641	548	576	691	546	685
FZ TI UR	1166	1028	1205	1104	1172	1173	1288	1171	1359	1165	1157	879
FZ TI LL	1650	1414	1617	1410	1526	1612	1699	1262	1557	1591	1408	1635
FZ TI LR	3155	2764	3124	2900	3087	3352	3155	2833	3044	3230	3084	2831
MR TI UL	100	71	88	97	108	107	90	80	100	86	90	97
MR TI UR	82	97	86	103	93	84	108	105	106	110	101	190
MR TI LL	82	97	105	85	80	95	63	90	81	88	73	77
MR TI LR	82	68	88	85	89	82	112	76	110	110	117	310
Points	62	69	63	70	67	67	62	64	66	66	64	48
Stars	3.5★	3.5★	3.5★	3.5★	3.5★	3.5★	3.5★	3.5★	3.5★	3.5★	3.5★	2.5★
CORA	0.93	0.91	0.90	0.83	0.94	0.91	0.90	0.89	0.91	0.92	0.89	0.84
DOE #	17	18	19	20	21	22	23	24	25	26	27	28
Head	6.3	10.3	3.5	3.5	6.3	10.3	2.8	9.0	8.5	7.5	6.8	0.0
Neck	25.0	24.5	25.0	25.0	25.0	25.0	25.0	25.0	24.5	24.5	25.0	25.0
Chest	5.8	9.3	9.3	19.5	11.0	7.5	9.3	5.8	7.5	9.3	7.5	14.5
Legs	25.0	25.0	25.0	21.5	25.0	23.9	25.0	24.3	25.0	25.0	25.0	8.0
Head dx [mm]	407	398	406	387	415	389	411	388	404	402	401	388
Head dy [mm]	181	186	170	167	184	185	166	175	187	184	173	171
Head dz [mm]	254	240	245	237	243	241	238	243	241	242	244	253

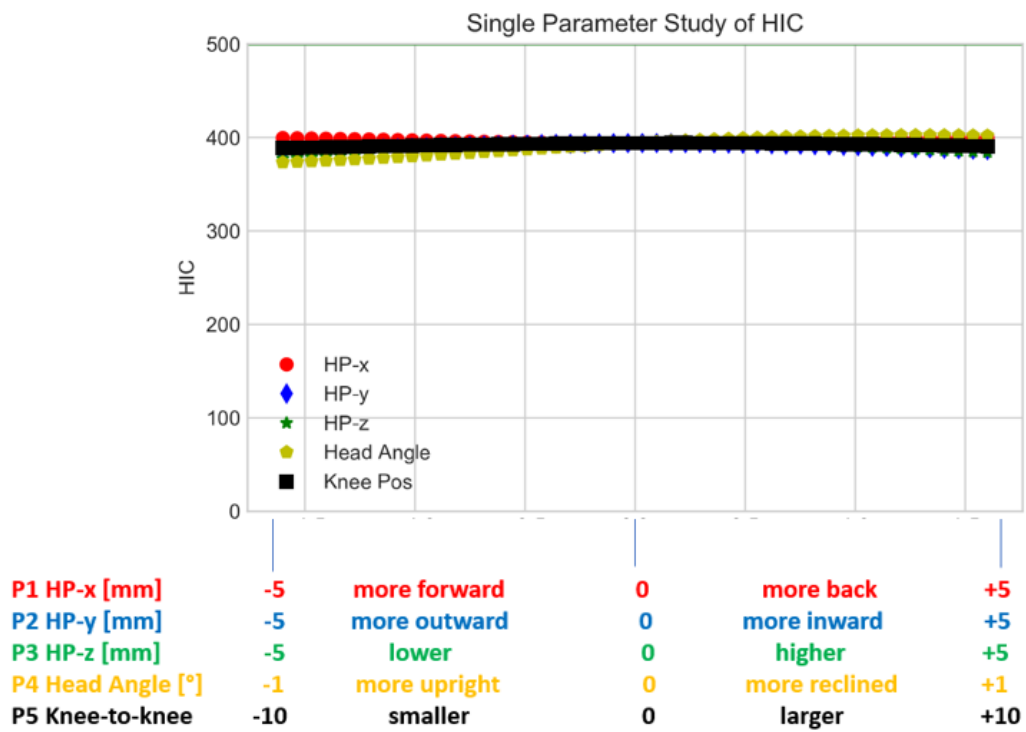
### B5. Repeatability Study – Driver Results Runs 29–41

DOE #	29	30	31	32	33	34	35	36	37	38	39	40	41
HP-x	0				0				0				0
HP-y	0				0				0				0
HP-z	5	5	-5	-5	5	5	-5	-5	0				0
Head Angle	1	-1	1	-1	0				1	1	-1	-1	0
Knee Pos	0				10	-10	10	-10	10	-10	10	-10	0
HIC	391	362	398	353	394	396	373	377	404	362	365	360	394
BRIC	0.98	0.86	0.95	0.82	0.92	0.97	0.89	0.88	0.96	0.96	0.87	0.85	0.88
Ntf	0.38	0.32	0.09	0.09	0.35	0.34	0.32	0.31	0.33	0.34	0.33	0.09	0.33
Ncf	0.3	0.2	0.21	0.19	0.15	0.21	0.23	0.22	0.22	0.17	0.2	0.16	0.19
Nte	0.37	0.41	0.39	0.4	0.38	0.37	0.38	0.36	0.37	0.34	0.39	0.38	0.38
Nce	0.1	0.19	0.1	0.09	0.14	0.18	0.09	0.09	0.1	0.1	0.09	0.17	0.11
Chest-UL	27	26	26	26	27	26	27	26	26	27	28	26	27
Chest-UR	49	48	46	47	48	49	48	47	46	46	48	48	48
Chest-LL	20	18	18	17	16	18	17	19	17	17	17	18	17
Chest-LL	30	33	31	32	32	30	33	32	29	31	33	32	34
ABDO-LE	51	51	55	53	53	51	53	53	54	54	52	53	54
ABDO-RI	48	50	54	52	54	50	52	51	54	54	52	50	52
ACET-LE	2173	2077	2446	2336	2220	2422	2371	2543	2421	2398	2267	2379	2163
ACET-RI	1264	960	1074	907	1008	1010	946	984	973	1098	931	927	1054
FEM-LE	5275	5122	4270	4232	4240	4838	4187	4839	3409	4177	4742	4303	4983
FEM-RI	5116	5367	4968	5182	4638	5004	5416	5205	4565	4308	5558	5075	4544
FZ TI UL	575	612	572	596	534	650	525	649	580	653	542	629	645
FZ TI UR	1144	1281	1103	1265	1361	1067	1191	1064	1104	897	1267	1185	1183
FZ TI LL	1446	1382	1360	1478	1685	1761	1317	1504	1693	1874	1252	1432	1692
FZ TI LR	2837	3307	2903	3210	3129	3004	3218	3163	3407	3100	2774	3013	3282
MR TI UL	105	84	76	69	97	76	96	97	100	101	93	74	95
MR TI UR	113	89	94	101	91	122	103	116	96	140	99	113	88
MR TI LL	83	78	67	89	66	180	86	70	57	68	75	83	69
MR TI LR	109	66	67	75	76	197	73	185	79	227	66	171	76
Points	60	67	67	72	65	57	66	68	66	56	67	69	67
Stars	3.0★	3.5★	3.5★	4.0★	3.5★	3.0★	3.5★	3.5★	3.5★	3.0★	3.5★	3.5★	3.5★
CORA	0.88	0.91	0.89	0.91	0.90	0.83	0.92	0.92	0.89	0.87	0.91	0.89	1.00
DOE #	29	30	31	32	33	34	35	36	37	38	39	40	41
Head	4.0	10.8	5.8	13.0	7.5	4.5	9.0	9.8	5.0	5.0	10.3	11.3	9.8
Neck	25.0	24.0	25.0	24.5	25.0	25.0	25.0	25.0	25.0	25.0	25.0	25.0	25.0
Chest	5.8	7.5	11.0	9.3	7.5	5.8	7.5	9.3	11.0	11.0	7.5	7.5	7.5
Legs	25.0	24.9	25.0	25.0	25.0	21.3	24.6	23.5	25.0	15.0	24.1	25.0	25.0
Head dx [mm]	415	387	414	386	406	401	401	397	411	416	389	387	401
Head dy [mm]	177	181	177	177	174	174	180	179	179	178	179	176	179
Head dz [mm]	243	246	240	245	245	254	250	242	246	244	243	240	243

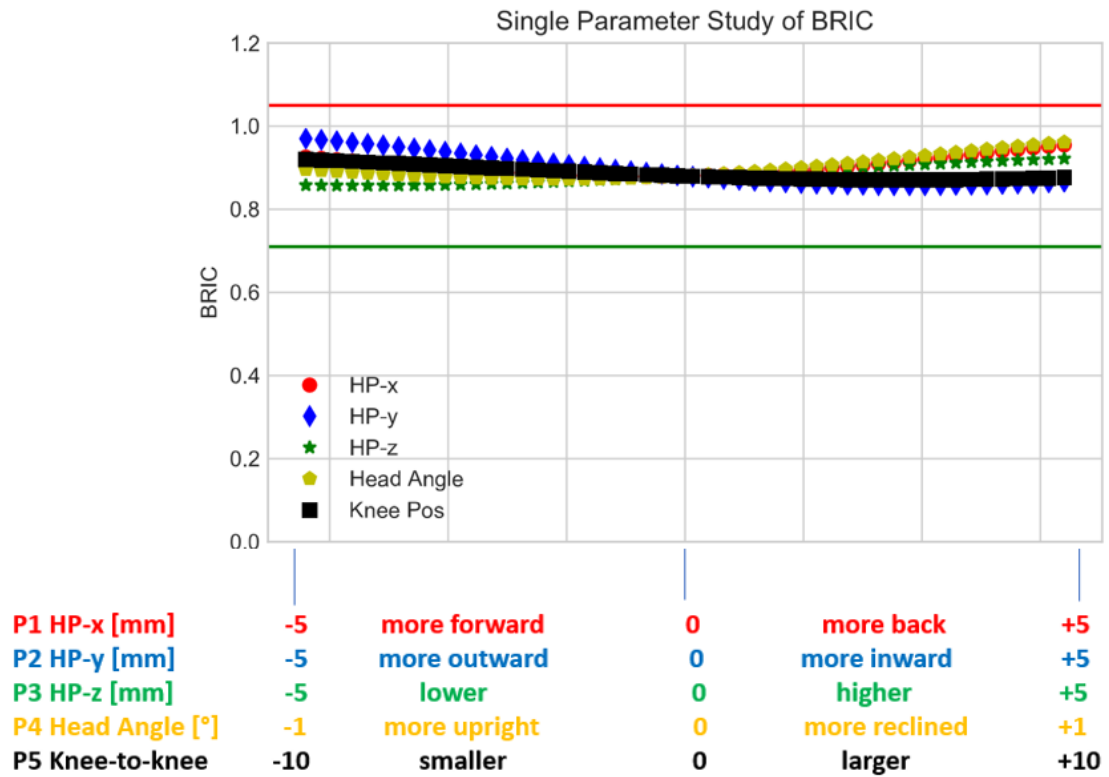
## B6. Driver Star-Rating – Effect of Individual Parameters



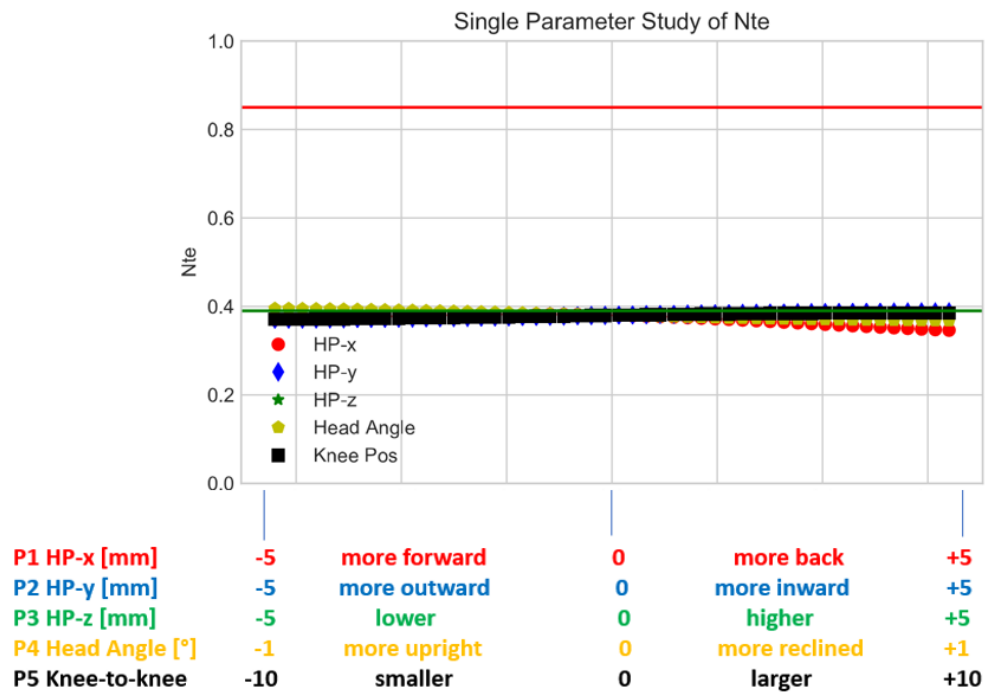
## B7. Driver HIC – Effect of Individual Parameters



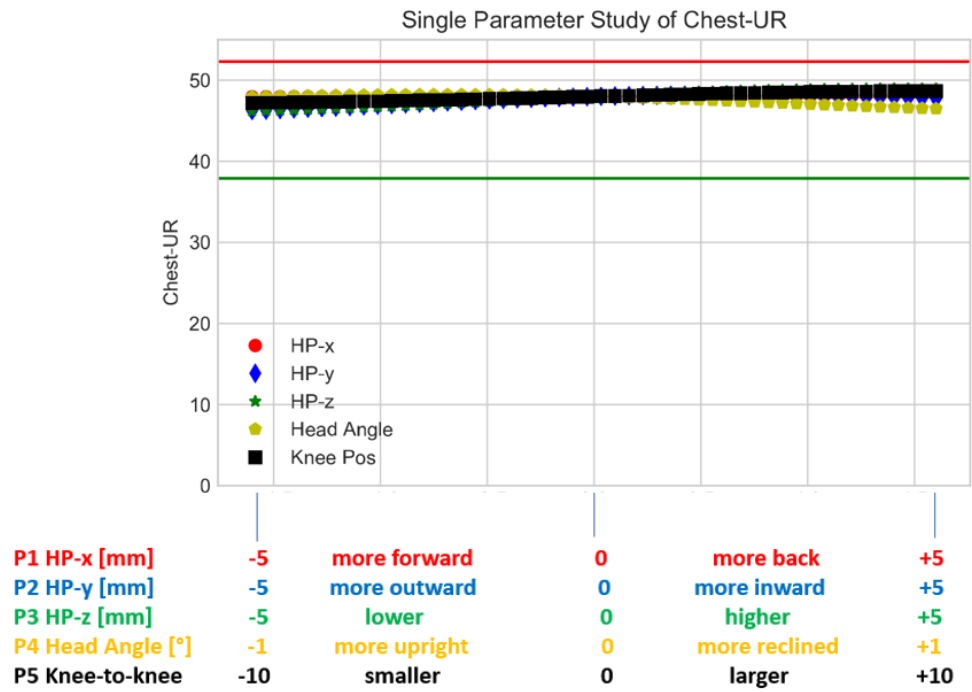
## B8. Driver BrIC – Effect of Individual Parameters



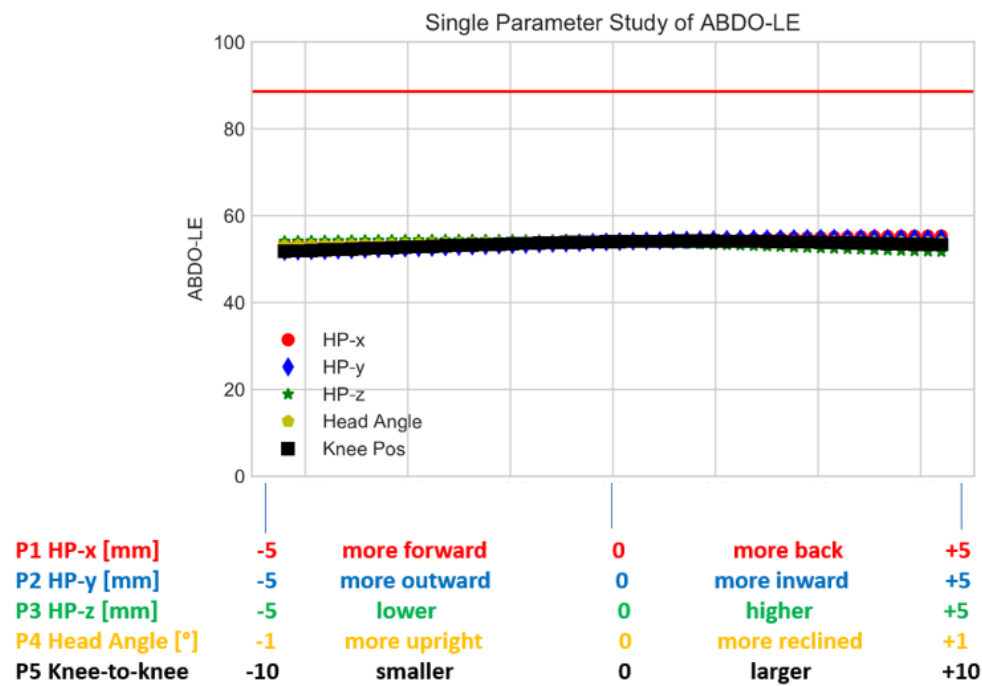
## B9. Driver Neck – Effect of Individual Parameters



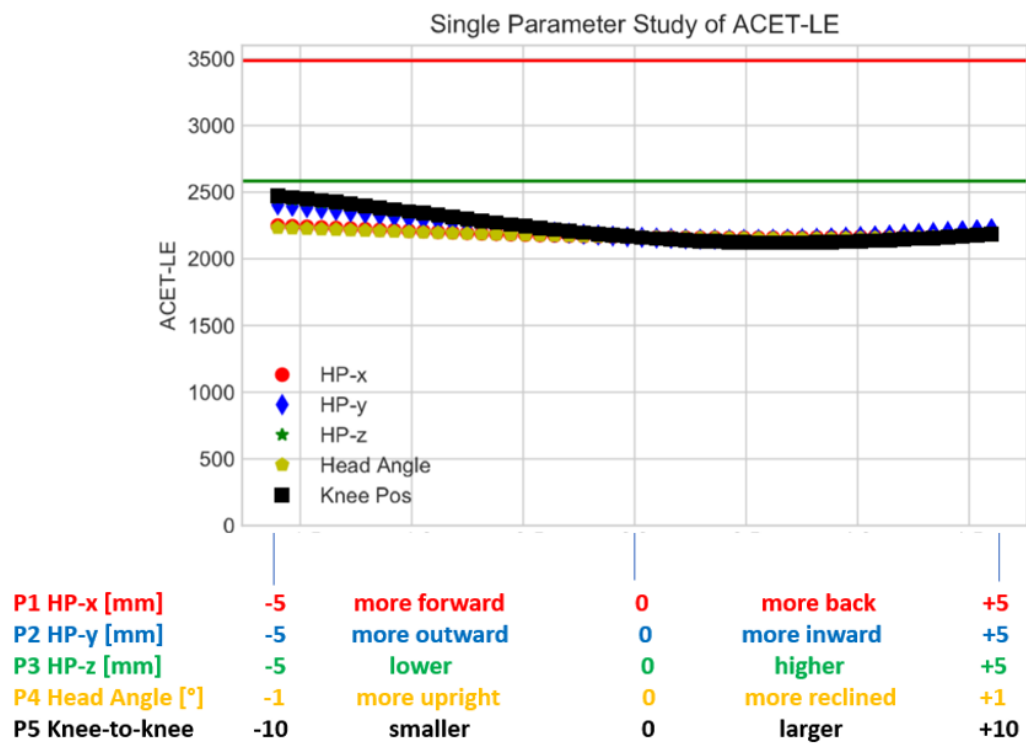
## B10. Driver Chest – Effect of Individual Parameters



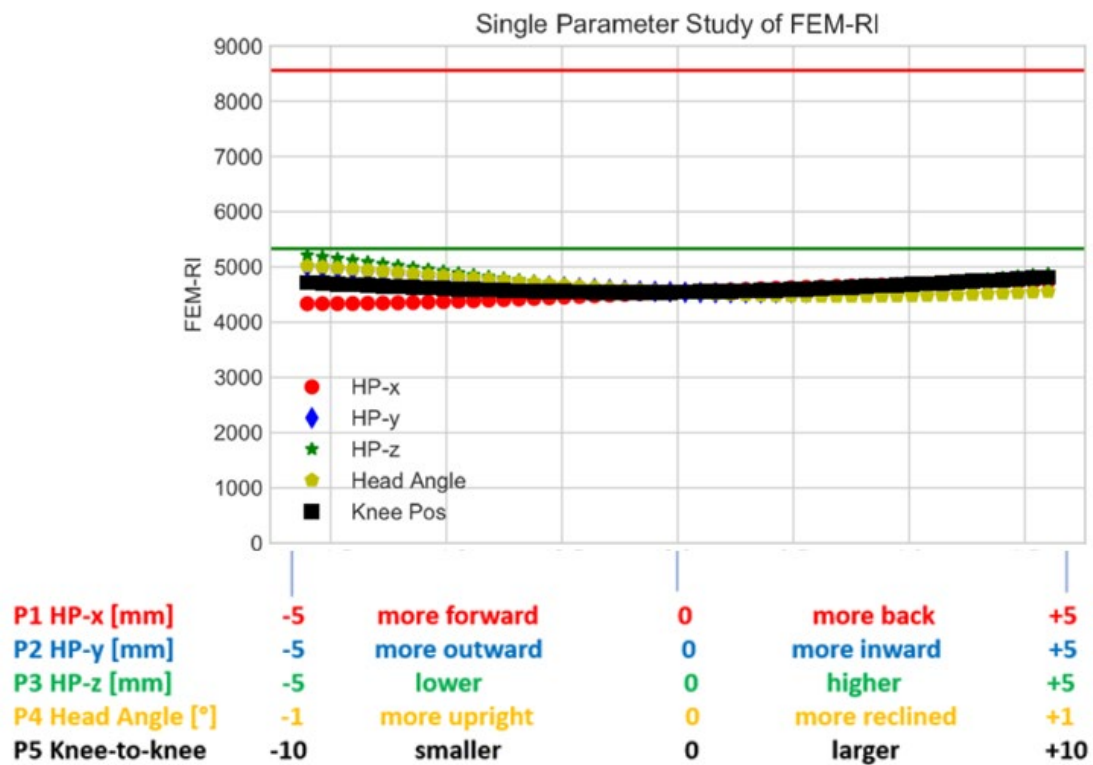
B11. Driver Abdomen – Effect of Individual Parameters



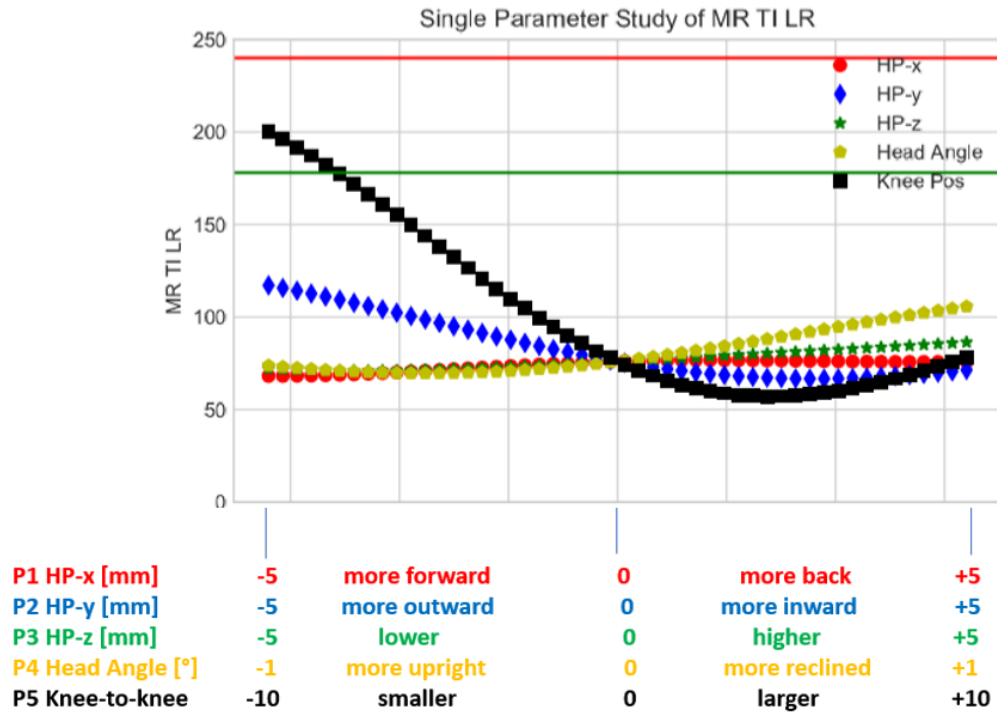
B12. Driver Acetabulum – Effect of Individual Parameters



### B13. Driver Femur – Effect of Individual Parameters



## B14. Driver Tibia – Effect of Individual Parameters



### B15. Sensitivity Study – Passenger Results Runs 1–16

DOE #	1	2	3	4	5	6	7	8	9	10	11	12	13	14	15	16
HP-x	20	20	-20	-20	20	20	-20	-20	20	20	-20	-20	20	20	-20	-20
HP-y	5	-5	5	-5	0	0	0	0	0	0	0	0	0	0	0	0
HP-z	10	10	10	10	20	0	20	0	10	10	10	10	10	10	10	10
Head Angle	0	0	0	0	0	0	0	0	5	-5	5	-5	0	0	0	0
Knee Pos	30	30	30	30	30	30	30	30	30	30	30	30	60	0	60	0
HIC	413	396	458	662	417	420	392	475	792	272	1115	251	407	829	600	708
BRIC	1.32	1.17	1.39	1.23	1.3	1.2	1.26	1.37	1.23	1.4	1.29	1.3	1.35	1.23	1.35	1.31
Ntf	0.5	0.47	0.68	0.52	0.45	0.47	0.49	0.62	0.47	0.51	0.55	0.52	0.43	0.44	0.58	0.66
Ncf	0.09	0.09	0.09	0.09	0.08	0.08	0.1	0.1	0.12	0.07	0.11	0.16	0.09	0.09	0.08	0.11
Nte	0.52	0.57	0.45	0.47	0.53	0.43	0.46	0.47	0.55	0.5	0.52	0.43	0.53	0.47	0.45	0.47
Nce	0.01	0.09	0.07	0.17	0.08	0.08	0.02	0.03	0.34	0.1	0.34	0.09	0.09	0.24	0.26	0.08
Chest-UL	29	30	28	28	29	29	28	25	33	31	32	29	30	30	30	29
Chest-UR	32	32	30	31	31	31	30	27	33	31	32	31	32	32	31	31
Chest-LL	40	38	38	36	41	39	38	36	44	39	41	38	42	42	40	40
Chest-LR	11	13	11	14	9	10	13	12	15	12	16	17	12	13	15	16
ABDO-LE	65	64	60	60	64	65	61	61	66	61	63	58	65	65	61	62
ABDO-RI	66	61	62	59	65	66	62	63	66	64	63	59	66	65	62	63
ACET-LE	2073	2003	3394	2501	2124	2260	2350	3844	1794	2569	2026	2790	2165	2346	2299	2593
ACET-RI	2488	2339	3915	3200	1986	2061	2569	3445	2381	2538	2256	2433	2362	2391	2923	2682
FEM-LE	4211	4003	7140	6274	3388	2834	5650	6344	3958	3431	6209	6061	4528	3448	7409	6678
FEM-RI	1134	1031	1732	1334	1203	1171	1253	1036	1316	942	1188	1227	1187	1001	1427	1330
FZ TI UL	1013	879	1153	1004	952	901	945	1124	983	870	909	850	1102	893	1014	974
FZ TI UR	780	877	1038	1040	870	857	1026	1009	708	758	902	1003	735	791	1051	995
FZ TI LL	3867	3257	2952	2880	3288	3505	2828	3158	3645	3598	2568	2711	3214	3568	2581	2741
FZ TI LR	3116	3497	3797	3886	3372	3446	3310	3276	3012	3019	3571	3589	2951	3101	3569	3642
MR TI UL	174	186	192	176	189	173	180	191	210	218	182	166	216	207	190	147
MR TI UR	279	315	150	179	294	318	199	209	286	289	150	192	364	214	188	131
MR TI LL	119	102	69	62	104	101	55	61	120	123	62	58	75	123	63	56
MR TI LR	145	151	71	80	142	159	94	90	131	145	72	101	181	103	91	75
Points	52	53	44	58	50	56	64	44	43	54	57	62	48	57	51	51
Stars	3.0★	3.0★	2.5★	3.0★	2.5★	3.0★	3.5★	2.5★	2.5★	3.0★	3.0★	3.5★	2.5★	3.0★	3.0★	3.0★
CORA	0.81	0.75	0.70	0.81	0.76	0.75	0.81	0.72	0.80	0.76	0.78	0.75	0.78	0.85	0.79	0.76
DOE #	1	2	3	4	5	6	7	8	9	10	11	12	13	14	15	16
Head	0	0	0	0	0	0	0	0	0	0	0	0	0	0	0	0
Neck	18	15.25	9.25	18	17.5	20.75	19.5	12.5	16.25	18.5	16.25	18	17.5	20.75	14.75	10.25
Chest	21.25	24.75	24.75	25	19.5	23	24.75	25	14.5	23	19.5	24.75	18	18	21.25	21.25
Legs	12.5	12.5	9.625	14.75	12.5	12.5	19.5	6.25	12.5	12.5	20.88	19.25	12.5	17.88	14.5	19.38
Head dx [mm]	570	566	506	537	570	557	530	490	619	508	590	479	560	565	534	535
Head dy [mm]	254	244	254	241	247	245	246	247	251	268	245	262	253	258	255	251
Head dz [mm]	425	449	411	374	449	444	435	406	368	448	349	420	455	387	372	394

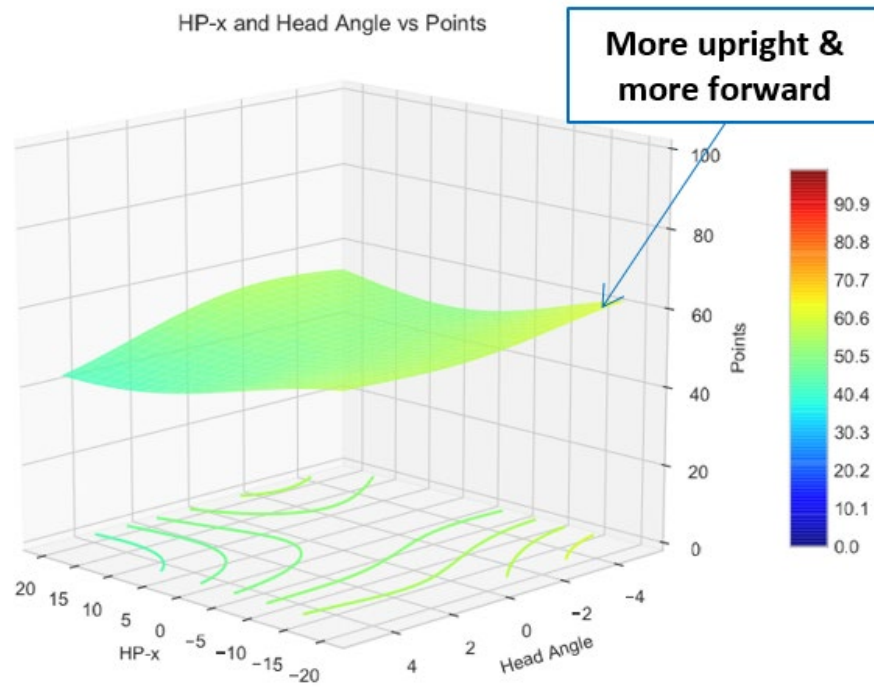
**B16. Sensitivity Study – Passenger Results Runs 17–28**

DOE #	17	18	19	20	21	22	23	24	25	26	27	28
HP-x	0	0	0	0	0	0	0	0	0	0	0	0
HP-y	5	5	-5	-5	5	5	-5	-5	5	5	-5	-5
HP-z	20	0	20	0	10	10	10	10	10	10	10	10
Head Angle	0	0	0	0	5	-5	5	-5	0	0	0	0
Knee Pos	30	30	30	30	30	30	30	30	60	0	60	0
HIC	388	709	740	1189	520	340	1236	323	666	513	1018	379
BRIC	1.43	1.5	1.26	1.3	1.42	1.38	1.26	1.44	1.5	1.39	1.21	1.27
Ntf	0.65	0.88	0.43	0.45	0.57	0.6	0.47	0.48	0.45	0.54	0.39	0.4
Ncf	0.08	0.09	0.09	0.08	0.12	0.07	0.11	0.09	0.19	0.09	0.08	0.08
Nte	0.53	0.58	0.48	0.52	0.5	0.53	0.53	0.48	0.58	0.58	0.47	0.5
Nce	0.07	0.03	0.19	0.27	0.11	0.03	0.37	0.06	0.24	0.03	0.23	0.08
Chest-UL	30	29	29	30	33	26	33	29	30	29	30	29
Chest-UR	31	30	31	31	31	30	34	33	32	31	31	31
Chest-LL	42	39	40	39	44	37	44	37	41	40	39	39
Chest-LL	11	10	15	15	14	11	17	10	14	10	14	16
ABDO-LE	62	62	63	63	65	59	65	57	65	61	61	63
ABDO-RI	63	63	63	64	66	61	65	58	65	62	63	63
ACET-LE	2939	3354	2105	2291	1786	3714	1821	3215	2093	3088	2209	2512
ACET-RI	3096	3244	2762	2734	2513	3593	2639	3709	2491	3572	2573	2932
FEM-LE	6925	5893	5878	5719	5492	5627	5336	6264	6134	6335	6268	5262
FEM-RI	1058	1114	1065	874	870	1198	896	1354	605	1519	1091	927
FZ TI UL	1004	979	962	1018	840	1060	937	1066	958	939	1096	901
FZ TI UR	927	1015	768	844	756	973	749	951	696	974	754	896
FZ TI LL	2819	2951	2693	2859	2932	3218	2610	2930	2421	3191	2848	3095
FZ TI LR	3076	3386	3016	2925	3276	3189	2997	3225	2404	3576	2733	3472
MR TI UL	222	199	241	251	225	205	236	232	246	170	228	203
MR TI UR	228	215	220	199	214	218	228	231	251	162	247	175
MR TI LL	72	81	72	78	64	95	67	72	72	102	85	103
MR TI LR	115	111	111	105	110	112	114	120	126	91	126	92
Points	37	30	51	51	45	43	45	47	44	49	53	57
Stars	2.0★	1.5★	3.0★	3.0★	2.5★	2.5★	2.5★	2.5★	2.5★	2.5★	3.0★	3.0★
CORA	0.80	0.79	0.90	0.84	0.80	0.76	0.82	0.78	0.86	0.78	0.85	0.83
DOE #	17	18	19	20	21	22	23	24	25	26	27	28
Head	0	0	0	0	0	0	0	0	0	0	0	0
Neck	10.75	0	20	18	15.25	13.5	17.5	20	14.75	14.75	20.75	19
Chest	18	23	21.25	23	14.5	25	14.5	25	19.5	21.25	23	23
Legs	7.75	6.875	10	10.38	14.88	4.375	12.5	1.75	9.375	12.5	8.875	15
Head dx [mm]	534	516	550	551	596	474	606	472	545	521	549	554
Head dy [mm]	267	269	255	244	249	289	239	264	257	258	262	237
Head dz [mm]	431	392	399	361	399	422	348	439	400	433	371	431

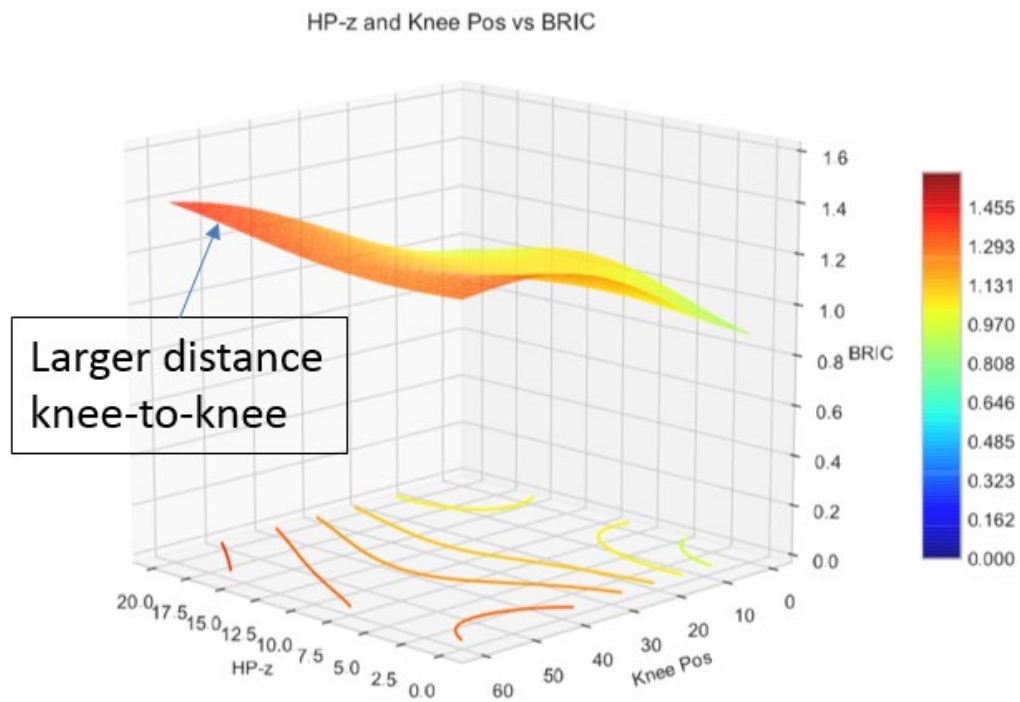
**B17. Sensitivity Study – Passenger Results Runs 29–41**

DOE #	29	30	31	32	33	34	35	36	37	38	39	40	41
HP-x	0	0	0	0	0	0	0	0	0	0	0	0	0
HP-y	0	0	0	0	0	0	0	0	0	0	0	0	0
HP-z	20	20	0	0	20	20	0	0	10	10	10	10	10
Head Angle	5	-5	5	-5	0	0	0	0	5	5	-5	-5	0
Knee Pos	30	30	30	30	60	0	60	0	60	0	60	0	30
HIC	1190	263	1287	382	332	396	902	377	1401	1195	343	408	762
BRIC	1.26	1.29	1.35	1.5	1.4	0.97	1.28	0.88	1.26	1.19	1.46	1.27	1.13
Ntf	0.46	0.43	0.54	0.59	0.42	0.34	0.76	0.31	0.54	0.48	0.56	0.43	0.44
Ncf	0.11	0.09	0.11	0.1	0.08	0.21	0.14	0.22	0.11	0.11	0.08	0.12	0.08
Nte	0.5	0.47	0.55	0.51	0.49	0.37	0.52	0.36	0.52	0.44	0.53	0.45	0.57
Nce	0.3	0.03	0.38	0.05	0.08	0.18	0.09	0.09	0.29	0.27	0.08	0.12	0.27
Chest-UL	32	30	33	27	30	26	30	26	33	32	27	29	28
Chest-UR	33	32	33	31	32	49	32	47	33	33	31	31	30
Chest-LL	44	39	43	36	41	18	39	19	44	43	36	38	39
Chest-LL	14	14	16	8	13	30	15	32	15	15	10	15	12
ABDO-LE	63	60	64	58	62	51	63	53	64	64	58	60	62
ABDO-RI	65	60	65	59	62	50	65	51	65	66	60	61	63
ACET-LE	1898	2518	1848	3614	1985	2422	2273	2543	1848	1839	3171	2985	2000
ACET-RI	2479	2623	2405	3639	2485	1010	2354	984	2500	2269	3664	2604	2362
FEM-LE	5943	5000	5668	5121	5756	4838	5678	4839	5544	4926	6119	4731	5496
FEM-RI	907	1136	796	1266	663	5004	611	5205	948	857	1412	1105	863
FZ TI UL	874	941	886	1081	946	650	1074	649	941	842	1191	857	1035
FZ TI UR	798	783	752	992	738	1067	797	1064	669	788	940	837	826
FZ TI LL	2642	3335	2520	3448	2313	1761	3017	1504	2387	3147	3327	3147	3120
FZ TI LR	3261	2825	3338	3264	2604	3004	2653	3163	2743	3276	2809	3248	3022
MR TI UL	210	199	230	173	262	76	246	97	274	192	210	145	216
MR TI UR	219	228	221	243	255	122	247	116	238	163	298	191	237
MR TI LL	70	75	65	95	84	180	86	70	73	82	76	97	84
MR TI LR	102	123	115	113	132	197	130	185	119	81	153	95	128
Points	48	58	46	39	50	57	39	68	43	59	41	63	51
Stars	2.5★	3.0★	2.5★	2.0★	2.5★	3.0★	2.0★	3.5★	2.5★	3.0★	2.5★	3.5★	3.0★
CORA	0.80	0.79	0.82	0.73	0.81	0.83	0.81	0.81	0.81	0.80	0.75	0.79	1.00
DOE #	29	30	31	32	33	34	35	36	37	38	39	40	41
Head	0	0	0	0	0	4.5	0	9.75	0	0	0	0	0
Neck	19	20.75	16.25	14.25	19.5	25	5	25	16.75	20	15.75	21.75	15.25
Chest	14.5	23	16.25	25	19.5	5.75	23	9.25	14.5	16.25	25	24.75	23
Legs	14.38	14.5	13.25	0	10.88	21.25	11.13	23.5	11.63	22.25	0	16.75	12.5
Head dx [mm]	606	496	606	467	548	548	542	546	606	604	469	494	552
Head dy [mm]	249	261	250	258	245	262	256	248	249	243	270	267	239
Head dz [mm]	371	448	343	424	439	422	390	390	336	347	443	410	379

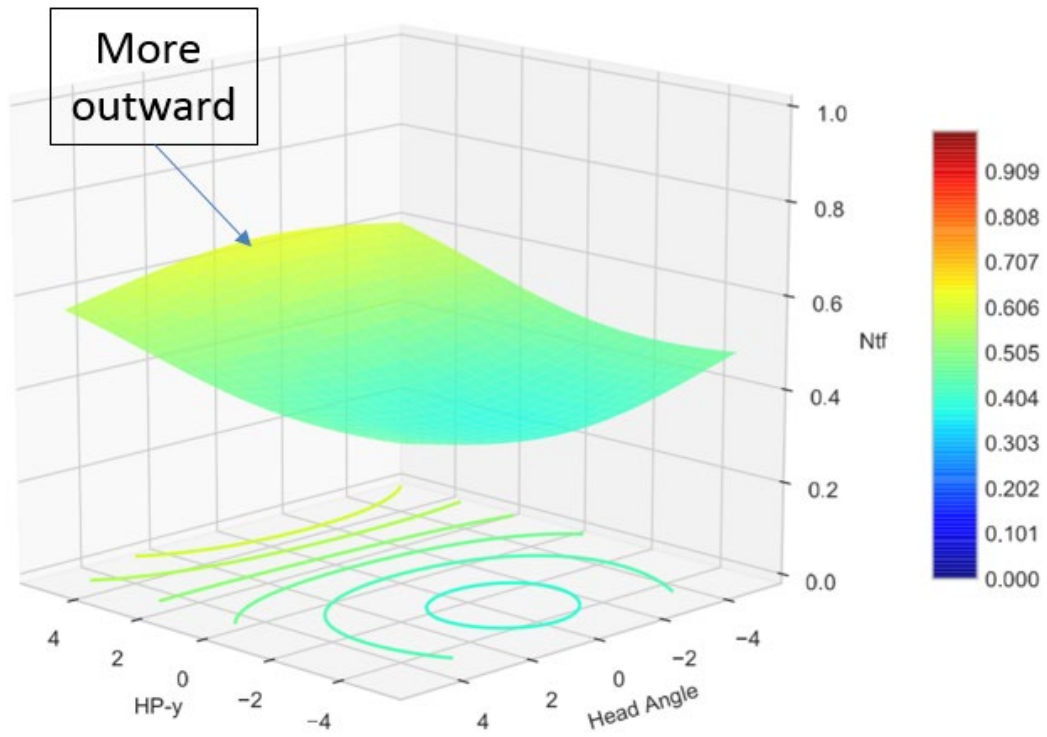
### B18. Passenger Point Score – Response Surface



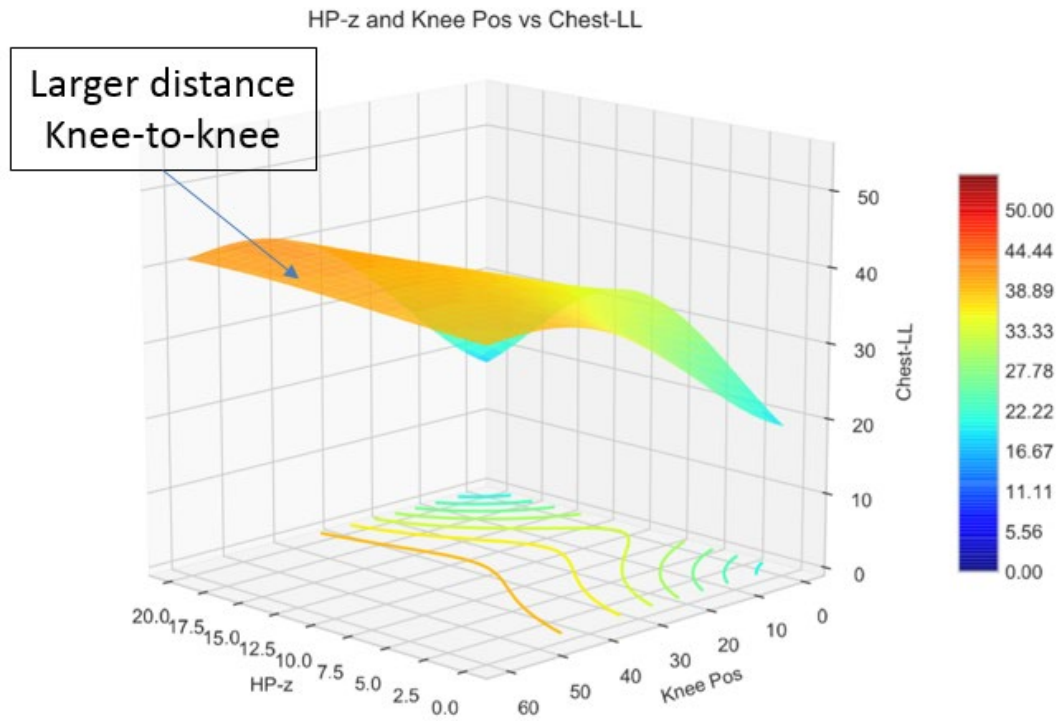
## B19. Passenger BrIC – Response Surface



## B20. Passenger Neck – Response Surface

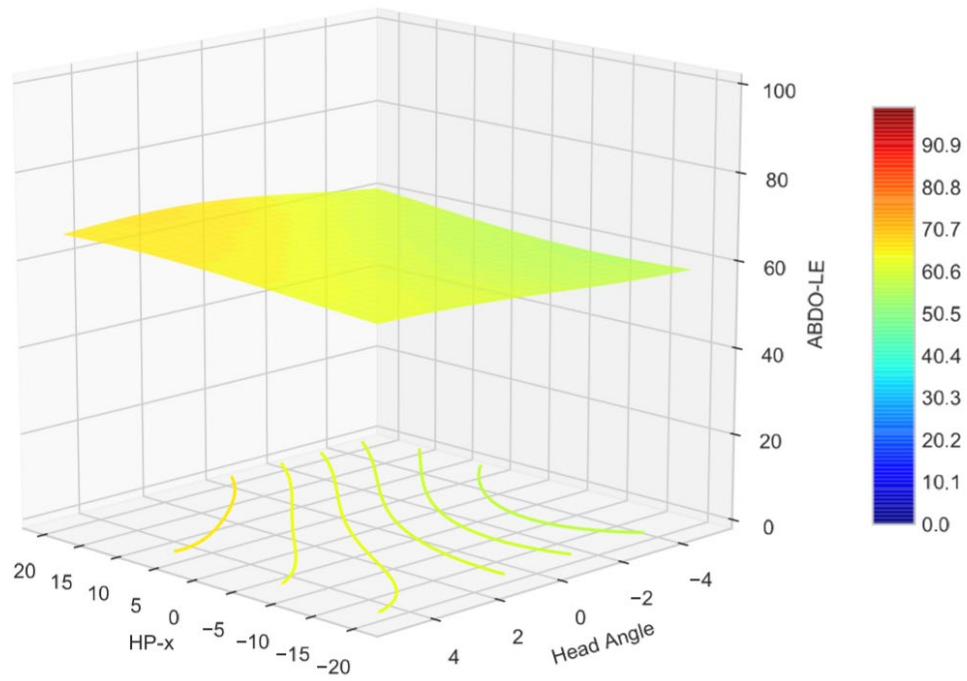


## B21. Passenger Chest – Response Surface

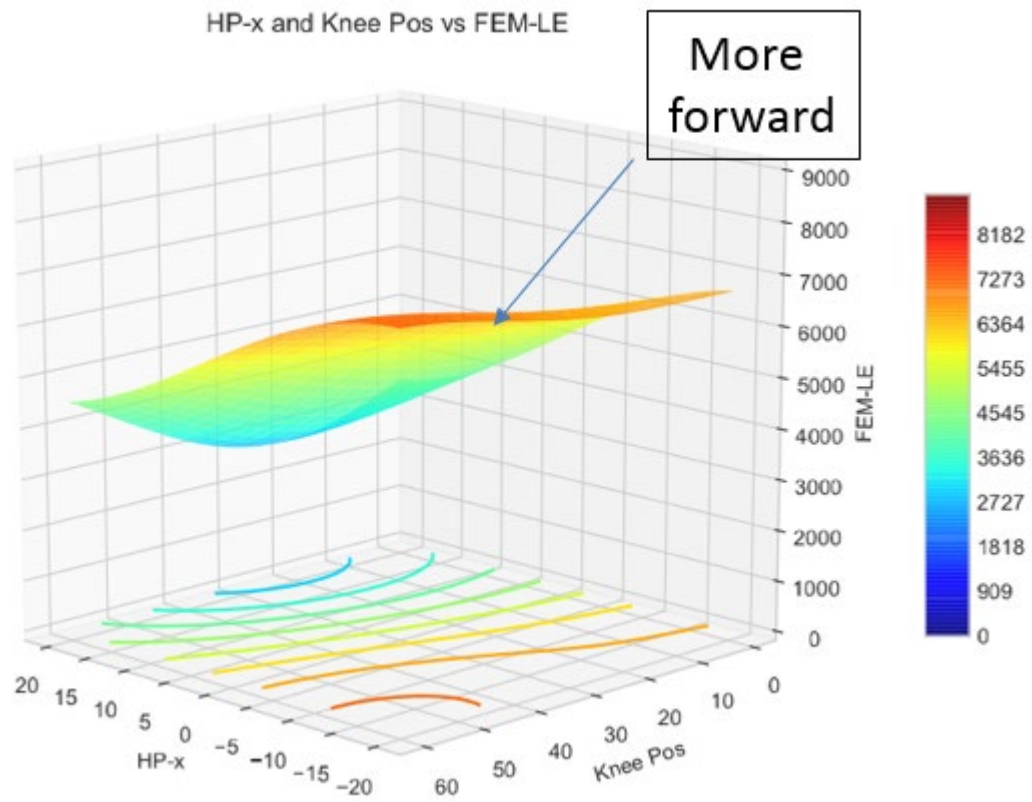


## B22. Passenger Abdomen – Response Surface

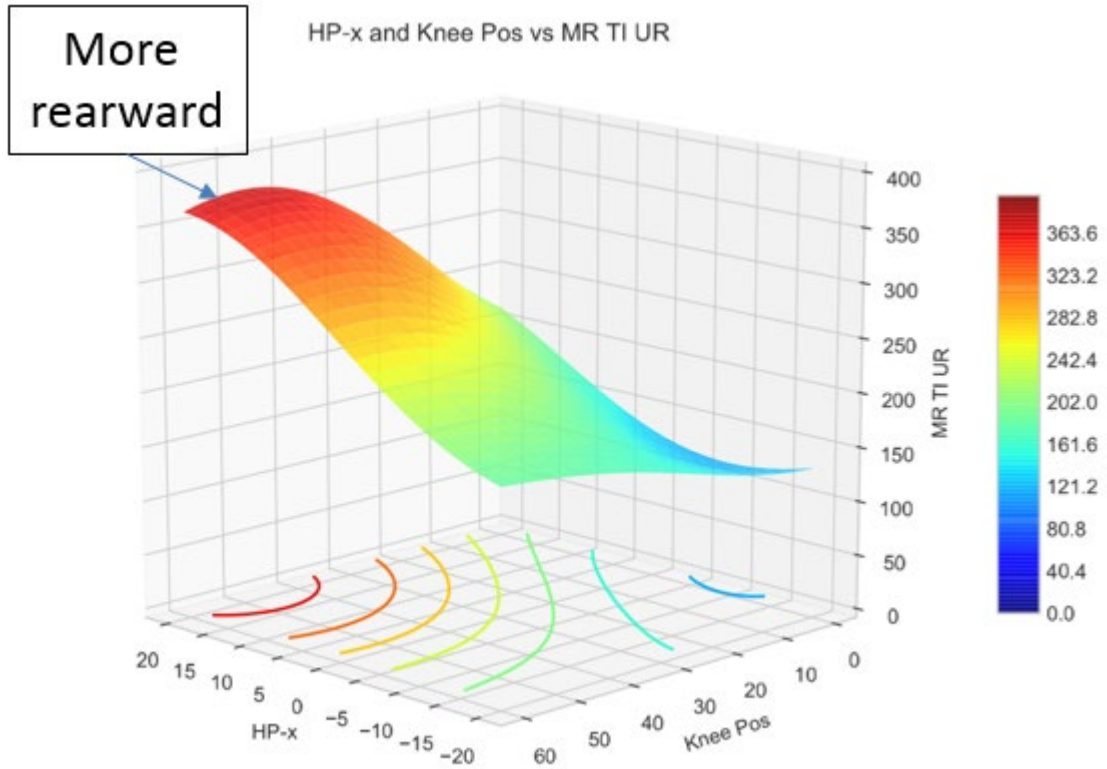
HP-x and Head Angle vs ABDO-LE



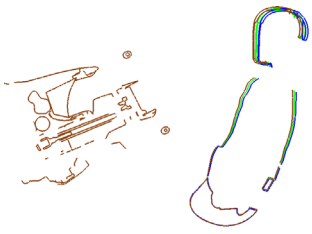
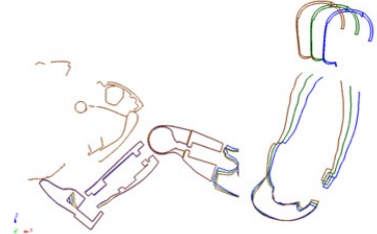
### B23. Passenger Femur – Response Surface



## B24. Passenger Tibia – Response Surface



### B25. THOR Position Study Results Overview

	Repeatability Study (Driver)	Sensitivity Study (Passenger)
		
$\Delta$ HP-x [mm]	10 +/-5	40 +/-20
$\Delta$ HP-y [mm]	10 +/-5	10 +/-5
$\Delta$ HP-z [mm]	10 +/-5	20 0/+10/+20
$\Delta$ Head/Torso Angle [°]	2 +/-1	10 +/-5
$\Delta$ Knee-to-knee distance [mm]	20 +/-10	60 0/+30/+60
$\Delta$ Star Rating	1.5 2.5 to 4.0	2 1.5 to 3.5
$\Delta$ Points	24 48 to 72	34 30 to 64
CORA Rating	0.81 – 0.93	0.7-0.9
$\Delta$ BrIC	0.12 0.85 to 0.97	0.37 1.13 to 1.50
$\Delta$ Chest Driver [mm]	2 47 to 49	8 36 to 44
$\Delta$ Head x-displacement [mm]	12 396 to 408	142 467 to 619
Head y-displacement [mm]	21 167 to 188	52 237 to 289

## THOR Position Study – Driver Summary

- **Results Repeatability Study (Driver): small variation of seating position**
  - 85% (35 of 41) of simulations showed same 3.5\* star rating
  - CORA ratings between 0.81 and 0.94 document good test repeatability

Response	Most important Param.	Effect
Star rating	Knee-to-knee distance	Smaller K-to-k => lower star rating
Head y-excursion	HP-y	More inward => higher head <u>dy</u>
HIC & BRIC	Head/Torso angle	More upright => lower HIC & BRIC
Neck Nij	HP-x	More rearward => higher Nte
Chest UR	HP-z	Lower seating => lower chest deflection
Abdomen	HP-y	No significant effect of any parameter
Femur	HP-x	More forward => higher femur load
Tibia	Knee-to-knee distance	Smaller K-to-K => higher tibia load

## THOR Position Study – Passenger Summary

- **Results Sensitivity Study (passenger): variation of seating position beyond test tolerances**
  - 37 of 41) of simulations showed 2.5-star or 3-star rating
  - CORA ratings between 0.7 and 0.9

Response	Most important Param.	Effect
Star rating	Knee-to-knee distance	Larger K-to-k => lower star rating
Head x-excursion	Head/torso angle	More reclined => more forward motion
HIC	Head/Torso angle	More reclined => higher HIC
Neck Nij	HP-y	More outward => higher Nte
Chest LL	Knee-to-knee	Larger k-to-k => higher chest deflection
Abdomen	Head/torso angle	More reclined => higher deflection
Femur	HP-x	More forward => higher femur load
Tibia	HP-x	More rearward => higher tibia load

DOT HS 812 845  
June 2020



U.S. Department  
of Transportation  
**National Highway  
Traffic Safety  
Administration**



14478-062520-v3